



Research Report



Retrofit of Wood Bridges

CTS
TG
365
.L46
1993

UNIVERSITY OF MINNESOTA
CENTER FOR
TRANSPORTATION
STUDIES

Report Documentation Page

1. Report No. MN/RC - 94/16	2.	3. Recipient's Accession No.	
4. Title and Subtitle Retrofit of Wood Bridges		5. Report Date February 1993	
		6.	
7. Author(s) Roberto T. Leon, Demetrios O. Beltaos, and Robert T. Seavy		8. Performing Organization Report No.	
9. Performing Organization Name and Address Civil & Mineral Engineering Department University of Minnesota 500 Pillsbury Dr. SE Minneapolis, Mn 55455		10. Project/Task/Work Unit No.	
		11. Contract(C) or Grant(G) No. (C) Mn/DOT 68575 TOC 66	
12. Sponsoring Organization Name and Address Minnesota Department of Transportation Office of Research Administration 200 Ford Building-Mail Stop 330 117 University Avenue St. Paul, Mn. 55155		13. Type of Report and Period Covered Final Report 1991-1992	
		14. Sponsoring Agency Code	
15. Supplementary Notes			
16. Abstract (Limit: 200 words) <p>A retrofit scheme to widen and strengthen nail-laminated timber bridges was evaluated in this project. The scheme consists basically of laying a second, transverse layer of timbers above the existing deck, and casting a grout layer between the two wood ones to insure good force transfer. An old wood bridge was evaluated before and after it was retrofitted in order to investigate the effectiveness of the retrofit technique. In addition, three laboratory specimens, representing portions of the retrofitted bridge deck (ungROUTed and grouted), were tested to investigate the strength and the effects of fatigue on the retrofitted bridge deck, and to evaluate the transverse load distribution of the original and retrofitted bridge deck. An analytical model of the retrofitted bridge deck was also developed utilizing the finite element method. the deflection and transverse distribution results from the model studies were compared favorably with the laboratory results.</p>			
17. Document Analysis/Descriptors Wood Bridges Bridge Retrofit Fatigue Grouts		18. Availability Statement No restrictions. This document is available through the National Technical Information Services, Springfield, Va. 22161	
19. Security Class (this report) Unclassified	20. Security Class (this page) Unclassified	21. No. of Pages 82	22. Price

RETROFIT OF WOOD BRIDGES

Final Report

Prepared by

Roberto T. Leon, Associate Professor
Demetrios O. Beltaos, Research Assistant
Department of Civil and Mineral Engineering

and

Robert T. Seavy, Research Associate
Department of Forest Products

The University of Minnesota - Twin Cities

February 1993

Submitted to

Minnesota Department of Transportation
Office of Research Administration
200 Ford Building, 117 University Avenue
St. Paul, MN 55155

This report represents the results of research conducted by the authors and does not necessarily reflect the official views or policy of the Minnesota Department of Transportation or the Local Road Research Board.

ACKNOWLEDGEMENTS

The financial and logistical support provided by the Local Roads Research Board, the Minnesota Department of Transportation, the Center for Transportation Studies at the University of Minnesota, Wheeler Consolidated Inc. and Sibley County for this work is gratefully acknowledged.

EXECUTIVE SUMMARY

A retrofit scheme to widen and strengthen nail-laminated timber bridges was evaluated for this project. The retrofit scheme was developed by Gene Isakson, County Highway Engineer, Sibley County. The scheme consists basically of laying a second, transverse layer of timbers above the existing deck, and casting a grout layer between the two wood ones to insure good force transfer. An old wood bridge was evaluated before and after it was retrofitted in order to investigate the effectiveness of the retrofit technique. In addition, three laboratory specimens, representing portions of the retrofitted bridge deck (ungrouted and grouted), were tested to investigate the strength and the effects of fatigue on the retrofitted bridge deck, and to evaluate the transverse load distribution of the original and retrofitted bridge deck. An analytical model of the retrofitted bridge deck was also developed utilizing the finite element method. The deflection and transverse distribution results from the model studies were compared favorably with the laboratory results.

The timber nail-laminated bridge chosen for the project was located southwest of Winthrop, Minnesota on County Highway 8 in Sibley County. The retrofit widened the clear roadway four feet (from 24 feet to 28 feet). The length of the bridge deck was extended two feet on each end (from 48 feet to 52 feet). The results of the field evaluations showed that the bridge was strengthened with the addition of the retrofit deck. With one lane loaded, the maximum deflection of the original bridge was 0.27 inches while the maximum deflection of the retrofitted bridge was 0.20 inches. This is approximately a 35 percent increase in stiffness. Since wood bridge design is often governed by deflection, this directly translates into a significant increase in the load rating for the bridge. With both lanes loaded, the increase in stiffness is roughly half of that for the single loaded lane.

The transverse load distribution of the retrofitted bridge was much better than the original nail-lam bridge. This was evident by looking at the relative deflection of adjacent deflection transducers. The relative deflections recorded by the deflection transducers were closer in magnitude for the retrofitted deck than for the original one. This showed that the load was being distributed over a larger portion of the deck. The improvement in the transverse load distribution was especially noticeable at high loads (large deflections).

The dynamic peak deflections also decreased for the retrofitted bridge. The deflections were reduced by about 15 percent. In addition, the speed associated with the maximum deflections decreased from 40 mph to 6 mph. This is important because it is much more likely that vehicles will be travelling across the bridge at 40 mph than at 6 mph. Thus, the likelihood of reaching these maximum dynamic deflections has been reduced with the retrofit deck.

The lab results showed that the maximum deflection of the grouted lab specimens is approximately 20 percent less than the ungrouted specimen. The grout not only fills the voids which may exist between the two decks but also appears to increase the strength.

All three specimens were not affected by the fatigue tests. Load-deflection curves were obtained after 1,000, 10,000, 100,000, and 1,000,000 cycles. Even after 1,000,000 cycles, there did not appear to be any loss of strength.

The lab results also showed that the transverse load distribution was considerably improved with the retrofit deck. The load was distributed over a much larger portion of the deck. The peak load was decreased and more of the specimen contributed in carrying the load.

The results of the analytical studies were compared to the lab results. The results showed that using the suggested value of 73% of the modulus of elasticity for the longitudinal direction, E_x , yields good results. The assumption of whether gaps exist or do not exist between the individual timber members does not appear to be critical. The analytical model of the grouted specimen yields somewhat greater deflections than recorded in the lab, 0.34 inches compared to 0.30 inches. However, the model is purposely conservative and this overestimation is not unexpected.

According to the AASHTO Standard Specifications for Highway Bridges, the effective width, b , for the original bridge deck should be taken as 40 inches. The elastic deflection computed using an effective width of 40 inches compared well to the field results of the static tests of the original bridge. In order to determine the deflection of the retrofitted bridge an effective width of 48 inches was used. This was estimated from the field results, using the fact that the static deflections were reduced between 16 and 25 percent. This new effective width worked fairly well in estimating the deflection in the field evaluation of the retrofitted bridge. It must be noted that this is for a deck depth of 10 inches. The percent increase in the effective width for other deck depths may not necessarily be 20 percent.

It is possible that this retrofit procedure could be applied to initial construction. With the decreasing availability of deep members (12 inches or greater), and the high cost of these deep members, new bridge decks could be constructed using the retrofit technique. The decks would have similar strength to the deeper decks but would use much shallower members and can be prefabricated for quick installation.

One issue which was not addressed was the long-term performance of the grout, especially in the area of the freeze-thaw response. It is likely that the composite action observed in the tests can be activated even if the grout deteriorates because of the large component of horizontal shear due to friction. Another area which seems to warrant more research is coming up with a reasonable effective width, b , for a retrofitted nail-lam bridge deck. The results from this project suggest a 20 percent increase in the effective width from the original bridge could be used. However, further research should be conducted in order to establish a method for assigning an effective width to a retrofitted bridge deck. Finally, the idea of using this retrofit technique for initial construction could be investigated further. It may be possible to construct cost-effective timber bridges using this technique. This possibility is important, especially in light of the shrinking budgets of many counties.

TABLE OF CONTENTS

Executive Summary
Acknowledgements
Table of Contents

Chapter 1,	FIELD TESTS	1
1.1	ORGANIZATION OF THE REPORT	2
1.2	ORIGINAL BRIDGE	2
1.2.1	Bridge Selection and Testing	2
1.2.2	Description of Instrumentation	3
1.2.3	Loading	3
1.2.4	Results of Static Load Tests	4
1.2.5	Results of Dynamic Load Tests	5
1.3	RETROFIT PROCEDURE	6
1.4	GROUTING PROCEDURE	7
1.4.1	Grout Mix	7
1.4.2	Grouting Procedure	7
1.5	TESTS ON RETROFIT BRIDGE	8
1.5.1	Results of the Static Load Cases	8
1.5.2	Results of the Dynamic Tests	9
1.6	SUMMARY OF RESULTS	10
1.6.1	Summary of Static Tests	10
1.6.2	Summary of Dynamic Tests	10
Chapter 2,	LABORATORY TESTS	11
2.1	INTRODUCTION	11
2.2	DESCRIPTION OF LABORATORY SPECIMENS	11
2.3	DESCRIPTION OF TEST SETUP	11
2.4	TESTING OF THE UNGROUTED SPECIMEN	11
2.4.1	Fatigue Tests	11
2.4.2	Monotonic Loading Tests	12
2.4.3	Discussion of Results	12
2.5	GROUTING THE LABORATORY SPECIMENS	13
2.5.1	Portland Cement Mix Specimen	13
2.5.2	Conbextra S Specimen	14

2.6	TESTING OF THE GROUTED SPECIMENS	14
2.6.1	Fatigue Tests	14
2.6.2	Monotonic Loading/Unloading Tests	15
2.6.3	Transverse Load Distributions	15
2.6.4	Discussion of Results: Grouted Specimens	15
2.7	SUMMARY OF LABORATORY RESULTS	16
Chapter 3,	ANALYTICAL STUDIES	17
3.1	INTRODUCTION	17
3.2	ANALYTICAL MODEL	17
3.3	MODEL ASSUMPTIONS	17
3.4	RESULTS AND DISCUSSION OF THE ANALYSIS	18
REFERENCES	18
APPENDIX A - CALCULATIONS FOR OLD BRIDGE	65

TABLES

Table 1 - Weight of trucks used for original bridge testing	19
Table 2 - Dynamic deflections for original bridge	19
Table 3 - Results of mortar mix cube tests	20
Table 4 - Weight of trucks used for retrofitted bridge testing	20
Table 5 - Dynamic deflections for retrofitted bridge	21
Table 6 - Stiffness of the ungrouted specimen	21
Table 7 - Stiffness from loading/unloading tests	22
Table 8 - Strength of the Conbextra grout	22
Table 9 - Strength of the Portland cement grout	22
Table 10 - Stiffness from fatigue tests (Conbextra S)	23
Table 11 - Stiffness from fatigue tests (Portland cement)	23
Table 12 - Stiffness from load/unload tests (Conbextra S)	24
Table 13 - Stiffness from load/unload tests (Portland cement)	24
Table 14 - Stiffness from load distribution tests (Conbextra, no deck)	25
Table 15 - Stiffness from load distribution tests (Portland, no deck)	25

FIGURES

Figure 1 - Elevation of the bridge (South view)	26
Figure 2 - View of the nail-laminated deck	26
Figure 3 - Location of transducers	27
Figure 4 - Geometry of loading axles	27
Figure 5 - Results of static test #1	28
Figure 6 - Results of static test #2	28
Figure 7 - Results of static test #3	29
Figure 8 - Results of static test #4	30
Figure 9 - Deflection profiles at midspan	31
Figure 10 - Deflection profiles at midspan	32
Figure 11 - Dynamic response at 6 mph	33
Figure 12 - Dynamic response at 20 mph	33
Figure 13 - Dynamic response at 40 mph	34
Figure 14 - Dynamic response at 60 mph	34
Figure 15 - Dynamic response at 40 mph	35
Figure 16 - Dynamic response at 60 mph	35
Figure 17 - Retrofit panels being installed	36
Figure 18. - Completed installation of the panels	36
Figure 19 - Cross-section of retrofitted bridge	37
Figure 20 - Elevation of retrofitted bridge	38
Figure 21 - Results of static test #1	39

FIGURES (Cont'd)

Figure 22 - Results of static test #2	39
Figure 23 - Results of static test #3	40
Figure 24 - Results of static test #4	40
Figure 25 - Deflection profiles at midspan for retrofitted bridge	41
Figure 26 - Deflection profiles at midspan for retrofitted bridge	42
Figure 27 - Dynamic response at 6 mph (retrofitted)	43
Figure 28 - Dynamic response at 20 mph (retrofitted)	43
Figure 29 - Dynamic response at 40 mph (retrofitted)	44
Figure 30 - Dynamic response at 60 mph. (retrofitted)	44
Figure 31 - Dimensions of laboratory specimen	45
Figure 32 - Plan view of laboratory specimen	46
Figure 33 - View of the testing frame	47
Figure 34 - Results of fatigue tests on ungrouted specimen	48
Figure 35 - Monotonic Test at 10 kips	48
Figure 36 - Monotonic Test at 20 kips	49
Figure 37 - Monotonic Test at 24 kips	49
Figure 38 - Monotonic Test at 28 kips	50
Figure 39 - Monotonic Test at 32 kips	50
Figure 40 - Monotonic Test at 36 kips	51
Figure 41 - Monotonic Test at 40 kips	51
Figure 42 - Monotonic Test at 41.6 kips	52

FIGURES (Cont'd)

Figure 43 - Results of pumping	53
Figure 44 - Initial load-deflection curve for the Conbextra test	54
Figure 45 - Initial load-deflection curve for Portland cement test	54
Figure 46 - Fatigue results for the Conbextra test (actuator)	55
Figure 47 - Fatigue results for the Conbextra test (external LVDT)	55
Figure 48 - Fatigue results for the Portland cement test (actuator)	56
Figure 49 - Fatigue results for the Portland cement test (external LVDT)	56
Figure 50 - Load-deflection curves for Conbextra S at 41.5 kips	57
Figure 51 - Load-deflection curves for Portland cement at 41.5 kips	57
Figure 52 - Strain gage layout	58
Figure 53 - Transverse load distribution (Conbextra at 10 kips)	59
Figure 54 - Transverse load distribution (Conbextra at 41.5 kips)	59
Figure 55 - Transverse load distribution (Portland cement at 10 kips)	60
Figure 56 - Transverse load distribution (Portland cement at 41.5 kips)	60
Figure 57 - Dimensions of laboratory model	61
Figure 58 - Nodal layout for finite element analysis	62
Figure 59 - Longitudinal deflections for analytical model (ungROUTED)	63
Figure 60 - Transverse deflections for analytical model (ungROUTED)	63
Figure 61 - Longitudinal deflections for analytical model (grouted)	64
Figure 62 - Transverse deflections for analytical model (grouted).	64

CHAPTER 1 - FIELD TESTS

Timber bridges have been used extensively throughout the state of Minnesota on county highways and roads. Many of the timber bridges in Minnesota are nail-laminated (nail-lam) bridges which were built in the 1950's and 1960's. Due to the age, the increase in traffic, and the increase in size of the traffic being driven across many of these bridges, there is a need to evaluate, strengthen, and widen many of these bridges. One issue which needs to be addressed is whether it is more cost-effective to replace or to retrofit the existing bridges.

The possibility of retrofitting timber bridges whose substructure and deck are in good shape is an appealing alternative to total replacement. If the existing substructure, such as the pilings, can be utilized, retrofitting the bridge may be less expensive to the county. Also, less traffic may be interrupted because traffic may continue to use the bridge while the retrofitting procedure is under way. This would eliminate the need for detours. It has been reported by Ken Johnson of Wheeler Consolidated, Inc., that retrofitting could be used to widen and strengthen some 1,372 timber bridges throughout the state of Minnesota.

Many existing wood bridges on secondary roads do not meet modern strength, serviceability, or safety standards. These bridges are generally short (less than 20 ft. simple spans), narrow (less than 24 ft. clear width), and were designed for HS15 or HS20 loadings. An economical strengthening and retrofitting scheme for this type of bridge is highly desirable since the counties and cities that own them do not have the financial resources to replace them.

This study examined a retrofitting scheme for older wood bridges on secondary roads proposed by Mr. Gene Isakson, the engineer for Sibley Co, MN. The scheme consists of:

- (a) removing the old bituminous layer,
- (b) laying down a series of pre-fabricated wood panels over the existing longitudinal timbers. These new panels cantilever 2 ft. on either side of the existing bridge in the transverse direction,
- (c) grouting the area between the old and new wood layers with a cementations mix,
- (d) adding a new bituminous surface.

This scheme is very economical because the panels are prefabricated, high skilled labor is not required, and the bridge is kept out of service for a minimum period of time. The scheme was used successfully in a retrofit in Sibley Co. in 1991, but a detailed study was needed to ascertain the performance of the retrofitted structure and to develop recommendations for widespread application.

In response to this need, and under the sponsorship of the Local Road Research Board, the Departments of Civil and Mineral Engineering and Forest Products at the University of Minnesota undertook an analytical and experimental study to provide this information. The study consisted of three main parts:

- (1) Testing of an existing bridge before and after the retrofit to ascertain differences in performance. For this task a three-span bridge on County Rd. 8 near Winthrop, MN was

selected. The bridge was tested statically and dynamically to determine the influence of the retrofit on the stiffness and load distribution on the bridge.

- (2) Laboratory testing of simulated portions of the retrofitted bridge to study the load distribution, stiffness, and fatigue characteristics of the bridge before and after the retrofit. For this task three large panels (18 ft. by 5.5 ft) were built and tested. One of the three specimens was ungrouted, while the other two were grouted with two different grouting mixes.
- (3) Finite element analysis of the laboratory specimens to model the behavior observed in the field and the laboratory. This task attempted to develop a theoretical solution to the problem in order to verify the reasonableness of the experimental data.

This report presents the results of the three tasks, and discusses the preliminary conclusions and further research needs.

1.1 ORGANIZATION OF THE REPORT

The organization of this report follows very closely the sequence of events that took place during this study. The study was divided into two experimental parts, one in the field and one in the laboratory, and one analytical part. Section 1 contains the description of the field tests. In Section 1.2 a description of the existing bridge selected for this study and its testing will be given. In Section 1.3 the retrofit scheme is detailed. In Section 1.4 the grouting problems and procedures are discussed. In Section 1.5 the testing of the retrofit bridge will be described, while in Section 1.6 the results of this phase are summarized.

Section 2 describes the laboratory tests, testing sequence, and results. Section 2.1 describes the specimens tested, Section 2.2 details the testing setup, and Section 2.3 describes the testing of the ungrouted specimens. Section 2.4 describes the grouting procedure in the laboratory, and Section 2.5 describes the tests of the grouted specimens. Section 2.6 contains a summary of the results.

Section 3 deals with the analytical studies. Sections 3.2 and 3.3 deal with the analytical model and its assumptions. Section 3.4 deals with the results and comparisons to the experimental data.

1.2 ORIGINAL BRIDGE

1.2.1 Bridge Selection and Testing

The bridge selected for the field studies is located on County Road 8, near Winthrop, Sibley Co., and was chosen because it was deemed representative of the type of bridge for which this retrofit scheme would be applicable and because it was already scheduled for renovation. The original bridge was a three span nail-laminated (or nail-lam) timber bridge. Figure 1 is an elevation view of the southern face of the bridge.

The nail-laminated bridge deck was 26 feet wide and 10 inches deep. The clear roadway was 24 feet. The center span is 16 feet center to center of the piers, and the two outer spans are 15.5 feet center to center of the piers. Longitudinal timbers are 10 x 3, 16 ft. long for the center span. At the center of each span, there are 6 x 12 inch transverse stiffener beams which are attached to the bottom of the nail-lam deck. Figure 2 shows the bottom of the nail-lam deck and the transverse

stiffener beam. All of the bridge members were treated with creosote. Some calculations, such as the live load deflection and the controlling ratings, of the original bridge are included in Appendix A.

1.2.2 Description of Instrumentation

In order to establish a baseline for use in comparing the effectiveness of the retrofit, the deflections of the original bridge under known loads were measured. The deflection of the center span was measured by attaching 4 linear variable differential transformers (LVDTs) to the bottom of the deck across the midspan. Each LVDT was calibrated before and after it is used in order to establish a direct correlation between voltage and displacement (i.e. 1.000 inch = 10.000 volts). The LVDT is infinitely accurate but the reading is limited to the accuracy of the data acquisition or displaying equipment. The digital voltmeters used to monitor the voltages during the static tests insured that deflections less than 0.001 in. could be resolved. The plotter used to monitor the deflections during the dynamic tests had similar capabilities, but of course the plots could only be read to a lower resolution (about 0.01 in.).

The LVDT's were placed at the midspan because the midspan is the most critical location for simply-supported members. Figure 3 shows a cross-section of the bridge with the precise placement of the LVDT's across the midspan. With this LVDT placement, an approximate transverse load distribution can be back-calculated from the deflections.

In order to attach the LVDT's, scaffolding was built across the center span about 5 feet below the bridge deck. Threaded rods were attached to the scaffolding and extended up to the bottom of the deck. Finger clamps attached onto the threaded rods held the LVDT's in position. In order to present the data the following designations will be used for the LVDT's. The LVDT on the edge of the North lane will be referred to as NL Edge. The LVDT located near the center of the North lane will be referred to as NL Center. The LVDT's located near the center of the roadway and near the center of the South lane will be referred to as RDWY Center and SL Center, respectively.

1.2.3 Loading

Sibley County provided two loaded trucks (#54 and #9103) for the field evaluations. These trucks were used because they represent an AASHTO HS-20 design load which is equivalent to the design load that was originally used. The truck weights and axle configuration are given in Table 1, while the dimensions are given in Fig. 4.

The field evaluation of the original bridge included 4 static load tests and 4 dynamic load tests. The static load tests involved the truck(s) stopping at given points along the bridge. With the truck(s) at each of these locations, the deflection at the midspan of the center span was recorded. The four static tests consisted of:

- (1) **STATIC TEST #1:** One pass of truck #54 from West to East in the North lane. The truck was referenced with respect to its front axle. In other words the front axle was placed at various points along the bridge, which included the center of the outer spans, the piers, and the quarter points of the center span.
- (2) **STATIC TEST #2:** One pass of truck #54 from West to East in the North lane. The truck in this test was referenced along the bridge with respect to its rear tandem. The deflection was

recorded when the rear tandem was centered over the midspan of each span.

- (3) **STATIC TEST #3:** One pass of truck #54 from East to West in the South lane recording the deflection when the rear tandem was centered over the midspan of each span.
- (4) **STATIC TEST #4:** One pass from West to East with truck #54 in the South lane and truck #9103 in the North lane (the trucks are side-by-side). The rear tandems were centered over the midspan of each span and the deflection was recorded.

The dynamic load tests involved the trucks being driven across the bridge at varying speeds. The NL Edge and RDWY Center LVDT's connected to an analog X-Y plotter in order to graph the bridge response as the trucks were driven across the bridge. Four separate passes were conducted at varying speeds with the trucks side-by-side going West to East. The passes were done at approximately 6 mph, 20 mph, 40 mph, and 60 mph.

1.2.4 Results of Static Load Tests

The results of the 4 static load tests are shown in Figures 5 through 8. In graphing the results, all 3 spans were assumed to be 16.0 feet center to center of the piers rather than the 16.0 foot center span and the 15.5 foot outer spans to simplify the labelling of the axes.

The results of the static load tests are plotted as single data points against the results of an elastic analysis of the bridge assuming a 40 in. wide influence width per line of tires. The curve shows the midspan deflection as the front axle (test #1) or rear axle (tests #2, #3, and #4) of the truck moves across the bridge, and can be thought of as an influence line for deflection. For example, in Fig. 5 the deflection begins to increase as the front axle of the truck gets to the second span (around 14.5 ft) and does not disappear until the back axle leaves that span (when the front axle is around 44 ft.). Because the rear axle is heavier than the front one, the larger deflections correspond to the rear axle near the midspan of the center span (about 36 ft.).

The elastic analysis, as noted before, is for the influence of a single line of tires and assumes a uniform deflection across the entire influence width. On the other hand, the experimental values plotted refer to specific points across that width and thus care should be exercised when interpreting this data. For example for static test #1 with the truck on the North lane (Fig. 5), the NL Edge sensor was placed almost immediately below one of the tire lines, the NL Center sensor was placed approximately halfway between the two lines of tires, the RDWY Center sensor was slightly outside one of the tire lines, and the SL was near the middle of the unloaded lane (see Fig. 3). Thus one would expect that the NL Edge sensor should be very close to the analytical value, while the NL Center should be slightly higher since it would feel the influence of two lines of tires and reflect some additional transverse bending. The RDWY Center sensor, on the other hand, was located about 30 in. from the line of tires, and thus should record much smaller deflection if the influence width of 20 in. on either side is assumed. The SL Center sensor, on the other hand, should see negligible deflections since it is well outside the influence width.

With these caveats in mind, the results shown by Figs. 5 through 8 are very reasonable. It should be remembered also that the analytical calculations are the result of an elastic analysis, and thus depend heavily on the assumed modulus of elasticity for the wood. In this case, E was assumed as 1800 ksi, a published value for this type of wood.

The maximum static midspan deflections are the most important part of the results. With one lane loaded, the maximum deflection is between 0.25 and 0.27 inches. With both lanes loaded the maximum deflection increases to just under 0.30 inches. The maximum deflection from the elastic analysis is approximately 0.34 inches.

The transverse load distribution can be investigated by looking at the relative magnitude of each deflection (LVDT) when the truck was at any given position along the bridge. Fig. 9 shows the deflection of each LVDT when the front axle is at 8 and 24 feet for Static Test #2 (single truck). Similar distributions for Static Test #4 (two trucks) are shown in Figure 10. From these and similar figures plotted at other locations of the trucks one can conclude that the transverse load distribution is not very good as the loads increase. One reason may be that at low loads there is a contribution from friction between the individual nail-lam members to help transversely distribute the load. As the load increases, the friction contribution decreases and, thus, the load is not distributed as well.

1.2.5 Results of Dynamic Load Tests

The dynamic responses for the NL Center and RDWY Center sensors with the two trucks side by side at speeds of 6 mph, 20 mph, 40 mph, and 60 mph are shown in Figures 11 through 14. Table 2 shows the peak maximum deflection of the front and rear axle for each pass.

These results lead to the following observations about the dynamic load tests:

- (1) The magnitude of the maximum dynamic deflections are similar to the maximum static deflections.
- (2) The maximum deflections occur at approximately 40 mph.
- (3) There is significant vibration after the truck leaves the bridge at 40 mph and especially at 60 mph.
- (4) The magnitude of the vibration (passes at 40 and 60 mph) may be due to the approach of the bridge because there was a small dip in the roadway just before the bridge. The dip before the bridge may cause the trucks to, in effect, bounce across the bridge at higher speeds (i.e. 40 and 60 mph).
- (5) The period of the free vibration due to the trucks can be determined from the graphs of the dynamic response. This free vibration has a natural period, T , of approximately 0.06 seconds. A dynamic analysis was done to obtain an estimate of the theoretical natural period of the bridge. A simply-supported member was assumed for the analysis. The experimental natural period from the dynamic responses correlates well with the theoretical natural period.
- (6) It is evident from Figures 13 and 14 that there is less damping than one would expect for a wood structure. The free vibration continues for 1.0 to 1.5 seconds after the trucks have passed over the bridge. The length of this vibration is significant when compared to the actual time of the response, which is roughly 0.625 to 0.875 seconds.

Figs. 15 and 16 show how the dynamic deflections of the NL Center and RDWY Center LVDT's varied with the speed of the trucks. The deflections graphed are the peak deflection values

associated with the rear tandem. In Fig. 16, the graph shows that at 40 mph the maximum dynamic deflection of the RDWY Center LVDT is greater than the maximum static deflection of 0.29 inches for the Static Test #4 (trucks side-by-side). In Figure 15, the NL Center LVDT does not exhibit this behavior. Its maximum dynamic deflection seems to be less than the maximum static deflection at all speeds.

1.3 RETROFIT PROCEDURE

The timber deck retrofit procedure examined in this study is fast, economical and simple. The procedure consists of the following steps:

- (1) Removal of the existing bituminous surface and rail posts, exposing the existing nail-lam deck. The full existing 26 ft. deck was cleaned and prepared for the installation of the transverse panels.
- (2) Placement of the retrofit panels. The panels were delivered to the site ready to be installed. They were pre-fabricated by Wheeler Consolidated, Inc. The panels were 4 ft. wide, 30 ft. long, 4 inches thick and contained pre-drilled grout holes spaced 3 feet on center in both directions. The placement proceeded as follows:
 - (a) First, a 2 inch wide x 1/2 inch thick styrofoam strip nailed to the edges of the existing deck. This was done to help contain the grout during the grouting procedure.
 - (b) Second, an interior 4 foot wide retrofit panel was placed 4 feet in from the West end of the existing bridge deck. The interior portion of the retrofit panels were fastened to the existing deck with 5/8 inch diameter x 11-1/2 inch dome head drive spikes, and 1 foot from the deck edges the retrofit deck panels were fastened with 5/8 inch diameter x 16 inch dome head bolts. Figure 17 shows some of the fastened retrofit panels and the existing nail-lam deck. Also shown in the figure are the styrofoam strips nailed to the edges of the existing deck. All the other interior panels were then installed in a similar manner. The panels were placed by a front-end loader equipped with a fork extension.
 - (c) Third, the end panels are placed. The two end panels were 6 feet wide and extended 2 feet beyond the existing deck.
 - (d) Fourth, after the end panels were fastened, the rail posts were attached. Figure 18 shows the completed structure.
 - (e) Fifth, the space between the old and new layers was grouted. This procedure is discussed in detail in the next section (Section 1.4).
 - (e) Finally, the approaches were paved so that the bridge could be opened to traffic before the grout was pumped.

The retrofit deck panel placement procedure took about a day. The panels can be installed easily because they are prefabricated and there is very little field construction associated with placing them.

1.4 GROUTING PROCEDURE

The voids between the two decks needed to be filled in order to prevent compression of the voids between the two wood layers. If the voids are not filled large vertical movements will result because of the compressibility of this space. This will lead to both problems with adherence between the bituminous and wood layers and cracking of the bituminous surface when the surface becomes brittle due to age and/or cold weather. This may adversely affect the serviceability life of the bituminous surface.

1.4.1 Grout Mix

Because the grout was an integral part of the retrofit scheme, initially an attempt was made at using a commercially available, pre-mixed, non-shrink, high strength grout. The idea was that while the cost would be significantly higher, this would minimize the quality control problems in the field. A grout called Conbextra S, consisting of portland cement, silica sands, and expansive agents, was selected. The initial attempt to grout the bridge was made using a mix of 5-1/4 quarts of water per 1 - 55 lb. bag. The 5-1/4 quarts of water per 1 - 55 lb bag would, according to the specifications, yield a 28 day strength of 8000 psi (based on ASTM C-109, 2 inch mortar cubes). This grout did not pump very well because the mix was not very workable and tended to clog up the parts of the equipment (the hose, the hose nozzle, and the outlet leading from the pump to the hose). In fact, only 2 or 3 grout holes were pumped before the pumping equipment jammed and the procedure had to be abandoned.

The Conbextra S did not work well because the original mix appeared too stiff and set quickly. Following the field experience, however, several different mixes were made in the laboratory using the Conbextra S, and it appeared that unless the grout was mixed very thoroughly, the sand tended to settle out causing narrow openings to clog up and making pumping nearly impossible. At this point, the consensus was that the Conbextra S and similar products would not be used on the next attempt.

A new grout was developed by the grouting contractor in order to avoid the workability problems encountered with the Conbextra S. This grout consisted of Type I portland cement, silica sand, water, and an admixture called Acryl 60. Acryl 60 is used to increase the bond strength of cement mixes and, thus, generally increases the compressive strength. The mix proportions by volume for the cement: silica sand: liquid mix were 8 : 8 : 5, with the liquid part made up of a 4:1 combination of water to Acryl 60.

1.4.2 Grouting Procedure

The following equipment was used to grout the bridge: a hose, long enough to reach across the bridge and fitted with a steel pipe with a diameter less than 1-1/4 inches (nozzle), and a mixer/pump. The supplies were delivered on a flatbed trailer. The mixer/pump was placed next to the trailer for efficiency and ease. A tank of water was also needed.

Starting on one end of the bridge, the grout was pumped hole by hole. The pipe end was inserted into the hole forcing the grout between the existing and retrofit decks. Pumping into a hole was stopped when there was some indication that the grout was not being pumped between the decks any further. This process continued until the entire deck was completely grouted.

During the grouting, 5 sets of 2 inch mortar cubes were taken in order to test the compressive strength of the grout. The samples were taken from different batches of grout. Four sets (of 2 cubes) of mortar cubes were left at the site to represent the field conditions. One set was taken back to the lab to be tested in accordance with ASTM C-109. Care was taken not to disturb the sample while transporting it to the lab, although there is no guarantee that the sample was not disturbed (i.e. vibration). The field samples were tested at roughly 7 days and 28 days, and the sample transported to the lab was tested at 28 days. Picking up the field samples and testing them on the same day was not always possible, but they were generally tested within 24 hours of the testing date. The results of the compression tests are shown in Table 3.

The 28 day field strength may not be very accurate. Due to vandalism, the cubes were found in the creek below the bridge. Since they were wet continuously, their strength is probably higher than that on the deck. Thus, these values should be used only as a rough estimate.

It was difficult to determine how effectively the voids between the decks were being filled. A heavy object (sledge hammer) was dropped, at between 2 and 3 foot intervals, on an area of the bridge deck which had been grouted. If the area sounded hollow, it was marked. A hole was then drilled, and the area was grouted again. In certain areas it was possible to visually determine if the grout was distributed well. In such areas the grout came up in the gaps between the individual members making up a retrofit panel, or grout started to come up through an adjacent grout hole. Another sign of good grout distribution found in the end panels was that small gaps opened between the end retrofit panel and the newly paved approach.

After the bridge was entirely grouted, it was closed to traffic for approximately one week before the first bituminous layer was put down and the bridge was opened to traffic. This gave the mortar ample time to cure and reach its intended strength. For future applications this interval can be shortened substantially once the strength gain curve for the mix used is ascertained. The second and final bituminous layer was put down one week later. The second layer of bituminous was put down so long after the first layer due to scheduling problems rather than problems associated with the retrofit procedure.

1.5 TESTS ON RETROFIT BRIDGE

The retrofit panels extended the existing 26 foot wide bridge deck by 2 feet on each side or a total of 4 feet. The new clear roadway is 28 feet +/- inches. This widens each lane by 2 feet, from 12 feet to 14 feet. Figure 19 is a cross-section through the new bridge deck, and Figure 20 is an elevation of the retrofitted bridge.

The evaluation procedure and tests for the retrofitted bridge were the same as the procedure and tests for the original bridge. Sibley County again provided two loaded trucks, #54 and #9103, for the field evaluation. They were the same two trucks used in the original bridge evaluation. The weights of the trucks are listed in Table 4. The weights are similar to the weights for the evaluation of the original bridge.

1.5.1 Results of the Static Load Cases

The results of the 4 static load tests are shown in Figures 21 through 24. For this case the choice of an EI for the analysis was not straight forward since the additional 4 in. of transverse plank cannot

be assumed to be working longitudinally. Therefore it was decided to backfigure an EI from the static tests. An EI value of 7,200,000 kin^2 was selected to fit the field data points. The modulus of elasticity, E, was taken as 1800 ksi as for the original bridge, resulting in an effective width, b, equal to 48 inches for the 10 in. deck.

When one lane was loaded the maximum static deflection was 0.20 inches. It is clear that the static deflections of the retrofitted bridge are significantly less than the static deflections of the original bridge. This decrease in deflection ranges between 26 and 29 percent. There is also a reduction in the maximum deflection when both lanes are loaded of roughly 16 percent. This is important because the design of timber bridges, in general, is limited by serviceability (i.e. deflection) rather than strength.

Insofar as transverse load distribution, it was hoped that the transverse load distribution would be improved considerably with the retrofit deck. Figures 25 and 26 show the deflection profile across the midspan at given points along the bridge for Static Tests #2 (single lane loaded) and #4 (both lanes loaded). Comparing these figures, it is evident that the transverse load distribution has been improved, especially at high loads (i.e. large deflections). This is easily seen if the relative deflection of two adjacent LVDT's are examined. For example, in Figures 25 and 26 the relative deflections of the SL Center and RDWY Center LVDT are closer in magnitude than in Figure 9 and 10. This suggests that the load is being distributed over a larger deck area with the retrofitted bridge deck than with the original nail-lam bridge deck. The improvement in the transverse load distribution at high loads may be due to the fact that the transverse direction is parallel to the grain for the retrofit deck. The retrofit deck is helping to transversely distribute the load so that the load is not only distributed by the dowels.

1.5.2 Results of the Dynamic Tests

The dynamic response of each pass is shown in Figures 27 through 30. Table 5 shows the peak maximum deflections for each pass. In some cases the peak deflections, particularly those of the front axles, were not evident. Below are a few comments about the dynamic response of the retrofitted bridge:

- (1) The maximum dynamic deflections have been reduced between 15 and 22 percent in comparison to the deflections in the evaluation of the original bridge.
- (2) There is some, but very little, vibration of the bridge as the trucks left the bridge, even at 40 or 60 mph.
- (3) The maximum deflections occur at approximately 6 mph rather than at 40 mph for the original bridge.

The magnitude of the free vibration after the trucks have left the bridge was very small. This is probably due to the fact that the approaches for the retrofitted bridge were much smoother than the approaches for the original bridge, and the trucks did not "bounce" across the bridge.

With the retrofit deck, the natural period of the bridge changed, but given the low levels of free vibration, it was not possible to determine this change accurately. Using the same EI value chosen for the elastic analysis used in the static tests, a dynamic analysis was done in order to obtain an estimate of the natural period. The calculated theoretical natural period was approximately .057

seconds. Thus the theoretical natural period of the retrofitted bridge (0.057 sec.) changes from that of the original bridge (0.06 sec.). This seems to be due to the fact that the change in the mass of the bridge due to the retrofit panels is roughly twice the change in the EI value of the bridge.

1.6 SUMMARY OF RESULTS

1.6.1 Summary of Static Tests

The following conclusions were reached from the static load tests:

- (1) The deflections were significantly reduced with the retrofit deck especially when one lane was loaded. This reduction ranged between 26 and 29 percent. With both lanes loaded the reduction in deflection was smaller, approximately 16 percent.
- (2) There was an improvement in the transverse load distribution in the retrofitted bridge, particularly at high loads. The original bridge could not count on friction between the members to contribute in distributing the load at high loads. The retrofit deck, because of its transverse orientation to the original deck, helped to distribute the load across the original bridge deck.
- (3) The elastic analysis of the bridge, using the effective width, compares well with the results of the static tests for both the original and retrofitted bridge. In both cases, the elastic analysis gives an upper limit for the actual deflections.

1.6.2 Summary of Dynamic Tests

The following conclusions were reached from the dynamic load tests:

- (1) The theoretical natural period of the bridge did change with the addition of the retrofit deck. The new bridge had a natural period of approximately 0.057 seconds versus 0.06 seconds for the original one. On the other hand, the results of the field test showing the speed versus the maximum peak deflection seem to suggest that the natural period of the bridge did change.
- (2) The peak dynamic deflections were reduced with the retrofit deck by about 15 to 22 percent.
- (3) The speed when the maximum deflections occur has changed with the retrofit deck. The maximum deflections with the retrofit deck occur at approximately 6 mph rather than 40 mph.

CHAPTER 2 - LABORATORY TESTS

2.1 INTRODUCTION

In addition to the field evaluations of the original and retrofitted bridge, the behavior of three laboratory specimens was investigated. The lab specimens were built to represent a section of the retrofitted bridge deck, and one ungrouted and two grouted lab specimens were tested. For the two grouted specimens, one was grouted with the Conbextra S grout and the other specimen was grouted with the Portland cement grout. The specimen grouted with the Conbextra S grout will be referred to as the Conbextra S Specimen. The specimen grouted with the grout mix used in the field will be referred to as the Portland Cement Mix specimen.

Fatigue, monotonic loading/unloading, and transverse load distribution tests were conducted on the three specimens, with the exception of the transverse load distribution test which was not done on the ungrouted specimen.

2.2 DESCRIPTION OF LABORATORY SPECIMENS

The lab specimens were built by Wheeler Consolidated, Inc. and delivered to the lab pre-assembled. The specimens represented the retrofitted nail-lam bridge deck. The original deck and the retrofit deck were 10 inches deep and 4 inches deep, respectively. The specimens were 65 inches wide by 18 feet long. The retrofit deck was fastened to the existing nail-lam deck by 5/8 inch diameter x 1 1/2 inch dome head drive spikes. There were 2 rows of 10 spikes, 3 feet center to center. Also, there were 2 rows of 1-1/4 inch diameter holes which were pre-drilled in the retrofit deck for grouting. There were 5 grout holes in each row, and they were also 3 feet center to center. The specimens were not treated with creosote. Figures 31 and 32 show schematics of the specimens.

2.3 DESCRIPTION OF LABORATORY SETUP

The load frame is shown in Figure 33. The specimens were placed on simple supports, 17 feet apart. A 40 kip MTS actuator provided the load. A 10 x 20 inch spreader beam was attached to the actuator to model the contact area of a truck tire. The load and deflection of the actuator were monitored by the MTS system which was calibrated before any of the tests were conducted.

2.4 TESTING OF THE UNGROUTED SPECIMEN

An ungrouted specimen was tested to compare the results of the ungrouted and grouted specimens in order to examine the effect of the grouting. The ungrouted specimen consisted basically of the testing of one of the panels as delivered to the laboratory.

2.4.1 Fatigue Tests

First, an initial load-deflection curve was established (Figure 34). The deflection was recorded by the actuator which monitored the deflection at the top of the specimen. The specimen was loaded up to a deflection of $L/400$ (where L is the distance between the supports), which corresponds to a deflection of 0.51 inches.

Next, load-deflection curves were determined for the following cycles:

- (1) 1,000 cycles
- (2) 10,000 cycles
- (3) 100,000 cycles
- (4) 1,000,000 cycles

The specimen was cycled at 2 Hertz (cycles/second), in compression, between 2 and 12 kips. A sine wave was the driving function. It was cycled between 2 and 12 kips to account for the fact that the deck is always in compression due to the railings and roadway surface. The load-deflection curve was conducted after each set of cycling. The results of the fatigue tests, in the form of load-deflection curves, are shown in Figure 34.

2.4.2 Monotonic Loading Tests

After the fatigue tests were completed, the specimens were loaded and unloaded monotonically up to a load of approximately 41 kips. This was the maximum load that the equipment would achieve. The specimen was first loaded up to 10 kips, followed by 20 kips. The load was then increased by intervals of 4 kips thereafter, to a maximum of approximately 41 kips. For this test, the deflection was also recorded at the bottom of the specimen by a LVDT in addition to the deflection recorded by the actuator. The LVDT was placed directly under the application of the load (i.e. the actuator). The results are shown in Figures 35 through 42.

2.4.3 Discussion of Results

The results of the fatigue tests, shown in Figure 34, show that the cycling had very little effect on the specimen. Table 6 shows the stiffness, rounded to the nearest 1/2 kip/inch, at each cycling stage.

The most striking feature of the results of the monotonic load/unload tests, shown in Figures 35 through 42, is the difference between the actuator and the LVDT load-deflection curves. At any given load, the actuator showed a larger deflection than the LVDT. This may be due to the fact that the deflection recorded by the actuator may include the closing of the gaps between individual members and/or the closing of the gaps between the retrofit and existing decks. The LVDT recorded the deflection at the bottom of the specimen. Thus the deflection recorded by the LVDT was smaller than the deflection recorded by the actuator.

The difference in deflection between the actuator and the LVDT is also shown in Table 7 which shows the stiffness calculated from the results of the monotonic load/unload tests. The deflection of the LVDT indicates a much stiffer specimen than the deflection of the actuator. If a LVDT had been attached for the initial load-deflection curve, the LVDT curve would also have shown a much stiffer specimen. The stiffness calculated from the deflection of the actuator in the monotonic load/unload tests correspond well with the results from the fatigue tests shown on Table 6.

Figures 35 through 42 show that the specimen is still in the elastic range at the maximum load of 41.5 kips. It was hoped that enough load could be applied to reach the inelastic range of the load-deflection curve, but with the equipment available, that was not possible. It should be noted that the maximum of 41 kips is more than double the AASHTO HS-20 Design Load of 32 kips per axle

which corresponds to 16 kips per tire. This shows that the specimens were controlled by deflection rather than strength, which is generally true for timber bridges.

The results of the monotonic load/unload tests also show the elastic delay behavior of wood. As the specimen was unloaded, it did not follow the load path although it was in the elastic range. In addition, immediately after the load was removed, there was some residual deflection recorded. This deflection was recovered after a short time.

2.5 GROUTING THE LABORATORY SPECIMENS

The laboratory specimens sat in the laboratory floor for about 30 days before the grouting and testing began. It seemed that the laboratory specimens shrank significantly during this time. This was probably due to the fact that the specimens dried from about a 18%-20% moisture content to about 8%. As the specimens shrank, the small gaps which existed between the individual members and decks expanded. At the time the specimens were grouted some of the gaps were as large as 1 inch.

In order to prevent the grout from leaking out, 1 inch diameter ethafoam was inserted into the gaps. Ethafoam is a filler used in expansion joints. After it was inserted, 1 x 6 inch or 1 x 5-1/2 inch plywood was nailed over the gaps to keep the ethafoam from being pushed out by the grout as it was being pumped.

The next step was the actual grouting of the specimens. A rotating drum mixer was used to mix the grout. An air compressor pump including the pump hose was rented. The grout was mixed in the rotating drum and poured into the funnel on the grout pump. The rotating drum mixer was used because it mixed the grout more thoroughly than the blade mixer on the grout pump.

2.5.1 Portland Cement Mix Specimen

The specimen grouted with the mix used in the field was grouted first because it was known to be easier to grout from the field experience. The proportions used to grout the actual bridge were used in the lab. As was done for the field tests, mortar cubes were made to determine the compressive strength of the mix. The grouting of this specimen went well. No major problems were encountered. When the grout was coming out of the edges of the specimen or up through the retrofit deck, a new hole was pumped.

After about one week, the plywood and ethafoam were removed. By visually inspecting the edges of the specimen where the ethafoam was inserted in the gaps, the effectiveness of the grouting was examined. It appeared that the grout had filled the voids between the decks fairly well. Also, as the grout was pumped, the retrofit panels where the grout holes were located were pushed up. This could actually be seen as the grout was pumped between the decks.

The same method of listening to the difference in the sound when a heavy object was dropped on the retrofit deck to determine whether any voids were present, was used on the grouted specimen. It appeared that the grout filled the voids between the decks very well. After the specimen was tested, the retrofit panels were removed, exposing the grout. Figure 43(a) shows the actual grout distribution. Overall, this grout worked well. It was easy to work with and easy to pump. Also, the grout filled the voids between the decks fairly well.

2.5.2 Conbextra S Specimen

After the Portland Cement Mix specimen was grouted, the equipment was cleaned, and the next specimen was grouted with the Conbextra S grout. From prior trial mixes done in the lab, it was determined that a workable mix was 5-2/3 quarts of water per 1 - 55 lb. bag of Conbextra S. Again, during the grouting, mortar cubes were made to determine the compressive strength of the mix.

The grouting of this specimen was very difficult. Even with the large amount of water, this mix was difficult to pump. It tended to clog up the equipment just as it had when the Conbextra S was attempted in the field. Also, it was difficult to determine if any of the grout was filling the voids. There was no indication of the grouting filling the voids such as the grout leaking out of the edges or coming up through the retrofit deck.

After the ethafoam and plywood were removed, the specimen was visually inspected. In some areas the grout was pumped to the edges, but the grout did not reach the edge of the specimen on the majority of the specimen. Also, there were no visible signs that the grout came up through the retrofit deck. Again, the method of dropping a heavy object and listening for a hollow sound to find the areas where the voids were not filled with grout was used in order to see how effective the grouting was. It appeared that the grouting was not very effective because the majority of the specimen seems to have some degree of voids between the decks. When the retrofit deck panels were taken off, the actual grout distribution was visible (Fig. 43(b)). In general, the grout did not spread out very much and the effectiveness, in this case, may not be very good.

Overall, the Conbextra S mix did not work very well. During the pumping, the grout tended to clog the equipment such as the hose and steel pipe connected to the hose. Also, the grout apparently was not very effective in filling the voids.

2.6 TESTING OF THE GROUTED SPECIMENS

The testing of the Conbextra S specimen started 9 days after it had been grouted. Table 8 includes the ASTM compressive strength of the trial mixes done prior to grouting, as well as the strength of the actual mixes at the start of testing. The Portland Cement specimen was tested after the testing of the Conbextra S specimen was completed, which was approximately 28 days after it had been grouted. Table 9 gives the relevant material data for this test. These strength values are only rough estimates because of the few number of cubes tested.

2.6.1 Fatigue Tests

The grouted specimens were subjected to a series of tests similar to those of the ungrouted one. First, a load-deflection curve was established for each specimen (see Figures 44 and 45). A LVDT was placed at the bottom of the specimens directly under the point of load application. For the fatigue tests on the grouted specimens, the specimens were cycled, in compression, between 2 and 16 kips. The 16 kips corresponds to the AASHTO HS-20 Design Load of 32 kips per axle, thus, 16 kips per tire. The specimens were cycled at 2 Hertz (cycles/second), and the driving function was a sine wave.

A load-deflection curve was obtained for each test. The results are in Figures 46 through 49. There are separate plots corresponding to the actuator and LVDT load-deflection curves.

2.6.2 Monotonic Loading/Unloading Tests

The specimens were loaded and unloaded up to a maximum of approximately 41 kips similar to the ungrouted specimens. The results for the last set of tests are shown in Figures 50 and 51. Tests at other levels showed similar behavior.

2.6.3 Transverse Load Distributions

The transverse load distribution is one of the most important aspects of the project. The retrofitted bridge should have significantly better transverse load distribution than the original nail-lam bridge.

In order to investigate the transverse load distribution on the lab specimens, strain gages (Bridge Weighing Systems) were attached to the bottom of the specimen across the midspan. Figure 52 is a drawing of the strain gage layout across the midspan of the specimen. Six strain gages were attached to the bottom of the specimen. They were placed at the center of each laminate (individual member) and attached with lag screws. The strain was recorded at varying levels of load. The load levels used were exactly the same as those used in the monotonic load/unload test.

First, the transverse load distribution tests were conducted on the grouted retrofitted specimen. Then, the retrofit panels were removed, the grout was chipped off the existing deck, and the specimen was tested again at the same load levels. This was done in order to get a comparison of the transverse load distribution with and without the retrofit deck. The results of the tests for 10, and 41.6 kips of the Conbextra S specimen are in Figures 53 and 54. The results of the tests of the Portland Cement Mix specimen are in Figures 55 and 56.

2.6.4 Discussion of Results: Grouted Specimens

The results of the fatigue tests (Figs. 48 and 49) show that the cycling had very little effect on the specimens. This is especially true looking at the LVDT load-deflection curves. Tables 10 and 11 show the stiffness, rounded to the nearest kip/inch, at each cycling stage. The tables also point out the fact that the cycling had no effect on the specimens. They also show the significant difference between the actuator and LVDT deflection.

The results of the monotonic load/unload tests are shown in Figures 50 and 51. Tables 12 and 13 show the stiffness from the monotonic load/unload tests. The stiffnesses from the fatigue tests match well with the stiffnesses from the monotonic load/unload tests, strengthening the conclusion that the fatigue loads had a negligible effect on the specimen strength.

Comparing the stiffnesses of the ungrouted specimen with the stiffnesses of the grouted specimens, one can note a significant increase in stiffness for the grouted specimens. Even the Conbextra S specimen which did not appear to be effectively grouted was significantly stiffer than the ungrouted specimen. The results of the monotonic load/unload tests also show that the load-deflection curve remains in the elastic range. The load-deflection curves remain linear up to the maximum load of approximately 41 kips.

The transverse load distribution test results indicate that the transverse load distribution was significantly improved with the addition of the retrofit deck. The maximum peak strain was reduced and the strain at the edges of the specimens was increased, creating a much more distributed strain

profile.

Tables 14 and 15 show the stiffness of the specimens when the retrofit panels are removed. It is quite evident that the stiffness of the specimens have been greatly improved with the retrofit deck. In very general terms, the stiffness has gone from approximately 29 kips/inch to approximately 44 kips/inch.

2.7 SUMMARY OF LABORATORY RESULTS

The following are the major conclusions from the laboratory tests:

- (1) The retrofit decks were not affected by the cycling in the fatigue tests.
- (2) The stiffness of the grouted specimens was significantly greater than the stiffness of the ungrouted specimen.
- (3) At the maximum load of 41 kips, the load-deflection curves for all three specimens remained in the elastic range. The maximum load of 41 kips achieved by the equipment was more than double the design load of 16 kips for one tire.
- (4) The load distribution with the retrofit deck on is much better than the existing nail-lam deck alone.

CHAPTER 3 - ANALYTICAL STUDIES

3.1 INTRODUCTION

An analytical study of the laboratory specimens was conducted in an attempt to model the retrofitted bridge deck by correlating the laboratory results with the analytical predictions. A three dimensional, non-linear finite element analysis was done.

In order to do the analytical analysis, an in-house finite element program was used. This program provided a better model of both the mechanistic and material properties of the wood elements used. This section describes some of the assumptions used in the model, compares the results of these assumptions, and compares the results to some of the laboratory results.

3.2 ANALYTICAL MODEL

An 8 node isoparametric plate element was used. Only a quarter of the lab specimen was needed to do the analysis due to symmetry. Figure 57 shows the dimensions of the specimen used in the analysis. The length was 17 feet, the clear distance between supports, and the width was assumed to be 5.5 feet (or 66 inches). Figure 57 also shows the x,y, and z directions which correspond to the longitudinal, transverse, and deflection directions, respectively. Figure 58 shows the mesh layout of the bottom-left quarter of the specimen. The load, P, from the actuator was assumed to be uniformly distributed to the specimen by the 10 x 20 inch spreader beam.

3.3 MODEL ASSUMPTIONS

The specimen was made of Douglas Fir which has a modulus of elasticity in the longitudinal direction, E_x , of 1800 ksi. A value of 73% of 1800 ksi was also considered because it has been shown to yield good analytical results. This value of E_x has been suggested by Oliva [Oliva, 1988]. For the analysis, the 2 cases considered were (1) $E_x = 1800$ ksi, and (2) $E_x = 73\%$ of 1800 ksi or 1314 ksi.

The members making up both the nail-laminated and retrofit deck in the real bridge are fastened together by nails. The individual wood members of the original and retrofit deck are not necessarily in perfect contact. This was particularly true for the lab specimens which had gaps between some of the individual wood members due to shrinkage. The following 2 cases were considered in the analysis:

- (1) Perfect contact between the individual members. For this case both the friction and the dowels transfer the load between the members.
- (2) Imperfect contact (or gaps) between the individual members. For this case only the nails transfer the load between the members. There is no friction contribution because of the gaps between the members.

In order to model the grout between the original and retrofit decks the following assumptions were made:

- (1) The original and retrofit deck are firmly grouted together.

- (2) There is no relative displacement between the surface and the bottom of this, now, composite plate.
- (3) There are no gaps in the bottom layer. The gaps will be filled with grout, but since the bottom deck is in tension the grout in the gaps can be neglected.
- (4) The modulus of elasticity in the longitudinal direction of each deck is equal to 73% of 1800 ksi.
- (5) The bottom and top layers are modelled as two different plates. They act compositely by the definition of the boundary conditions.

Assumptions (1) and (2) state that when the specimen deforms the original and retrofit deck are firmly connected and, thus, no slip will occur. This assumption is reasonable because under the service loads applied the friction force between the two decks should prevent any slip.

3.4 RESULTS AND DISCUSSION OF THE ANALYSIS

The results presented in this section are based on comparisons with an actuator load of 14.1 kips. This load was assumed to be uniformly distributed on the specimen by the 10 x 20 inch spreader beam (Area = 200 sq. in.). Figures 59 and 60 show the results of the ungrouted model. Figure 59 shows the longitudinal deflection along the centerline of the specimen. Figure 60 shows the transverse deflection across the midspan of the specimen. The deflection of 0.37 inches from the lab tests on the ungrouted specimen is also plotted in both figures.

The curves in Figs. 59 and 60 show that the modulus of elasticity assumption has a significant affect on the results. On the other hand, the contact assumption does not affect the results very much. Comparing the deflection of the ungrouted specimen (LVDT deflection) to the analysis, using a value of 73% of the modulus of elasticity yields very good results.

Figures 61 and 62 show the results of the grouted model. The figures again show the longitudinal and transverse deflection. Also, plotted on the figures are the deflections of Portland Cement Mix specimen and the Conbextra S specimen which are 0.30 and 0.31 inches, respectively.

The results of the grouted model clearly show the uncertainty in modelling the grouted specimen. The results for this model do not match as well with the lab results as the ungrouted model. It should be noted that the results of the grouted model are conservative and, thus, could be used as a tool for estimating the deflection on the grouted bridge deck.

REFERENCES

- [1] Oliva, M.G., and Dimakis, A., Behavior of Stress-Laminated Timber Highway Bridges, Journal of Structural Engineering, ASCE, Vol. 114, No.8, August 1988, pp. 1850-1869

	Weight (lbs)	
	Rear Tandem	Total
Truck #54	32,420	47,260
Truck #9103	32,740	47,880

Table 1 - Weight of trucks used for original bridge testing.

	axle	LVDT Deflection (inches)	
		RDWY Center	NL Center
6 mph	front	0.114	0.125
	rear	0.231	0.250
20 mph	front	0.137	0.127
	rear	0.247	0.247
40 mph	front	(*)	(*)
	rear	0.292	0.265
60 mph	front	0.077	0.078
	rear	0.217	0.203

(*) peak reading could not be clearly determined

Table 2 - Dynamic deflections for original bridge.

Type of Specimen/Age		Compressive Strength (psi)
Field	7 days	5400
	28 days	9700
ASTM C-109	28 days	6800

Table 3 - Results of mortar mix cube tests.

	Weight (lbs)	
	Rear Tandem	Total
Truck #54	32,180	47,360
Truck #9103	32,960	48,020

Table 4 - Weight of trucks used for retrofitted bridge testing.

	axle	LVDT Deflection (inches)	
		RDWY Center	NL Center
6 mph	front	0.130	0.095
	rear	0.249	0.209
20 mph	front	0.109	0.080
	rear	0.199	0.175
40 mph	front	(*)	(*)
	rear	0.174	0.168
60 mph	front	(*)	(*)
	rear	0.127	0.109

(*) peak reading cannot be clearly detected

Table 5 - Dynamic deflections for retrofitted bridge.

Number of Cycles	Stiffness (kips/in)
1	29.0
1000	30.0
10000	30.5
100000	31.0
1000000	31.0

Table 6 - Stiffness of the ungrouted specimen.

Load (kips)	Actuator LVDT Stiffness (kips/in)	External LVDT Stiffness (kips/in)
10	31	37
20	31.5	39
24	32.	39.5
28	32.	40.
32	32.	39.
36	32.5	38.5
40	32.	38.
41.6	31.	38.
Average	31.75	38.63

Table 7 - Stiffnesses for the Conbextra S specimen

Water (qts.)	ASTM C-109 (psi)	9 day (psi)
5.25	7700	(*)
5.66	6500	6100
7.0	5200	(*0

(*) no mortar cubes tested

Table 8 - Compressive strength of the Conbextra grout

ASTM C-109 (psi)	Laboratory Mix (psi)
6800	5300

Table 9 - Strength of the portland cement grout (28 days).

Number of Cycles	Actuator LVDT Stiffness (kips/in)	External LVDT Stiffness (kips/in)
1	29.	42.
1000	32.	44.
10000	31.5	44.
100000	31.5	44.
1000000	32.	44.

Table 10 - Stiffness from fatigue tests (Conbrextra s).

Number of Cycles	Actuator LVDT Stiffness (kips/in)	External LVDT Stiffness (kips/in)
1	29.5	41.5
1000	35.5	44.5
10000	36.	44.5
100000	35.5	45.5
1000000	36.	48.

Table 11 - Stiffness from fatigue tests (Portland cement).

Load (kips)	Actuator LVDT Stiffness (kips/in)	External LVDT Stiffness (kips/in)
10	33.4	44.5
20	33.5	45.
24	34.	45.
28	34.	44.5
32	38.	45.
36	34.	44.5
40	34.	44.5
41.3	35.5	43.5
Average	34.6	44.4

Table 12 - Stiffness from load/unload tests (Conbrextra S).

Load (kips)	Actuator LVDT Stiffness (kips/in)	External LVDT Stiffness (kips/in)
10	36.5	44.
20	37.	45.5
24	38.	46.
28	38.	46.5
32	37.5	45.5
36	37.	45.5
40	36.5	44.5
41.6	36.5	44.
Average	37.1	45.2

Table 13 - Stiffness from load/unload tests (Portland cement).

Load (kips)	Actuator LVDT Stiffness (kips/in)
10	22.5
20	26.5
24	25.5
28	26.
32	26.
36	26.
40	25.5
41.3	20.
Average	24.8

Table 14 - Stiffness from load distribution tests (Conbrextra, no deck).

Load (kips)	Actuator LVDT Stiffness (kips/in)	External LVDT Stiffness (kips/in)
10	21.7	30.7
20	23.5	30.1
24	23.5	29.8
28	23.5	29.3
32	23.2	28.6
36	22.9	27.9
40	22.8	27.6
41.6	23.0	27.9
Average	23.0	28.9

Table 15 - Stiffness from load distribution tests (Portland, no deck).

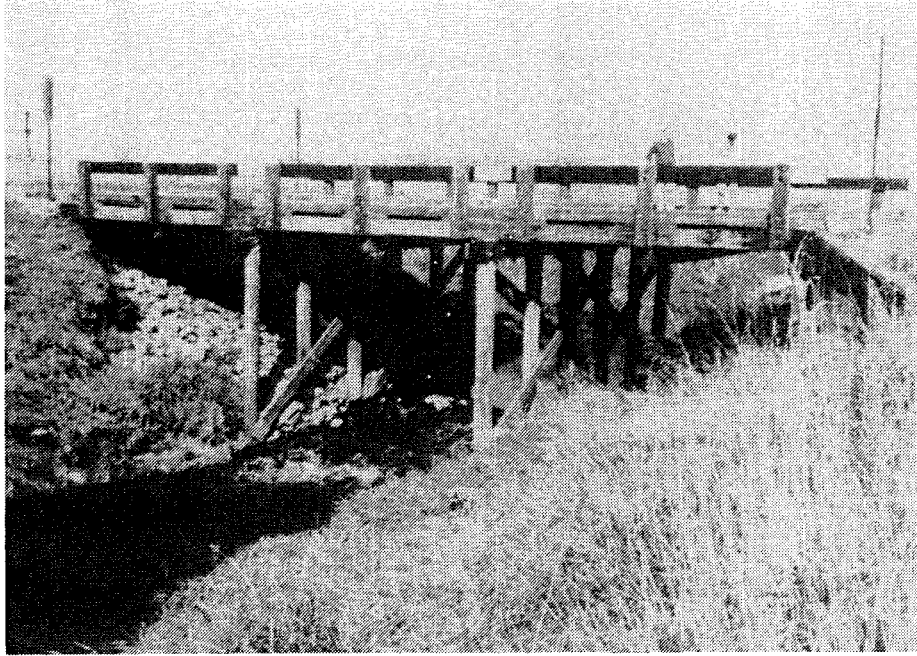


Figure 1 - Elevation of the bridge (South view).

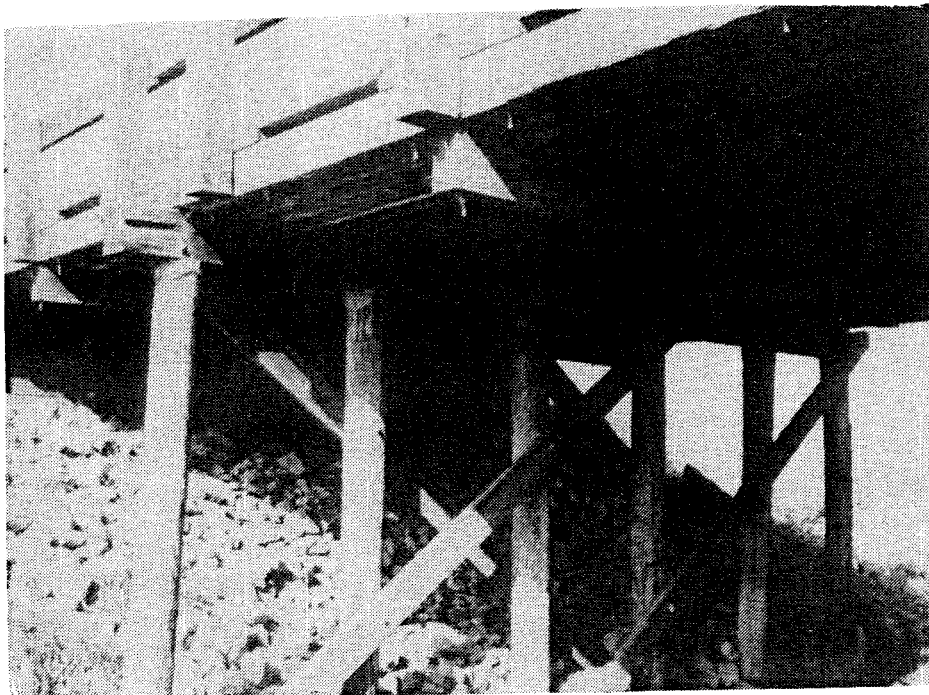
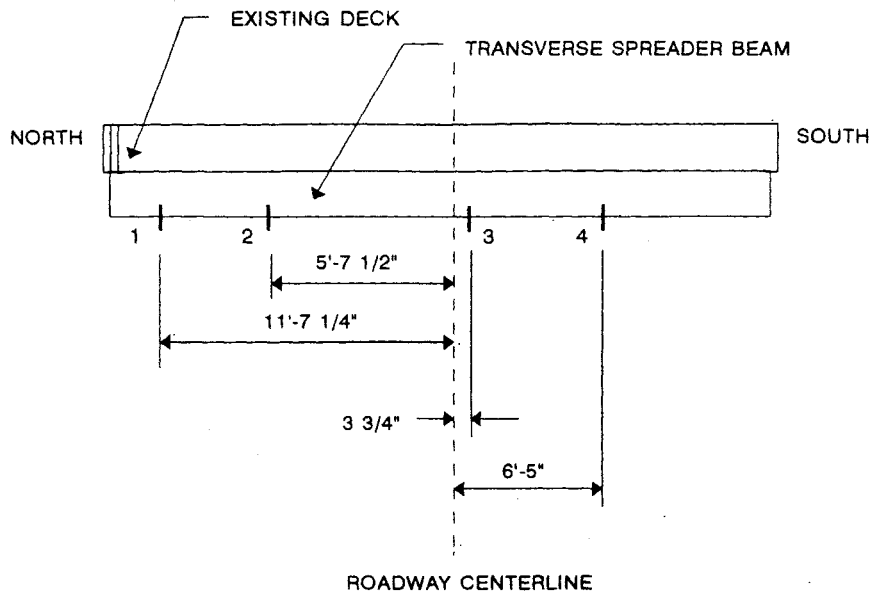


Figure 2 - View of the nail-laminated deck.



- 1: NORTH LANE EDGE LVDT (NL EDGE)
- 2: NORTH LANE CENTER LVDT (NL CENTER)
- 3: ROADWAY CENTER LVDT (RDWY CENTER)
- 4: SOUTH LANE CENTER LVDT (SL CENTER)

Figure 3 - Location of transducers.

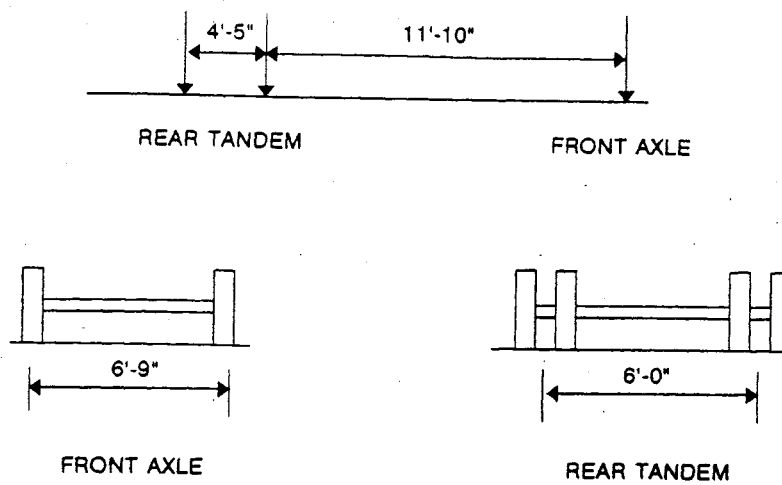


Figure 4 - Geometry of loading axles.

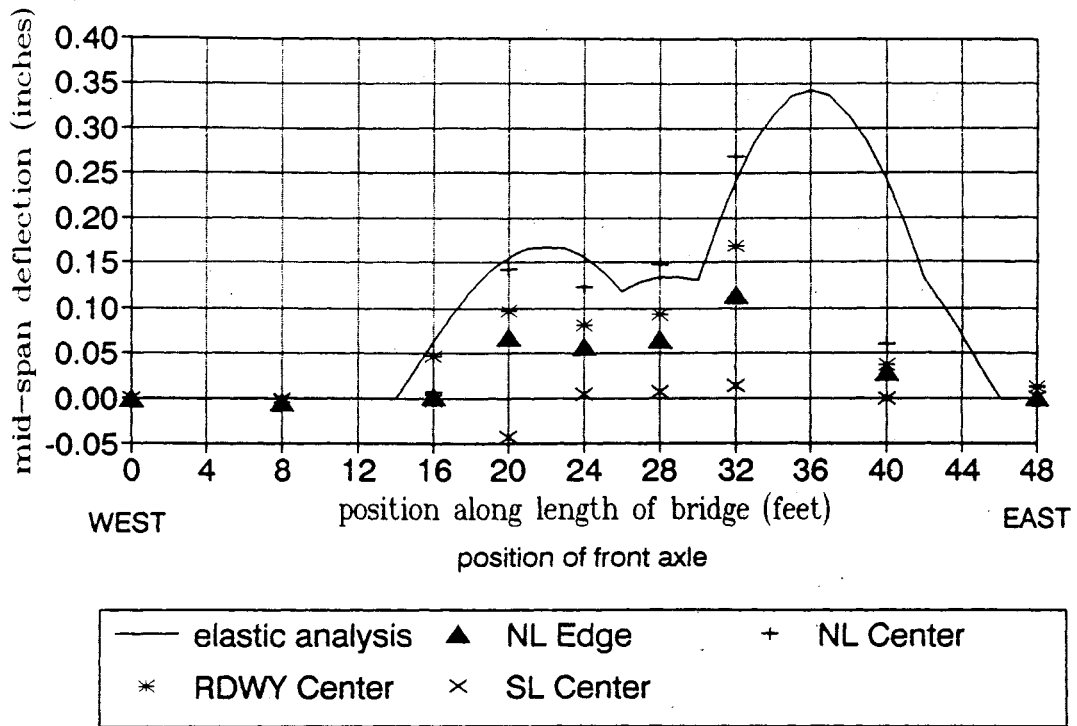


Figure 5 - Results of static test #1.

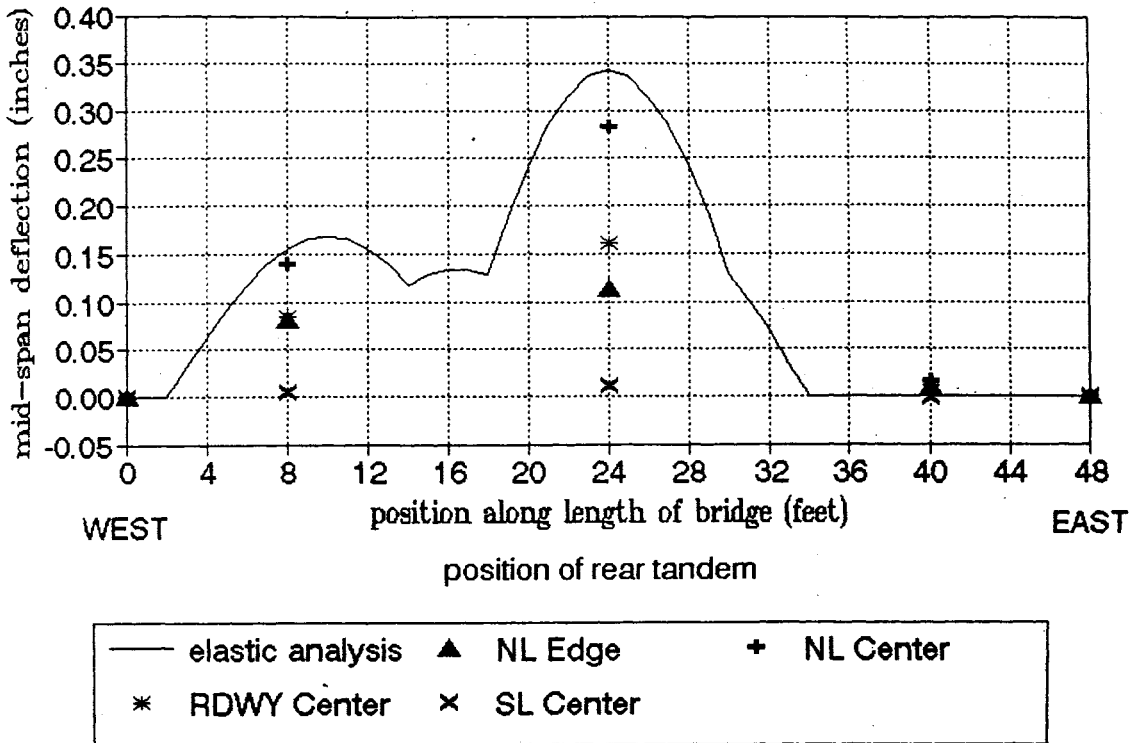


Figure 6 - Results of static test #2.

STATIC TEST #3 ORIGINAL BRIDGE

East to West, South Lane, Truck #54

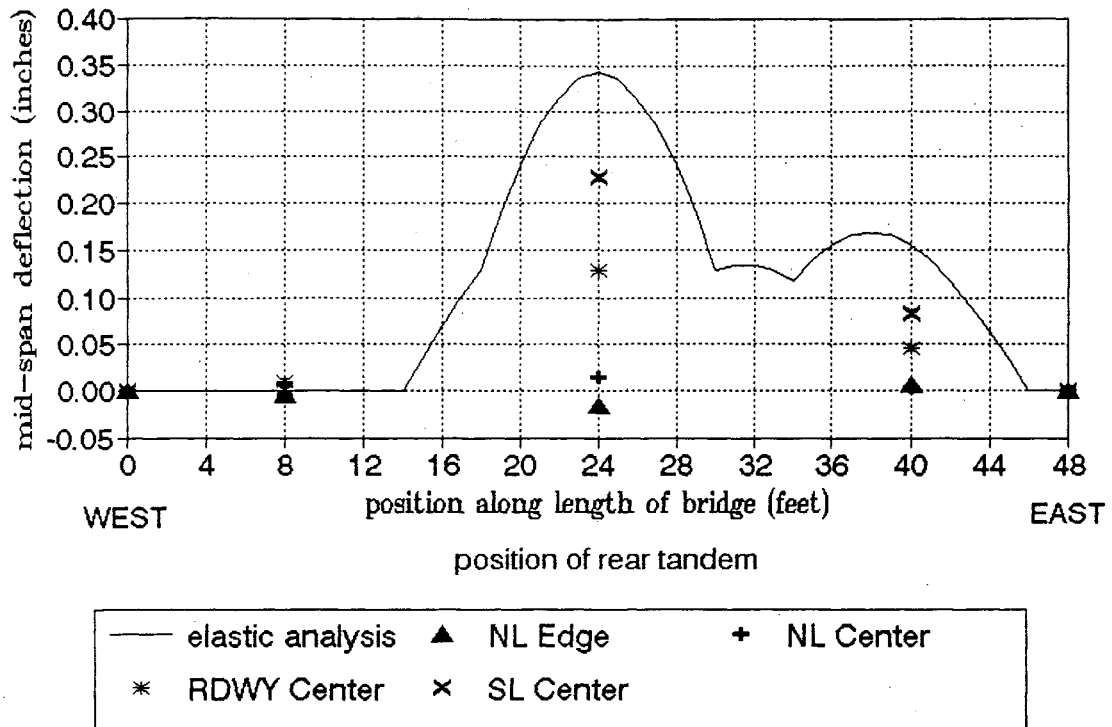


Figure 7 - Results of static test #3.

STATIC TEST #4 ORIGINAL BRIDGE

West to East, T #54(SL) T #9103(NL)

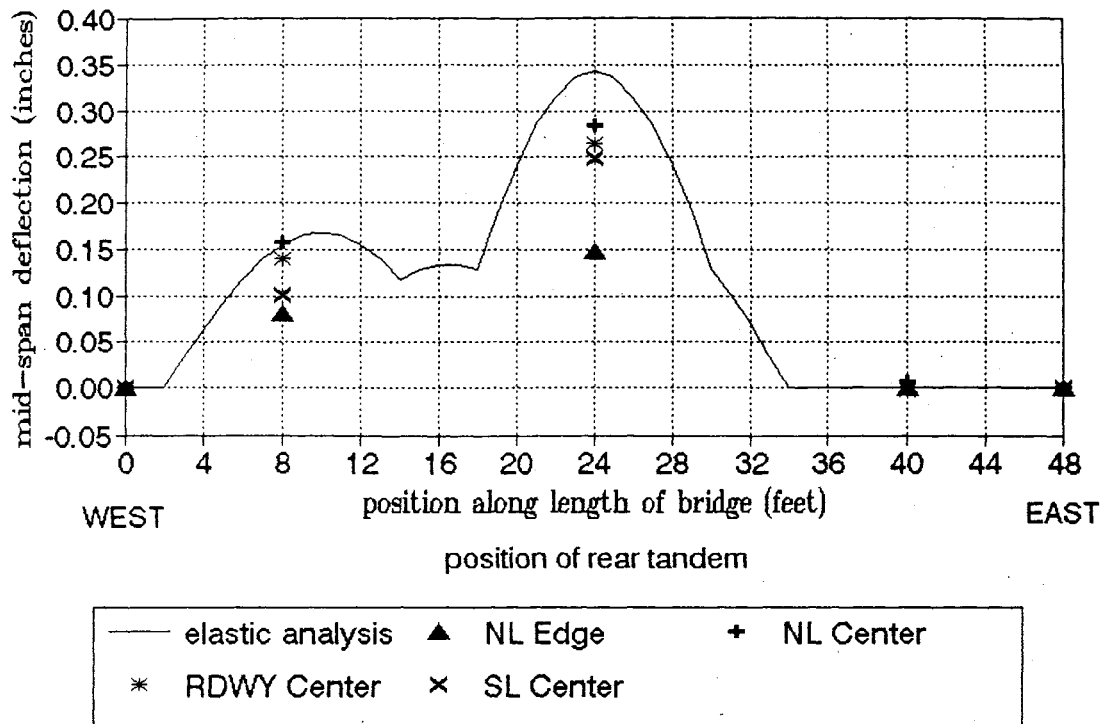
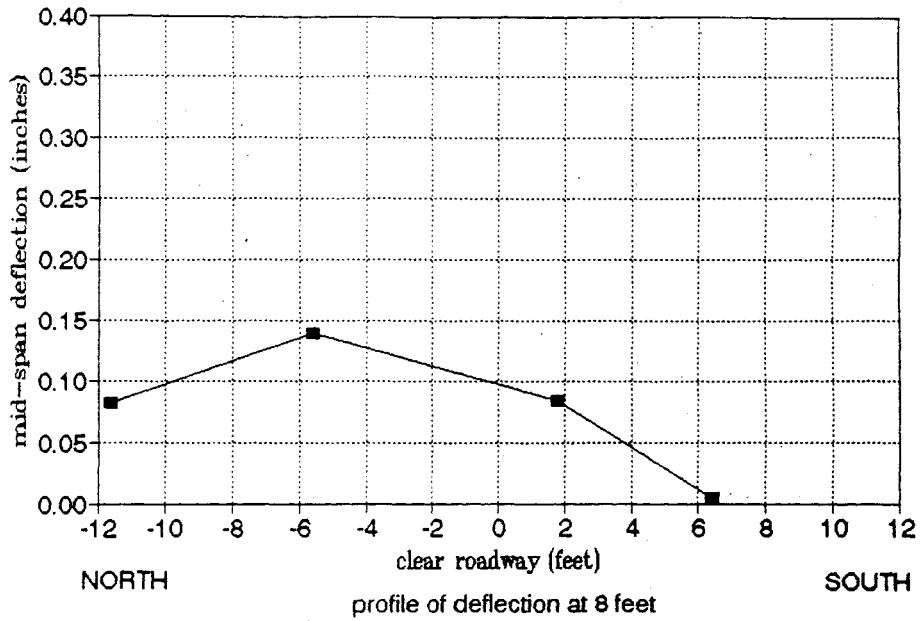
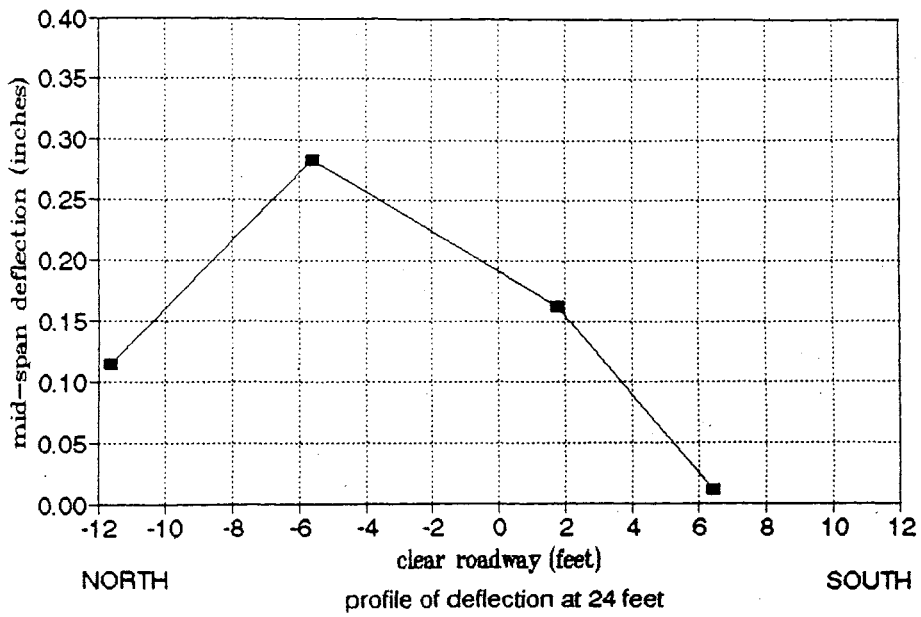


Figure 8 - Results of static test #4.

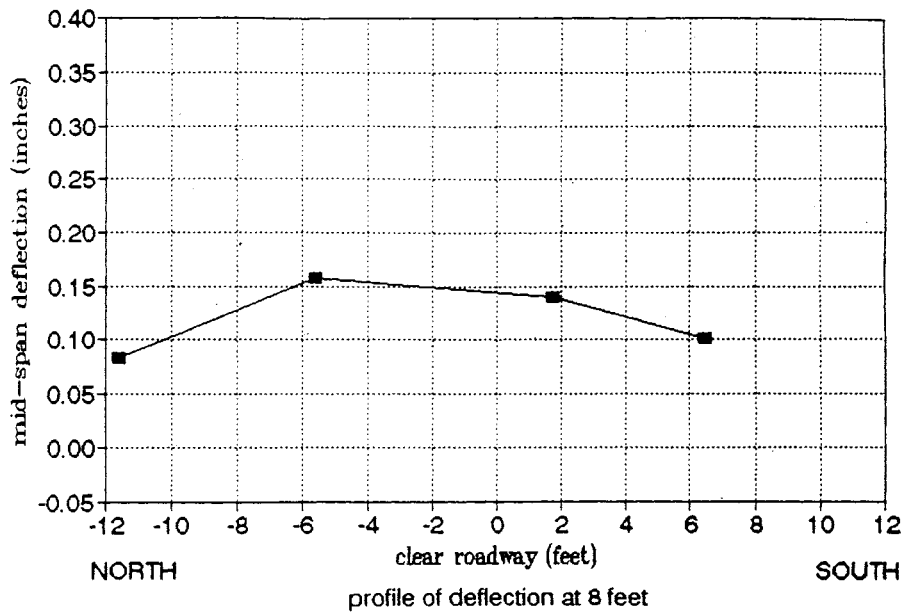


(a) Deflection profile for test #2, with load at 8 ft.

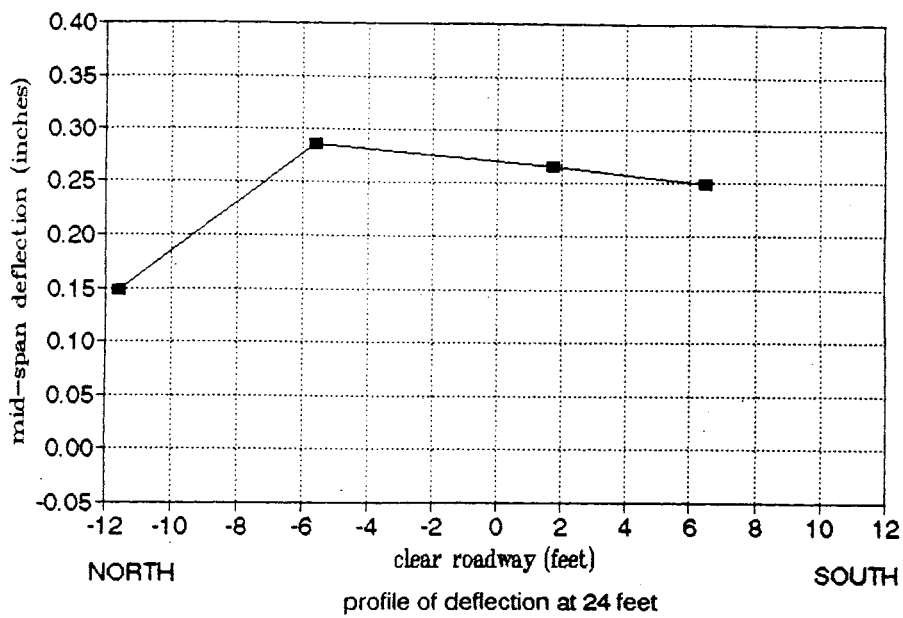


(b) Deflection profile for test #2, with load at 24 ft.

Figure 9 - Deflection profiles at midspan.



(a) Deflection profile for test #4, with load at 8 ft.



(b) Deflection profile for test #4, with load at 24 ft.

Figure 10 - Deflection profiles at midspan.

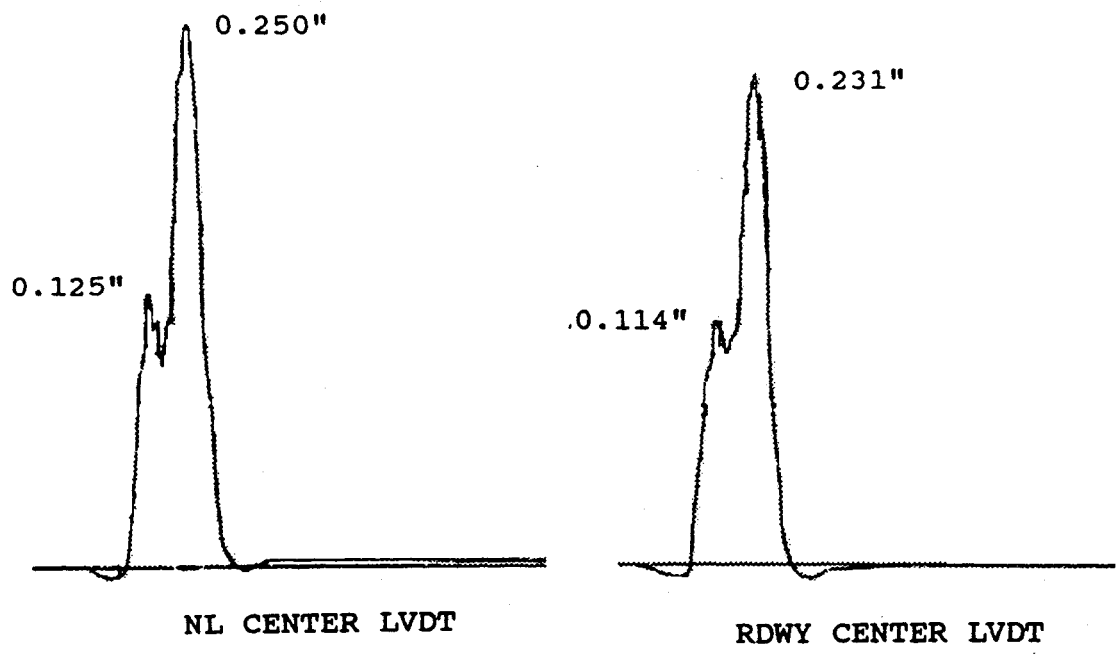


Figure 11 - Dynamic response at 6 mph.

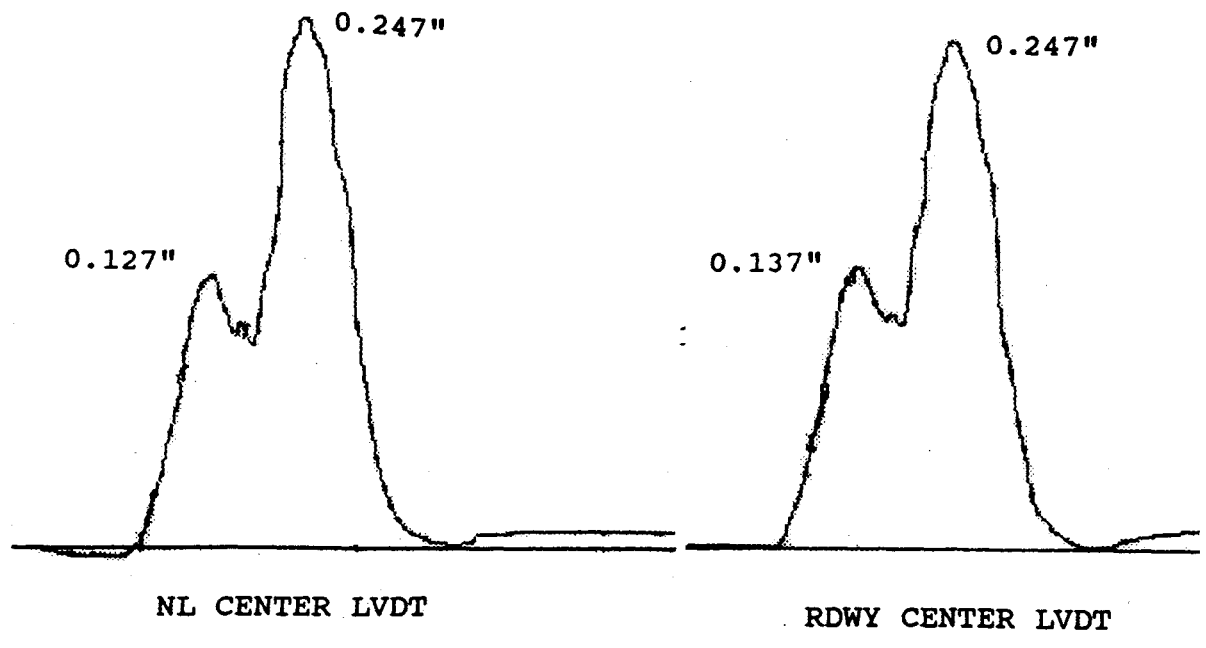


Figure 12 - Dynamic response at 20 mph.

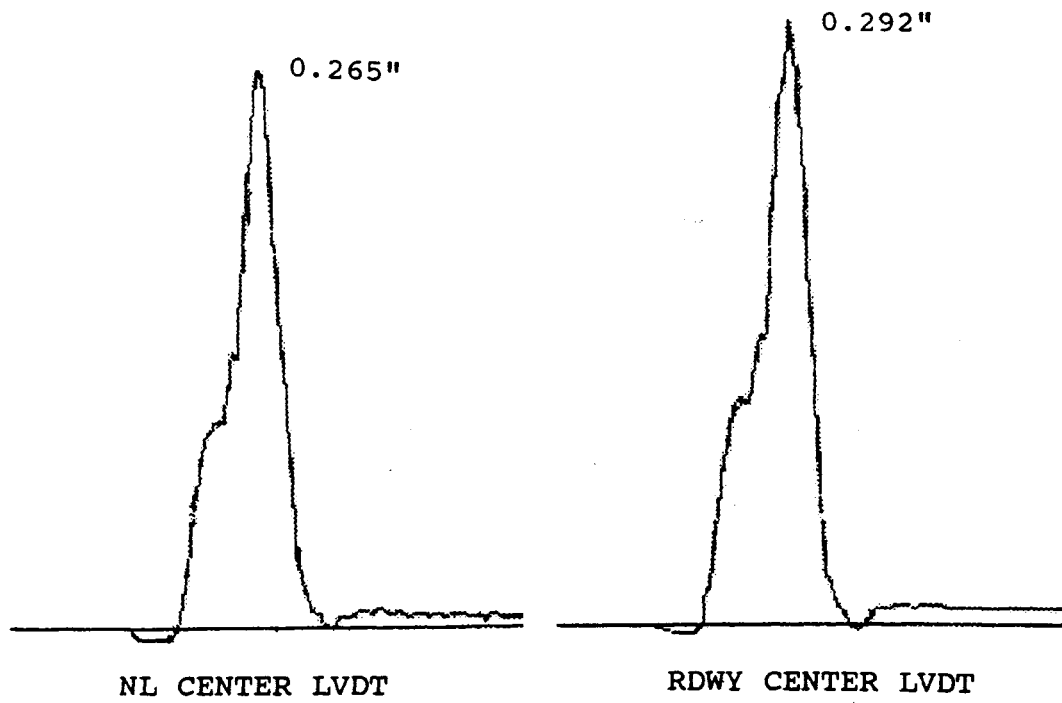


Figure 13 - Dynamic response at 40 mph.

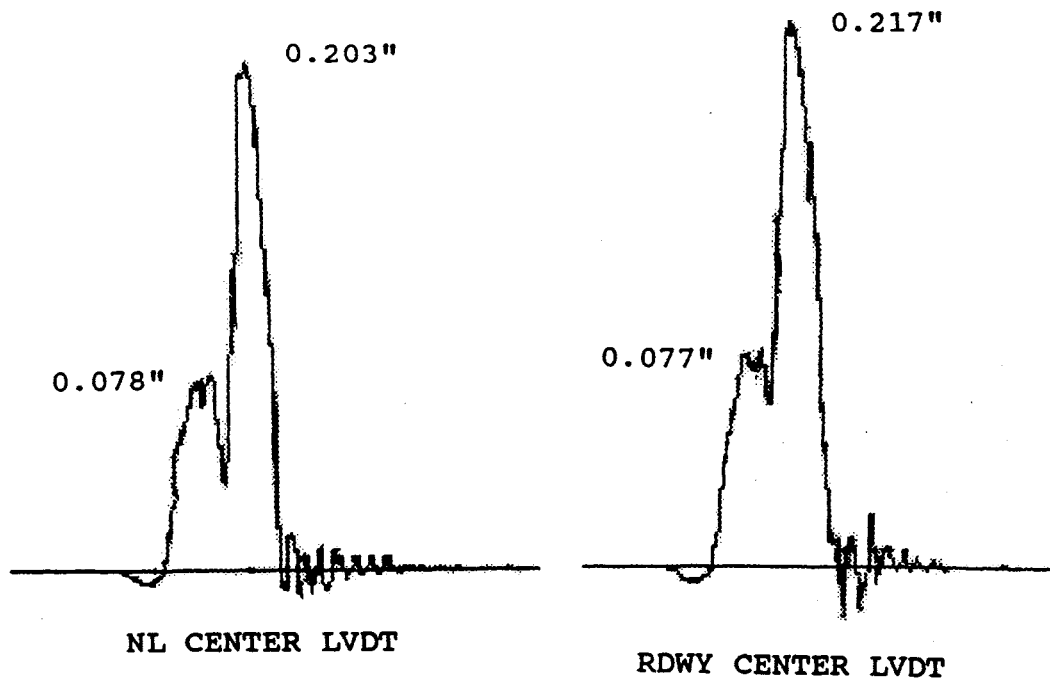


Figure 14 - Dynamic response at 60 mph.

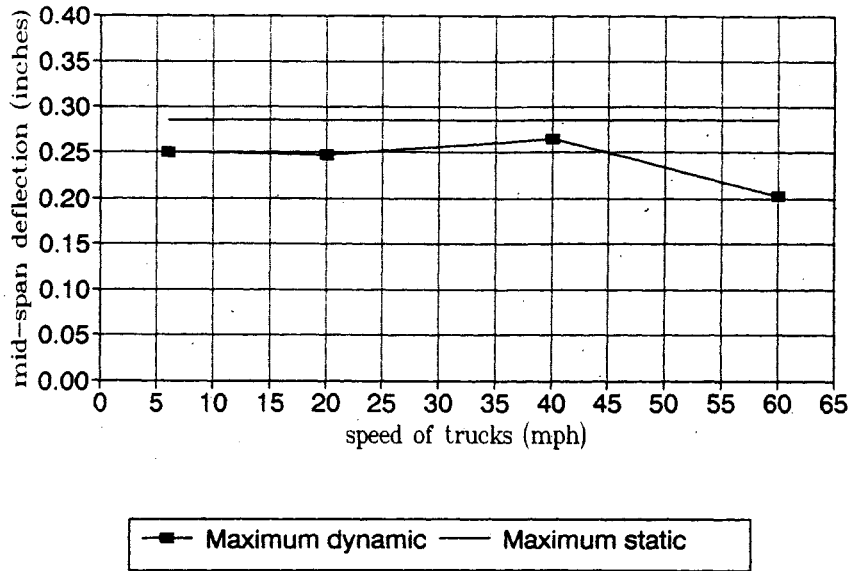


Figure 15 - Dynamic response (NL Center LVDT).

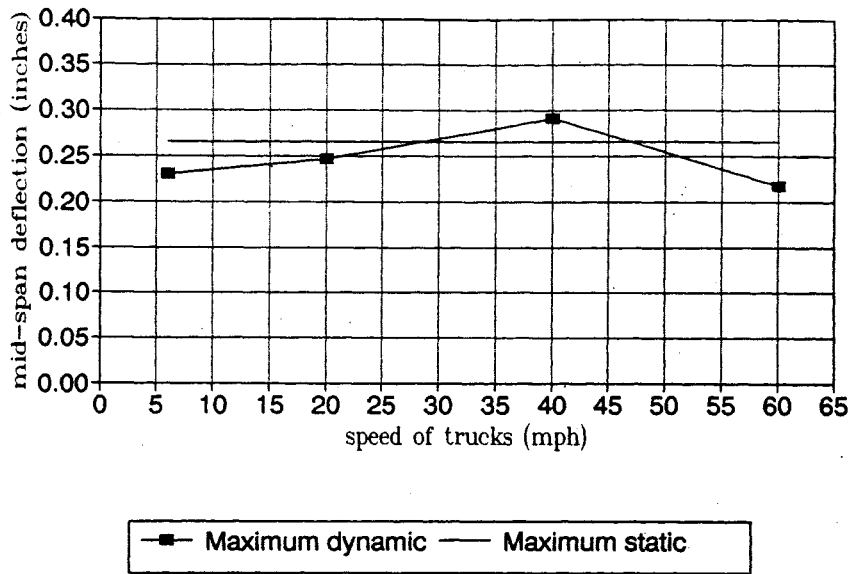


Figure 16 - Dynamic response (RDWY Center LVDT).

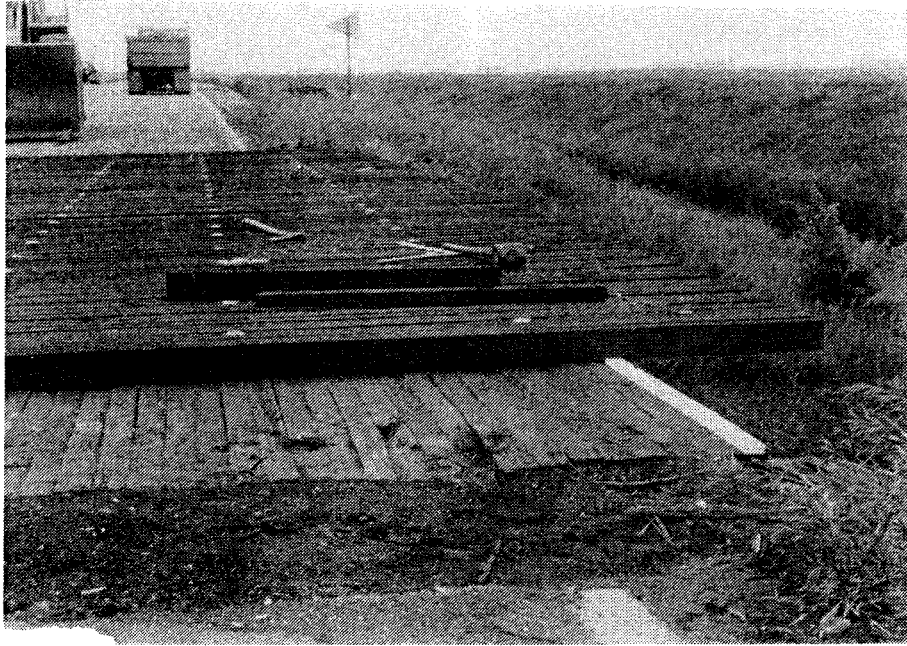


Figure 17 - Retrofit panels being installed.

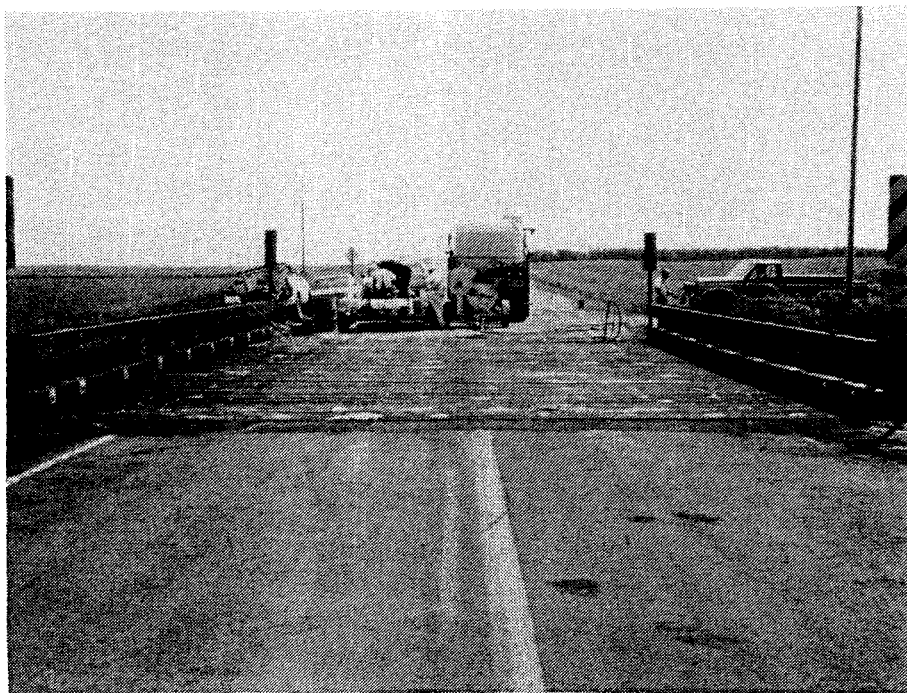


Figure 18. - Completed installation of the panels.

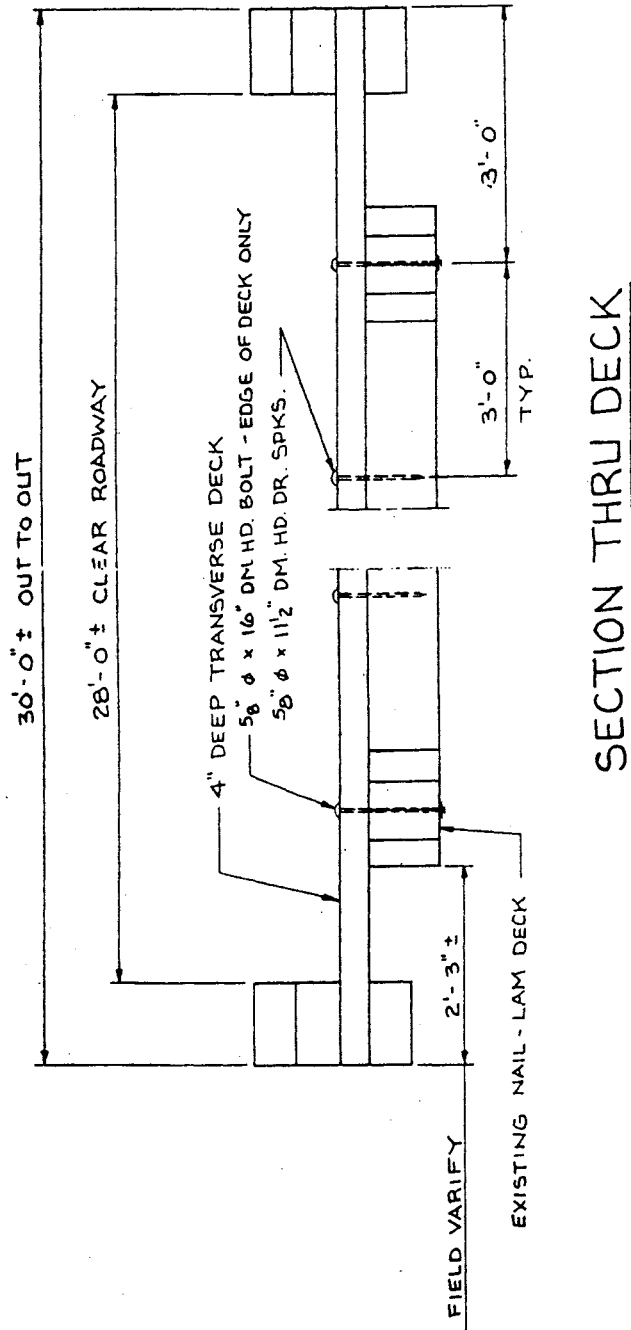


Figure 19 - Cross-section of retrofitted bridge.

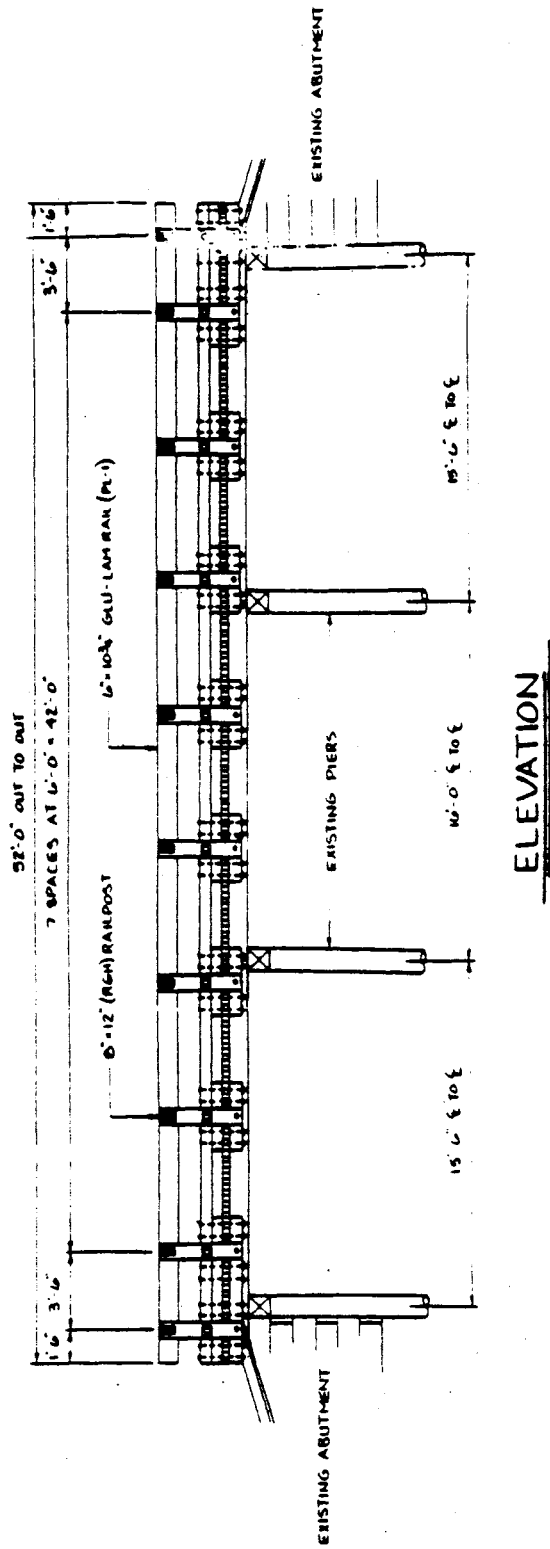


Figure 20 - Elevation of retrofitted bridge.

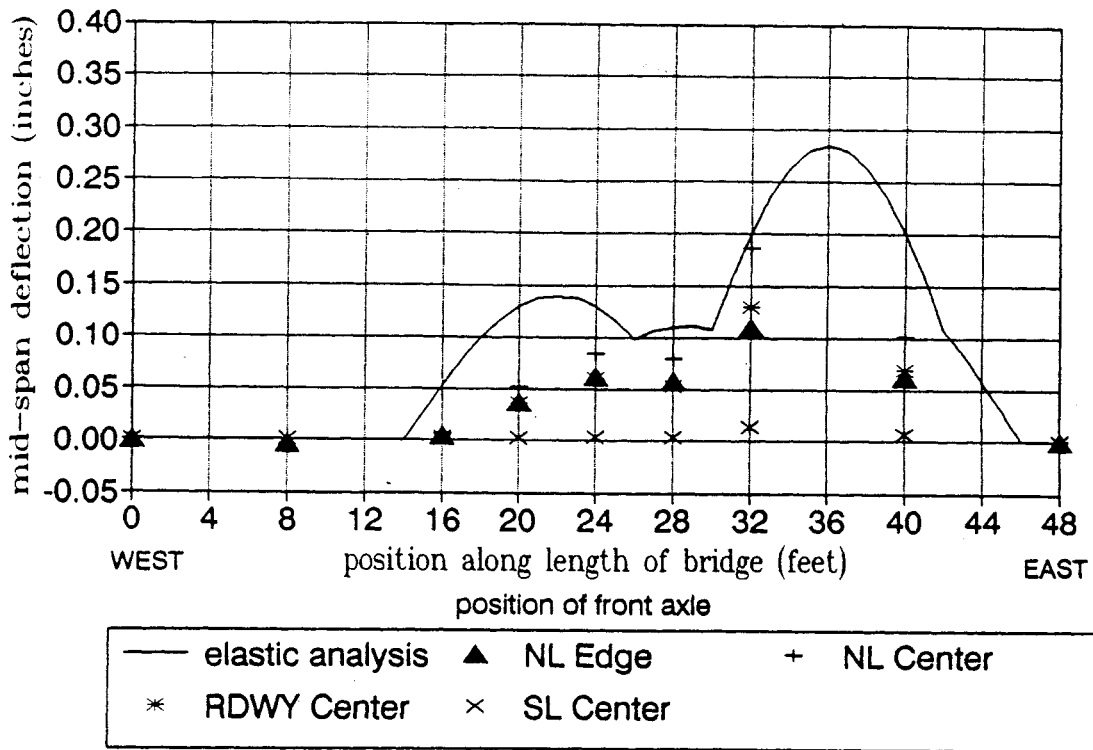


Figure 21 - Results of static test #1.

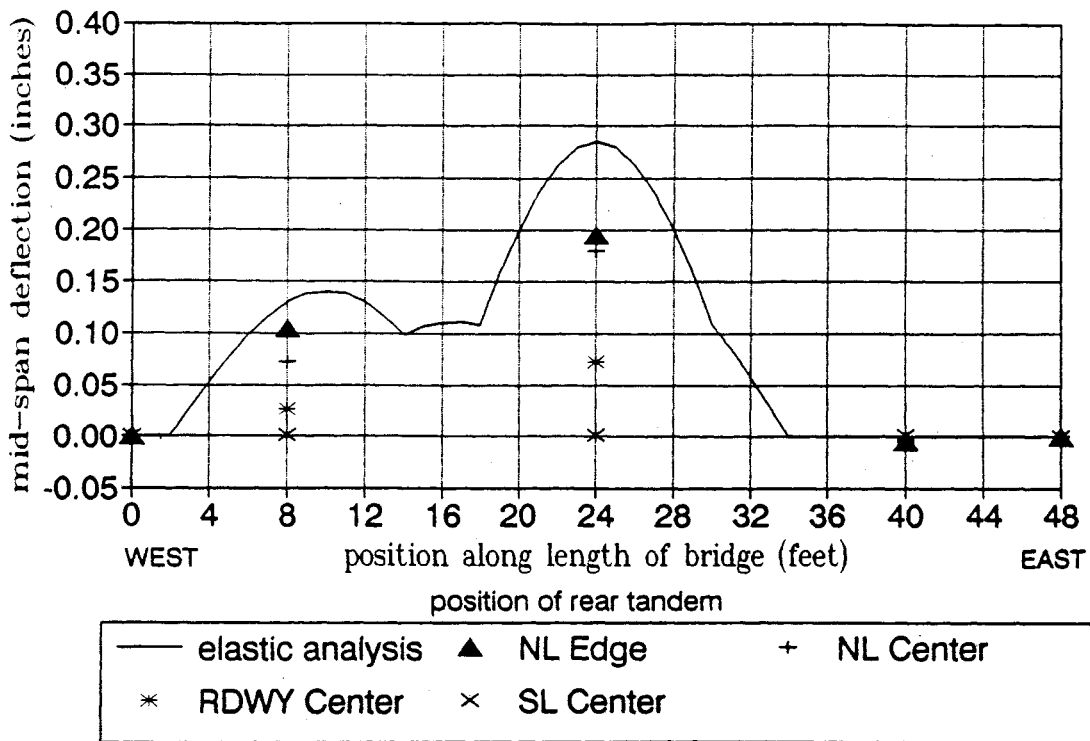


Figure 22 - Results of static test #2.

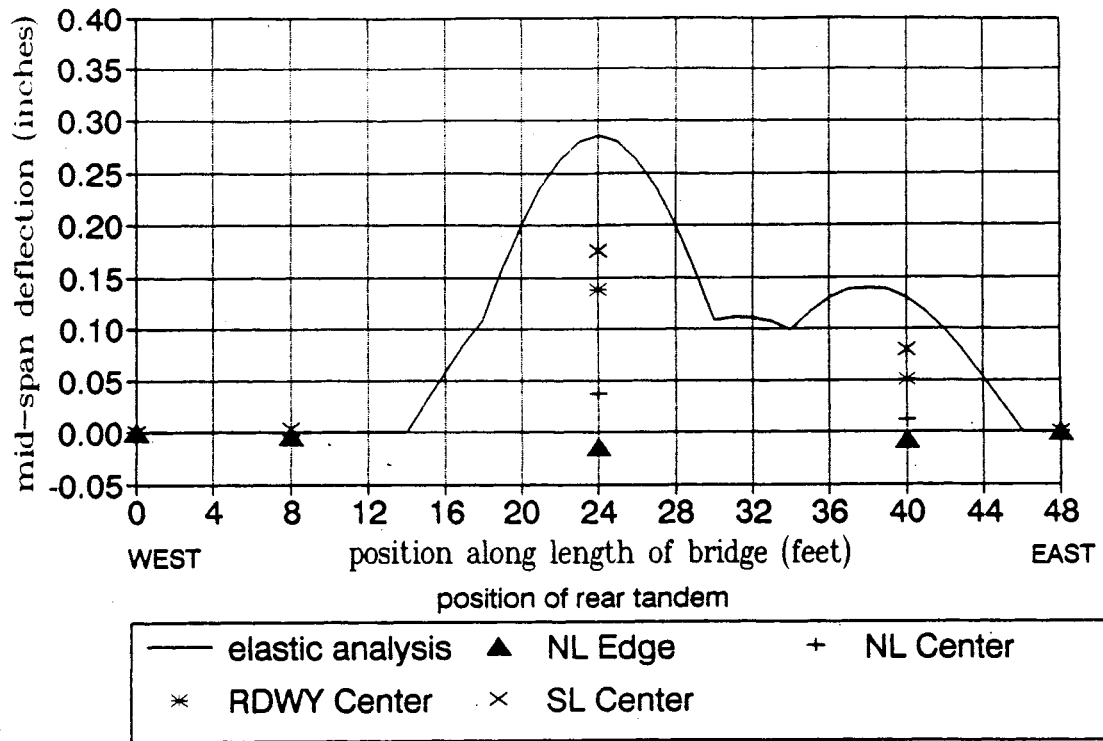


Figure 23 - Results of static test #3.

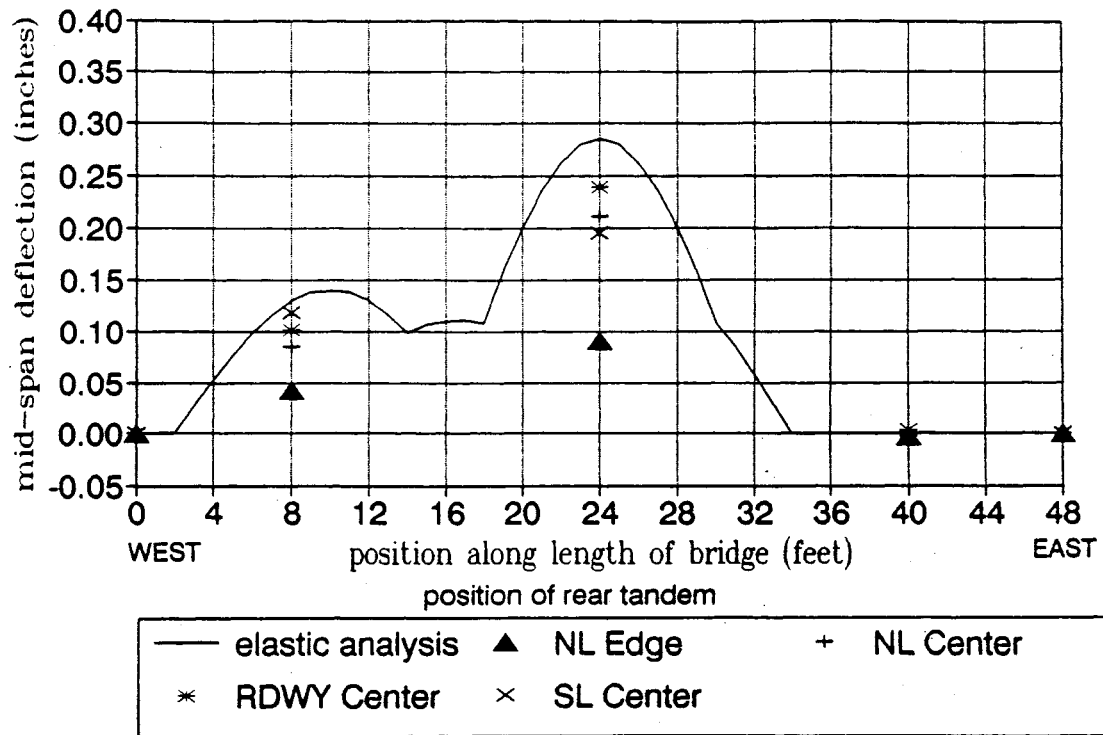
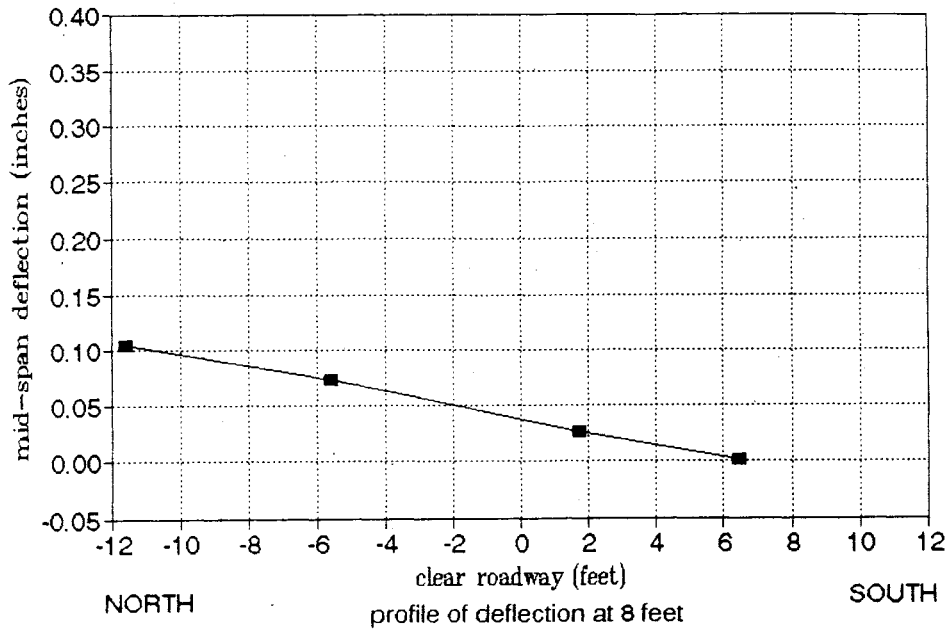
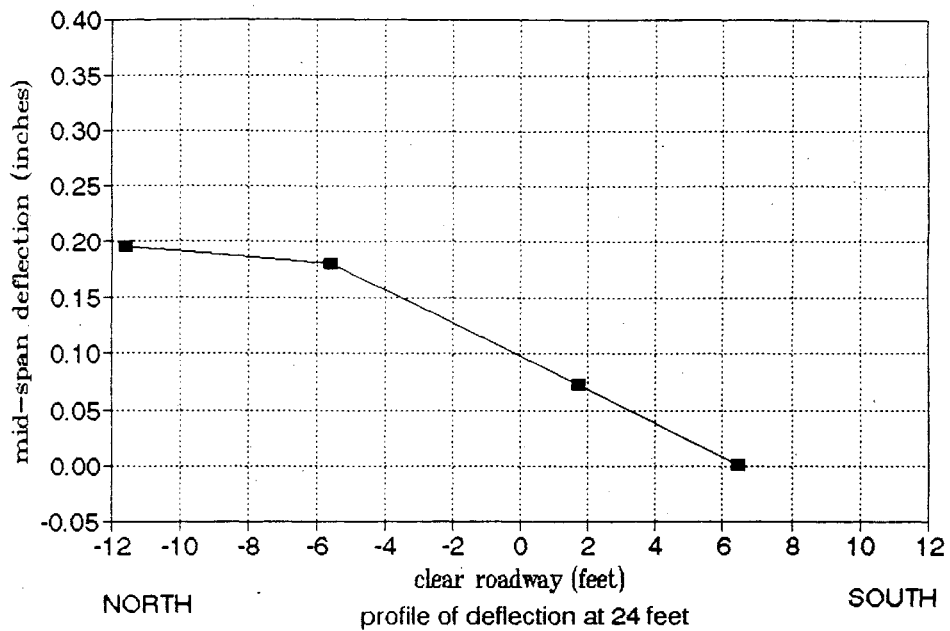


Figure 24 - Results of static test #4.

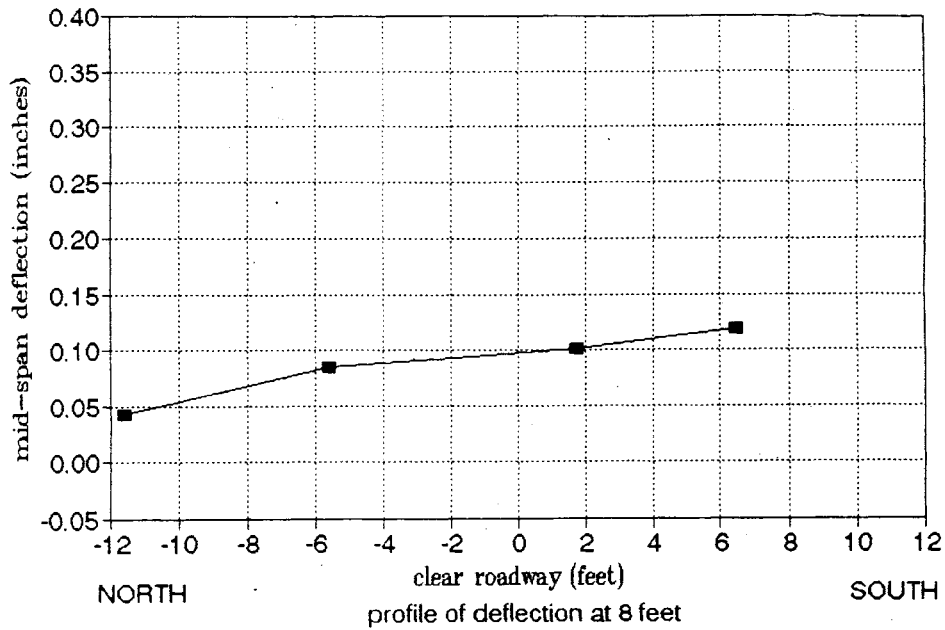


(a) Deflection profile for test #2, with load at 8 ft.

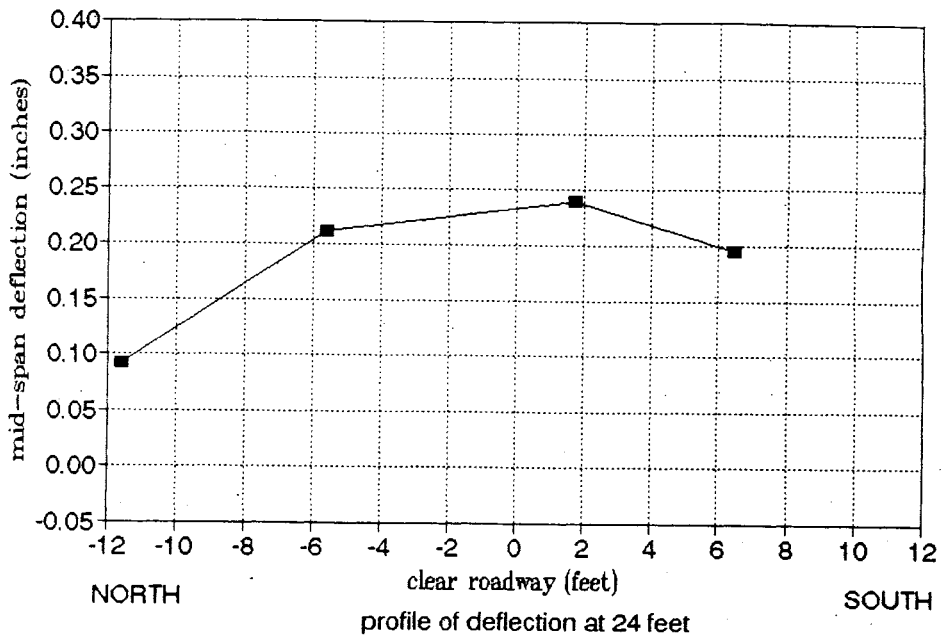


(b) Deflection profile for test #2, with load at 24 ft.

Figure 25 - Deflection profiles at midspan for retrofitted bridge.



(a) Deflection profile for test #4, with load at 8 ft.



(b) Deflection profile for test #4, with load at 24 ft.

Figure 26 - Deflection profiles at midspan for retrofitted bridge.

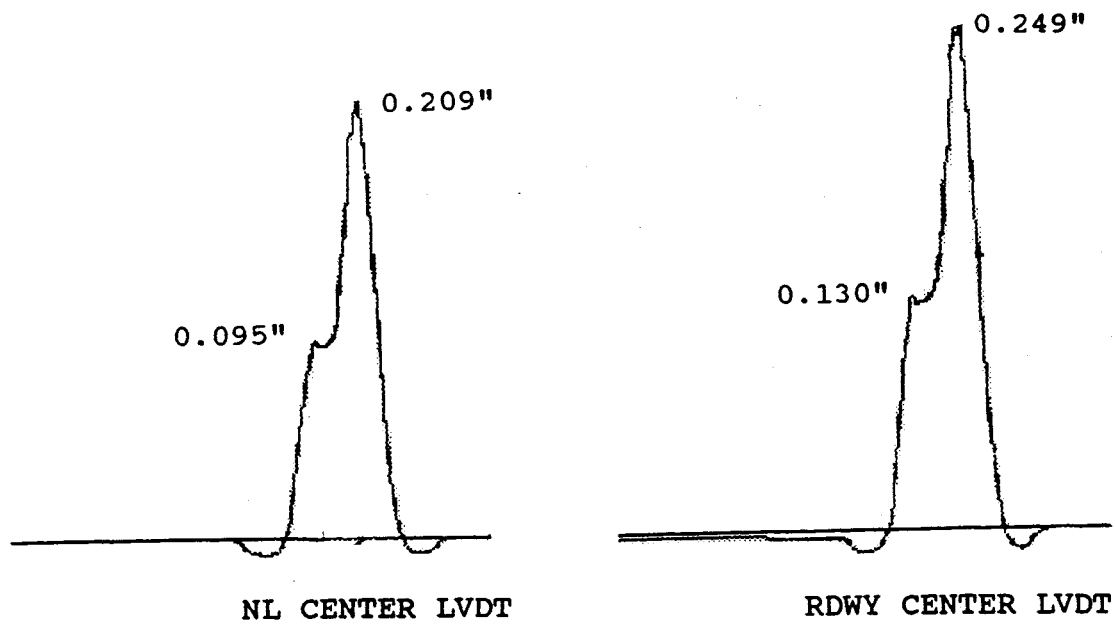


Figure 27 - Dynamic response at 6 mph (retrofitted).

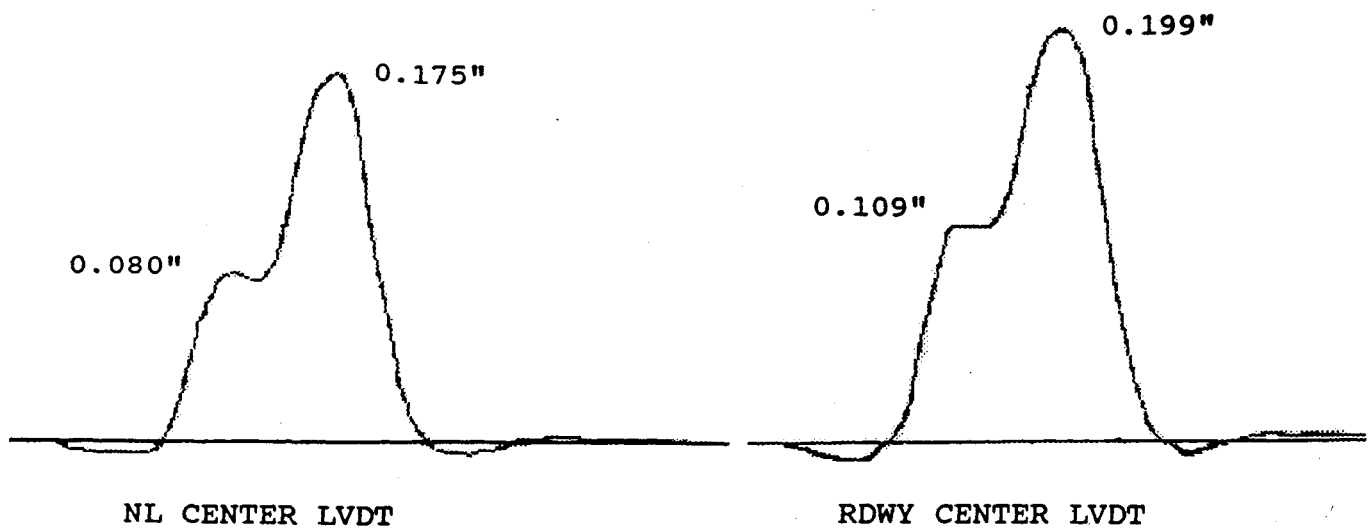


Figure 28 - Dynamic response at 20 mph (retrofitted).

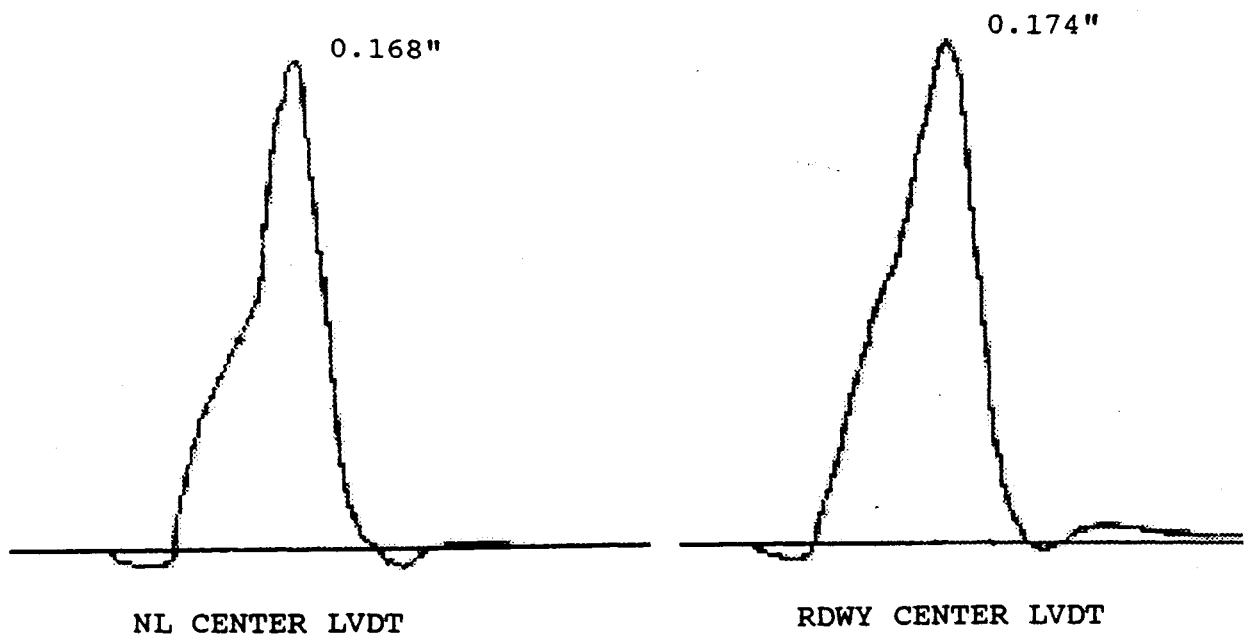


Figure 29 - Dynamic response at 40 mph (retrofitted).

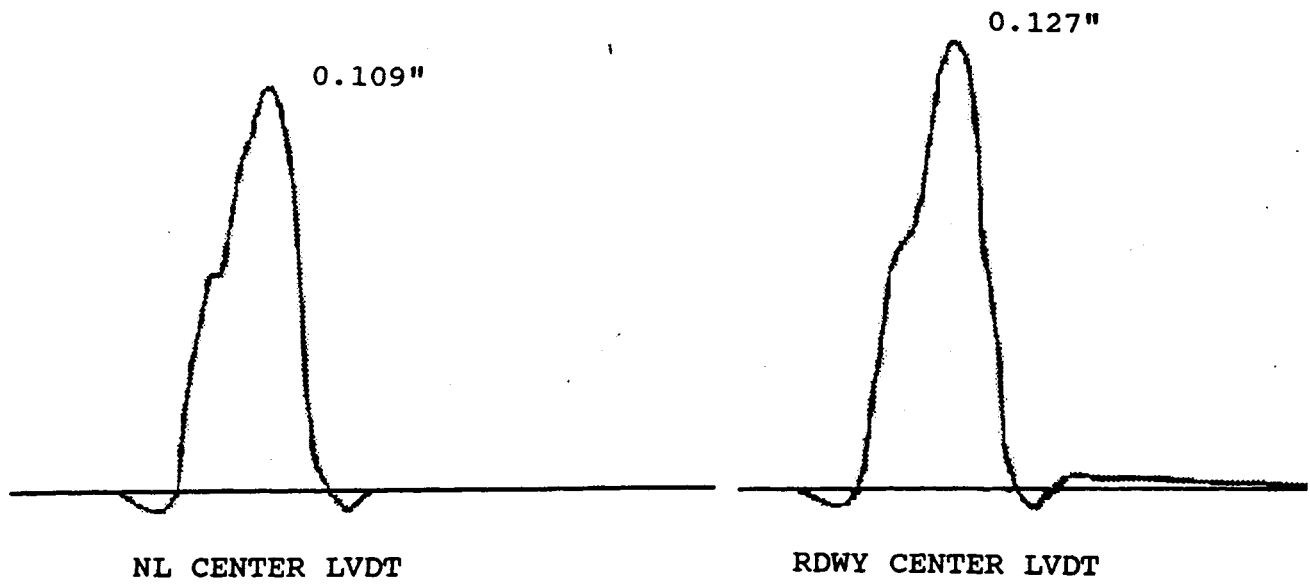


Figure 30 - Dynamic response at 60 mph. (retrofitted).

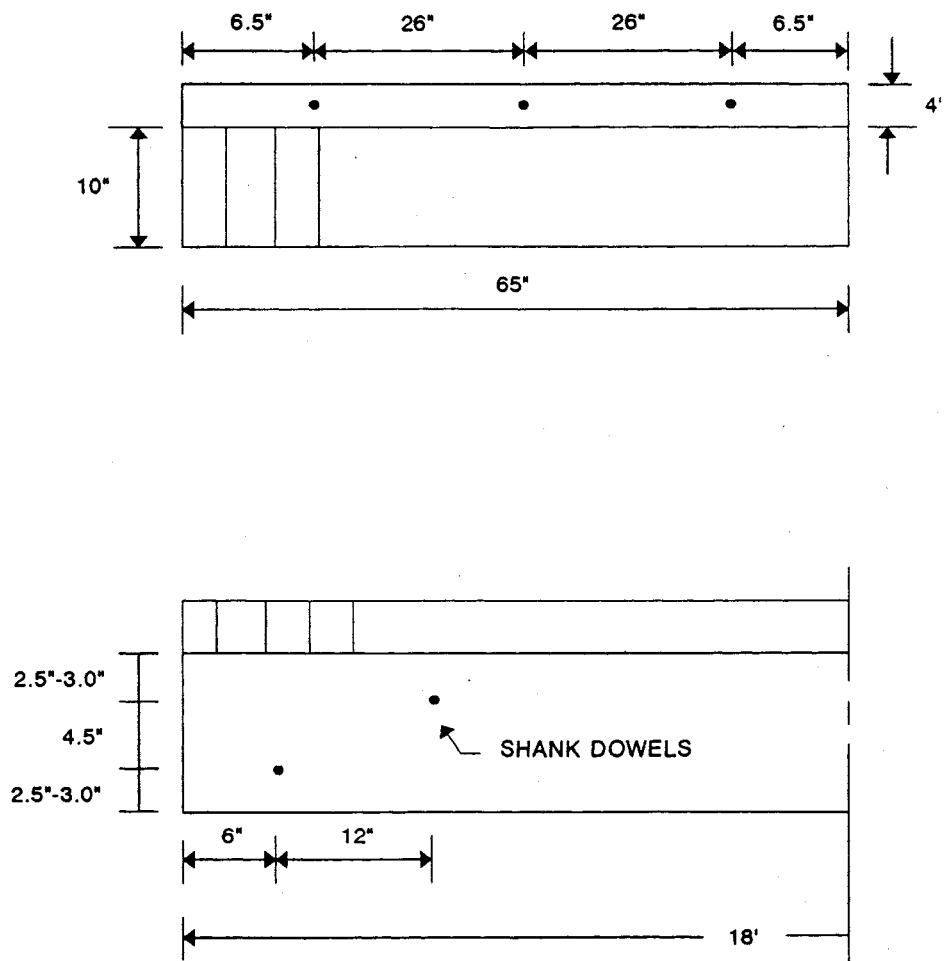


Figure 31 - Dimensions of laboratory specimen.

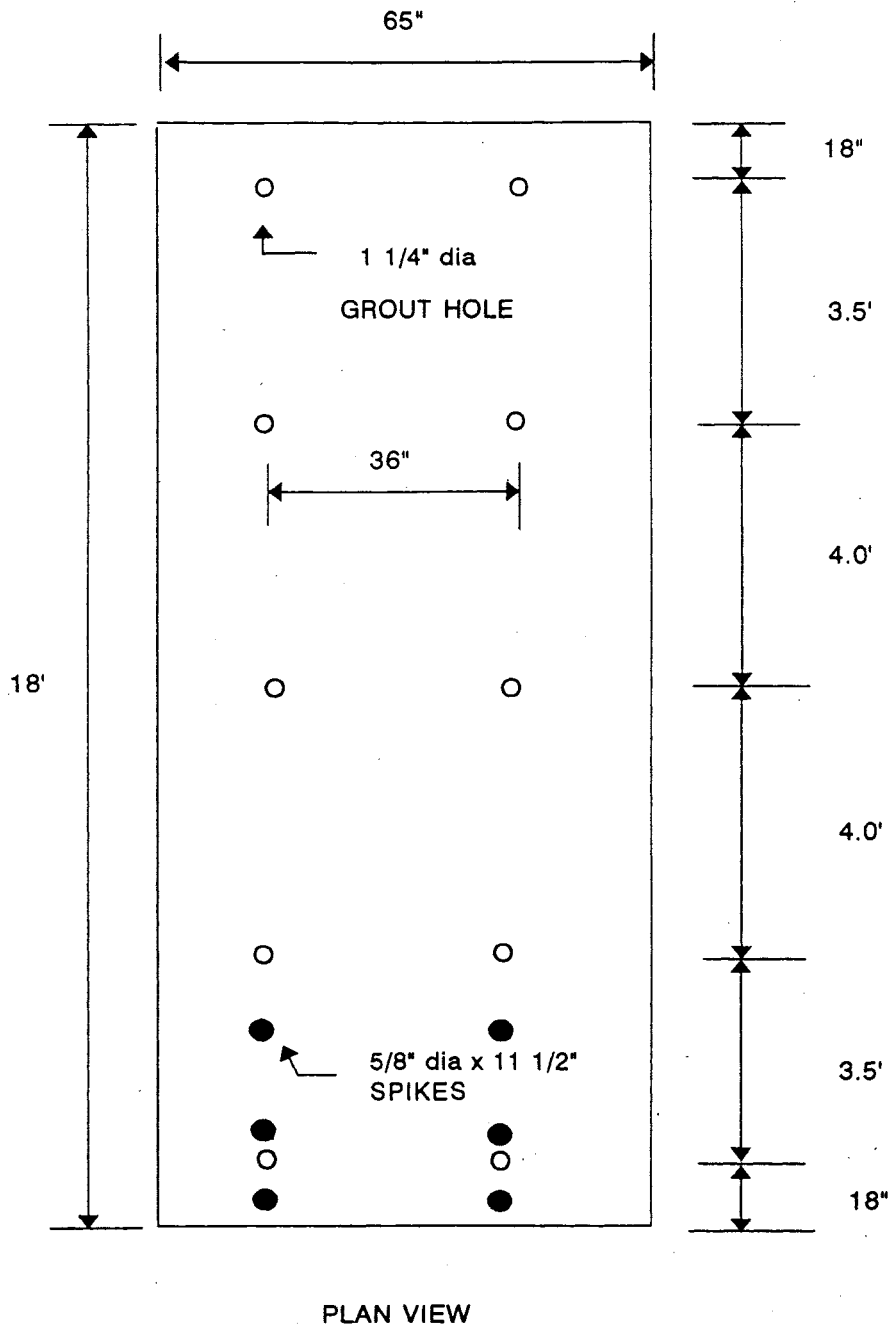


Figure 32 - Plan view of laboratory specimen.

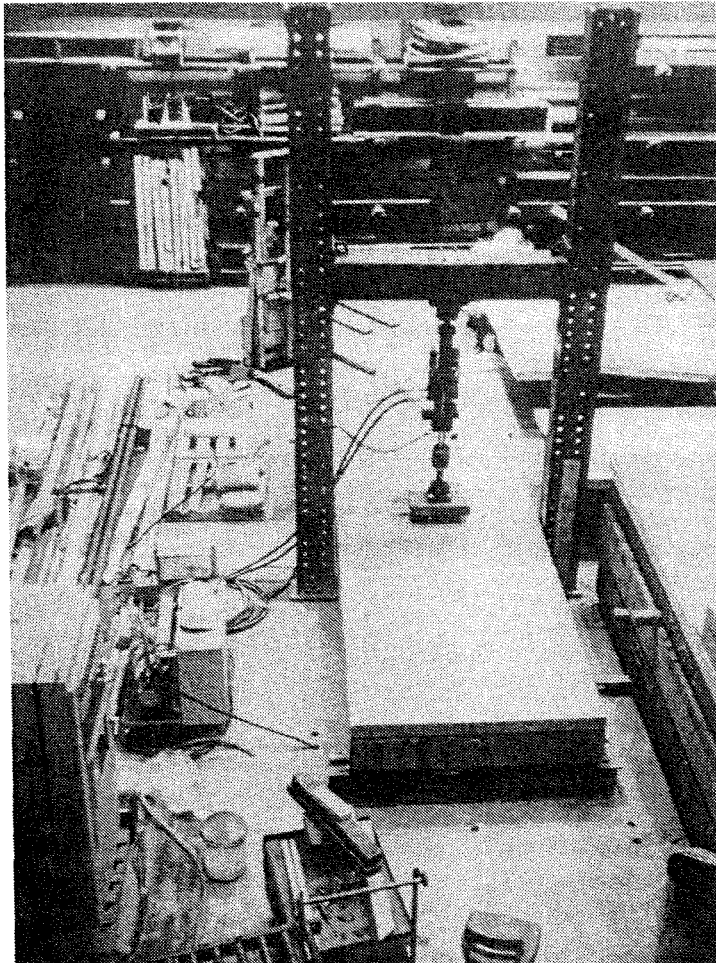


Figure 33 - View of the testing frame.

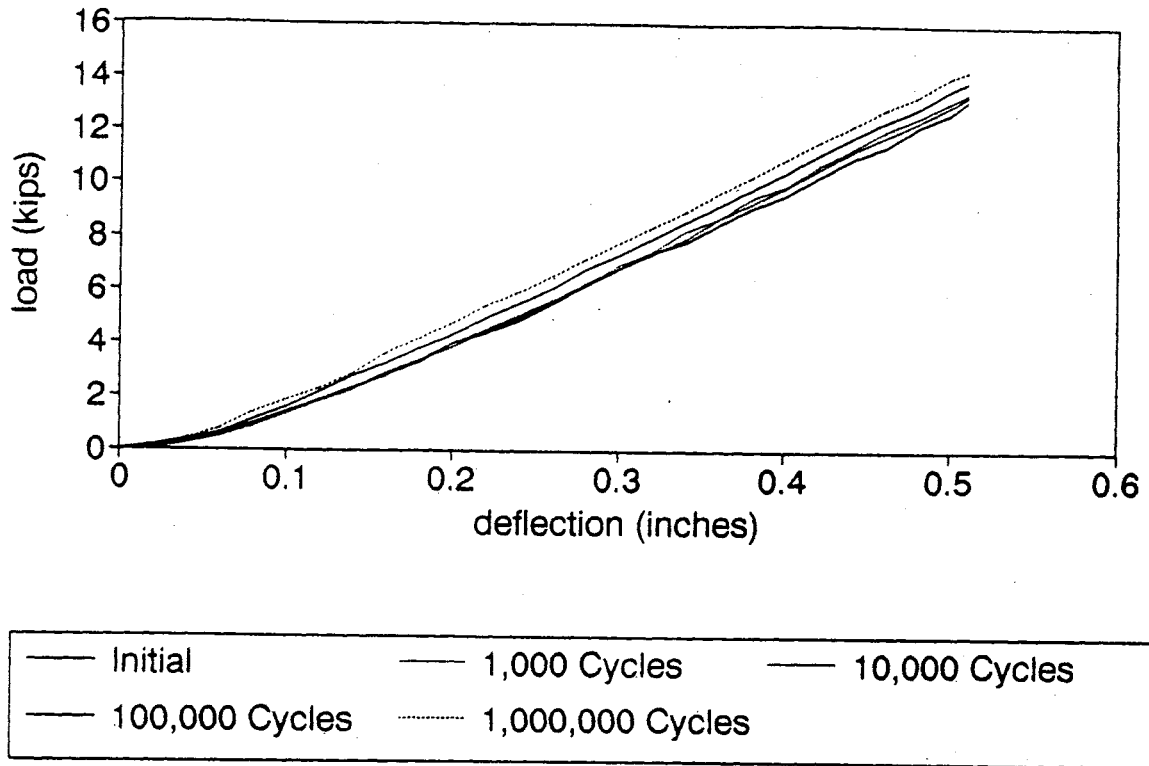


Figure 34 - Results of fatigue tests on ungrouted specimen.

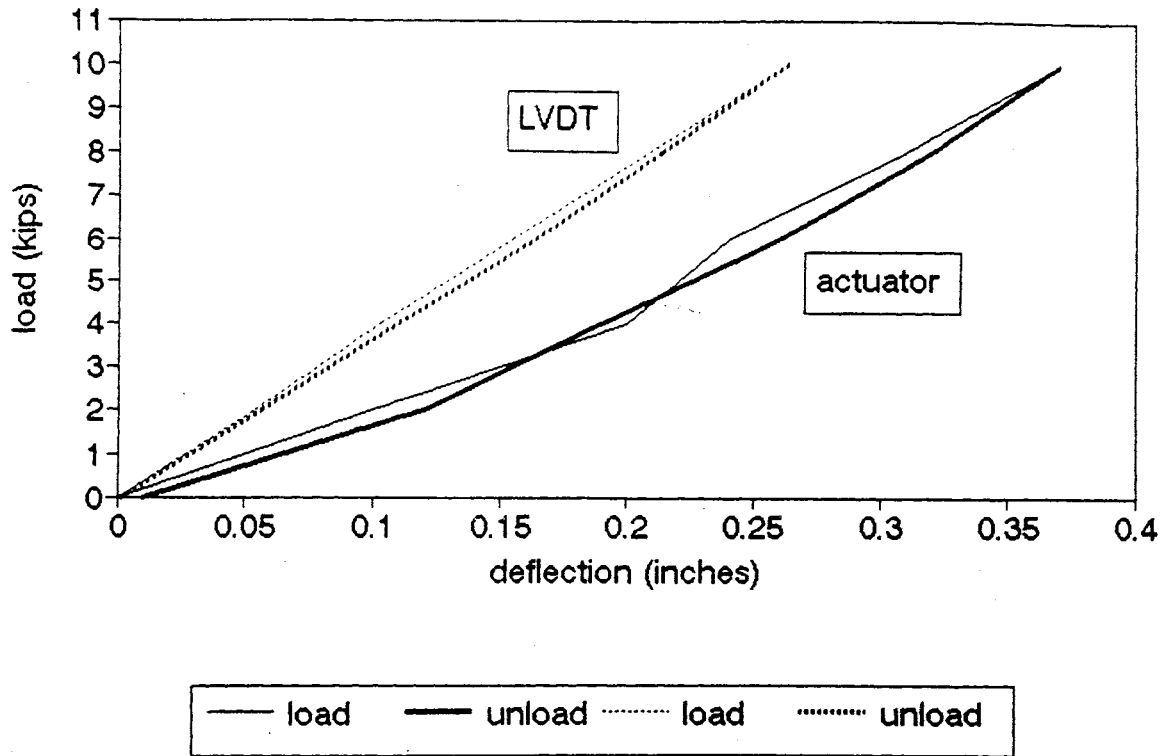


Figure 35 - Monotonic Test at 10 kips.

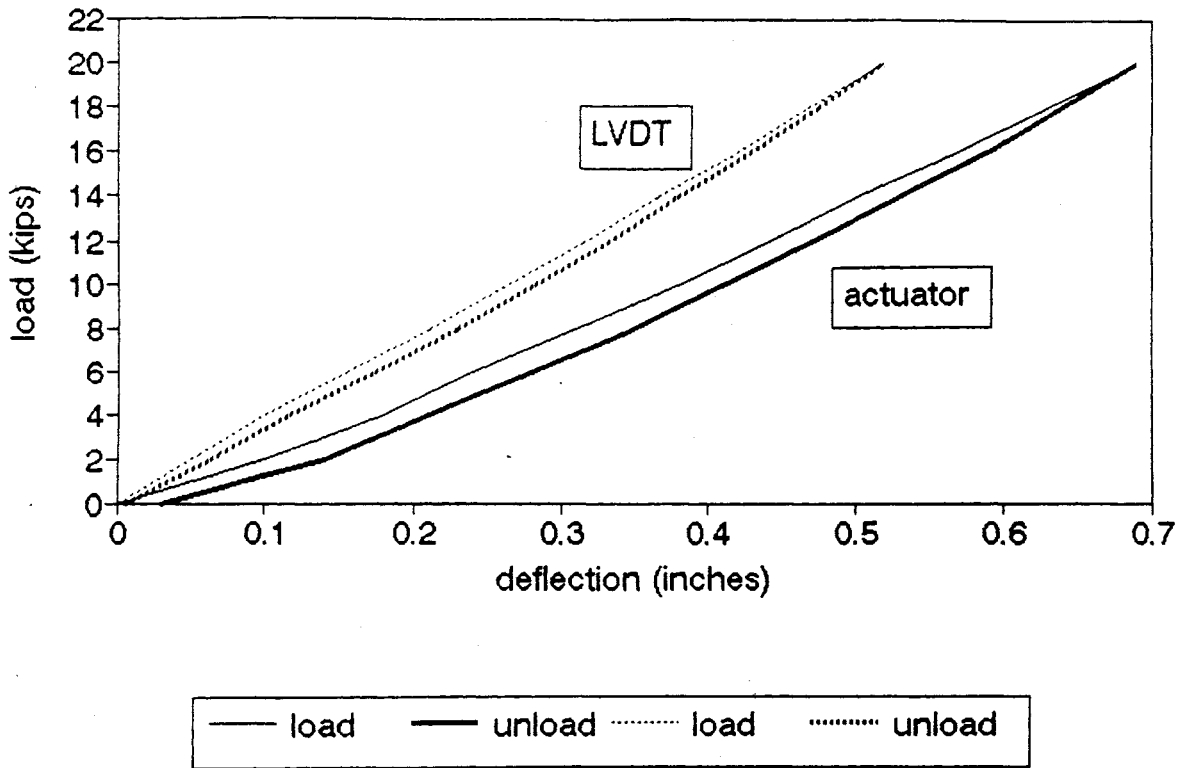


Figure 36 - Monotonic Test at 20 kips.

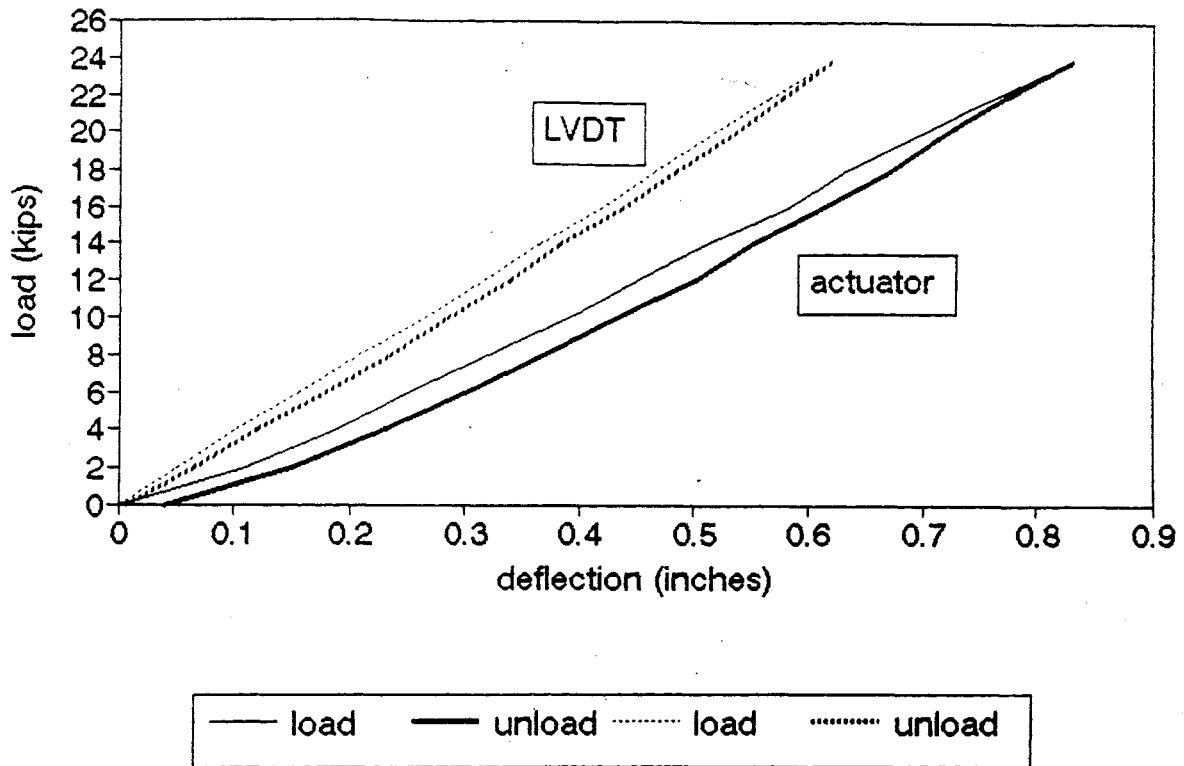


Figure 37 - Monotonic Test at 24 kips.

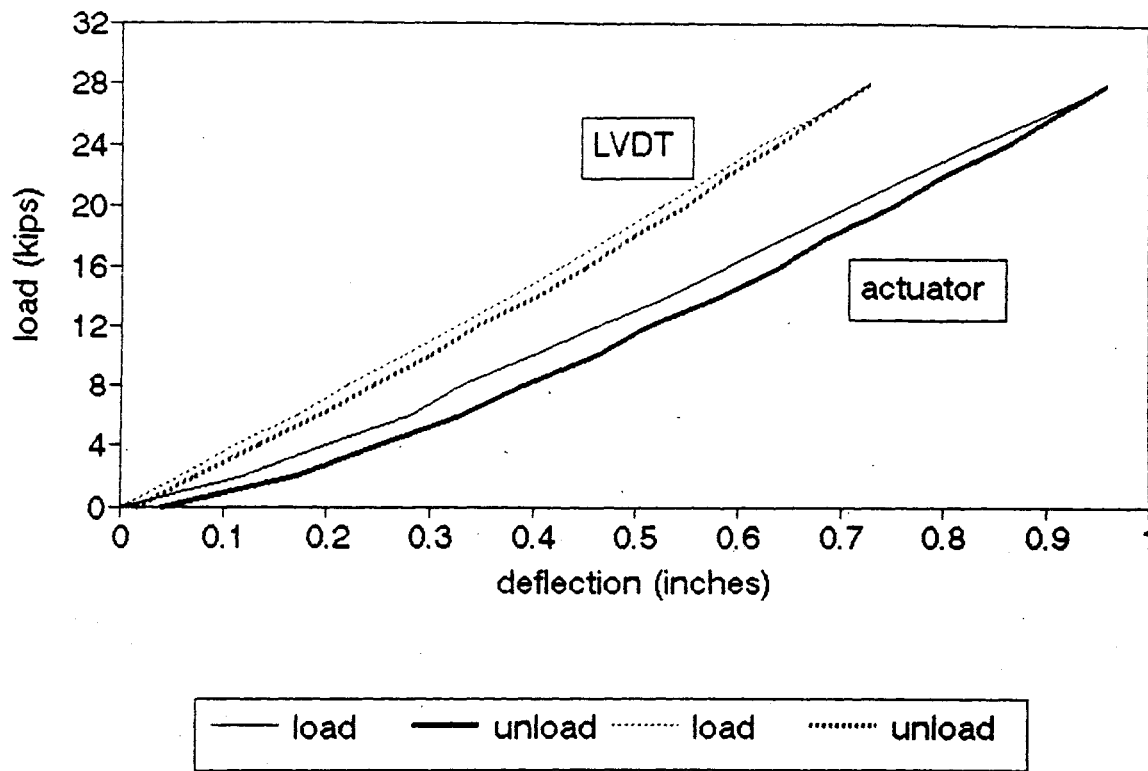


Figure 38 - Monotonic Test at 28 kips.

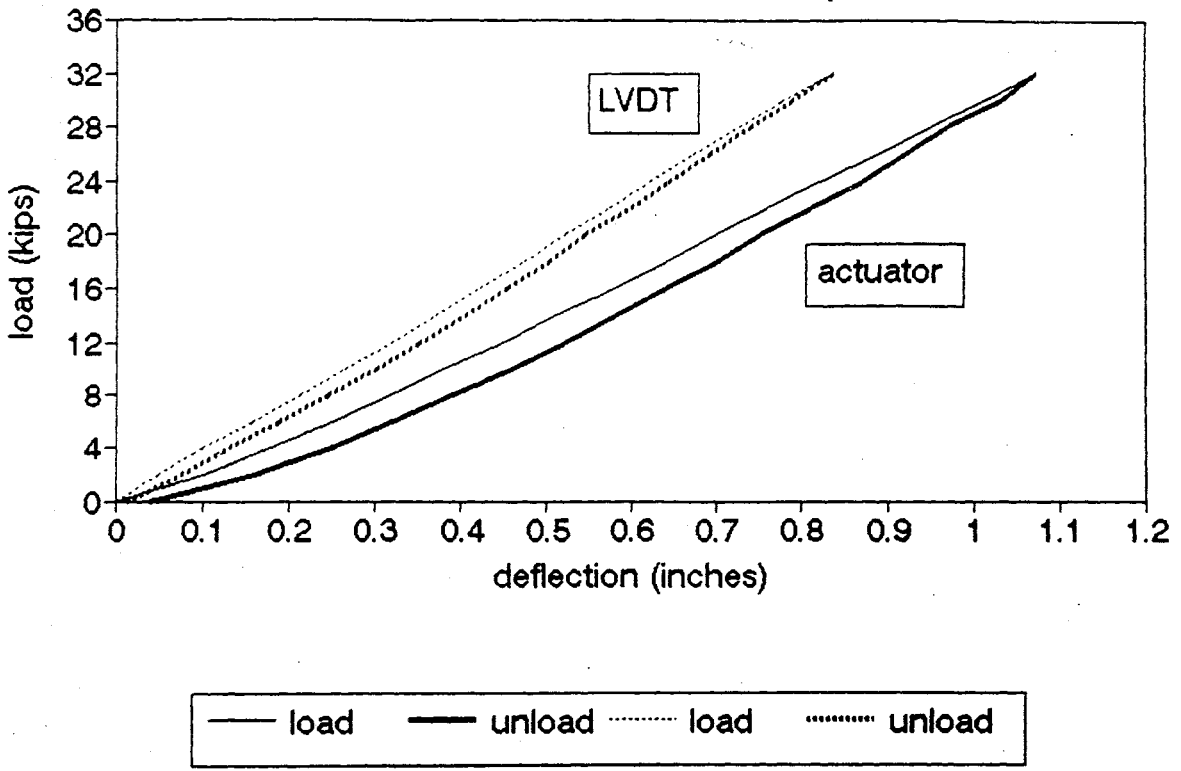


Figure 39 - Monotonic Test at 32 kips.

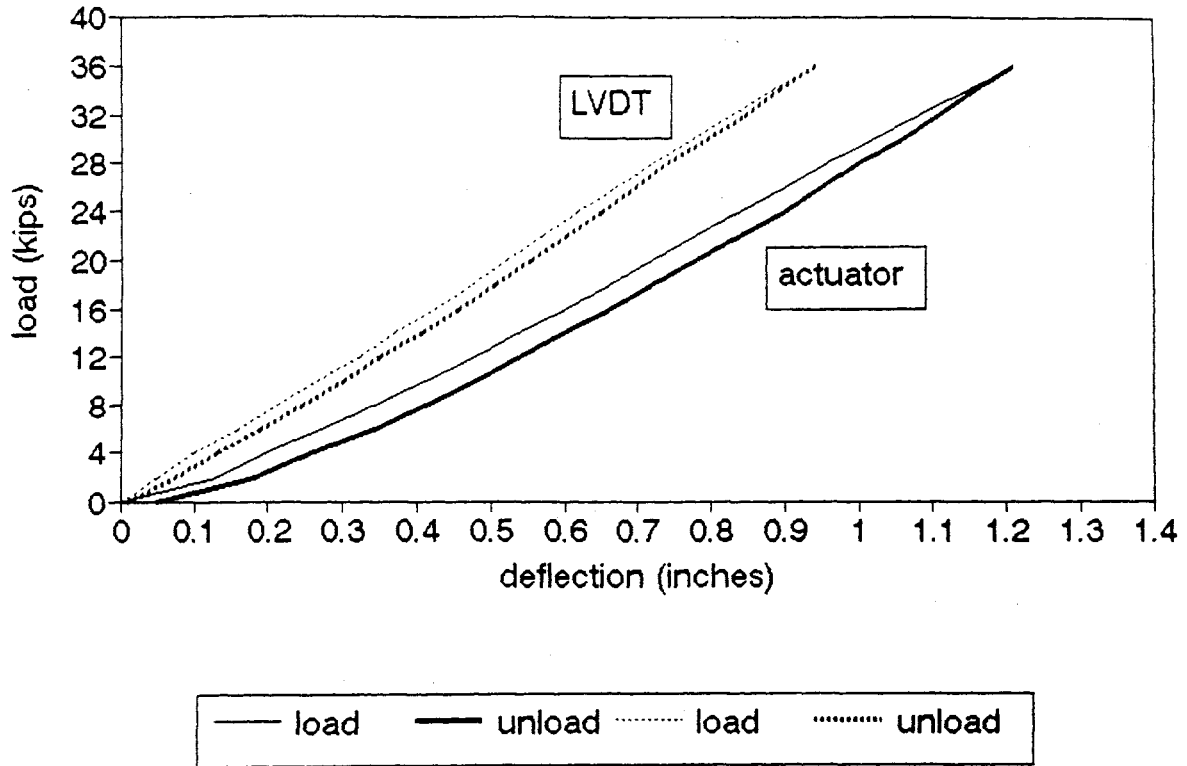


Figure 40 - Monotonic Test at 36 kips.

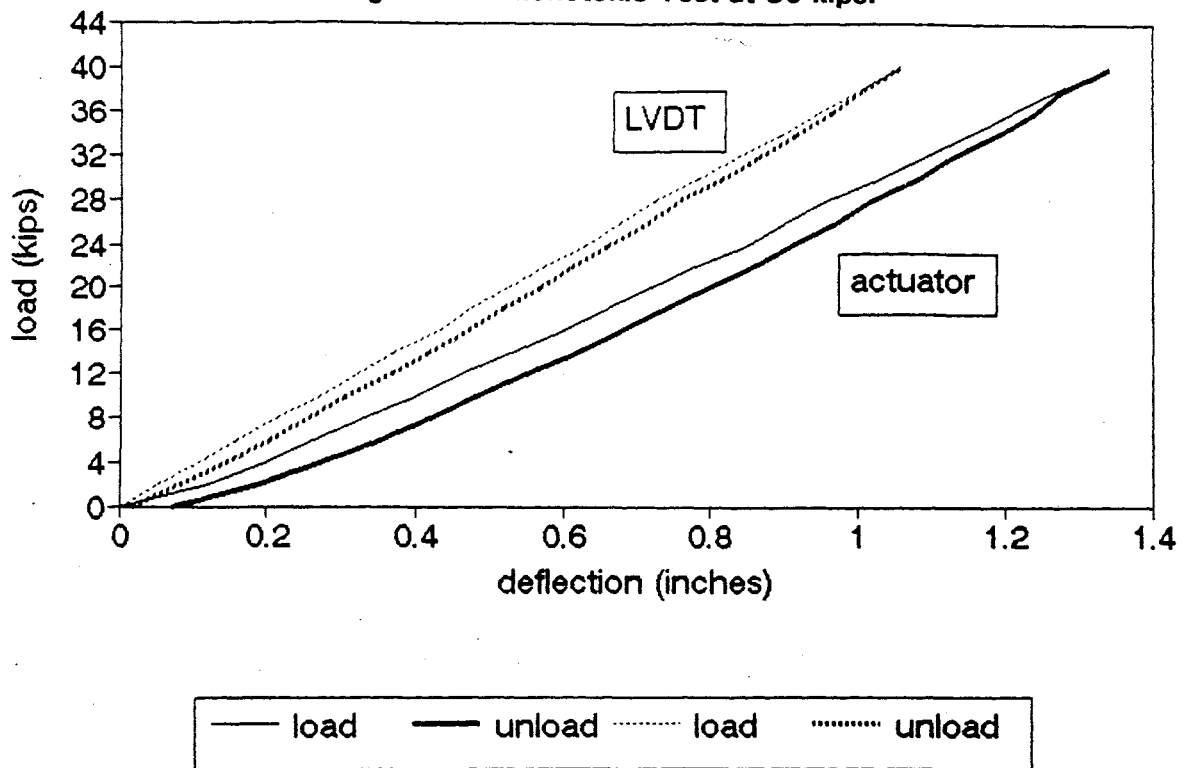


Figure 41 - Monotonic Test at 40 kips.

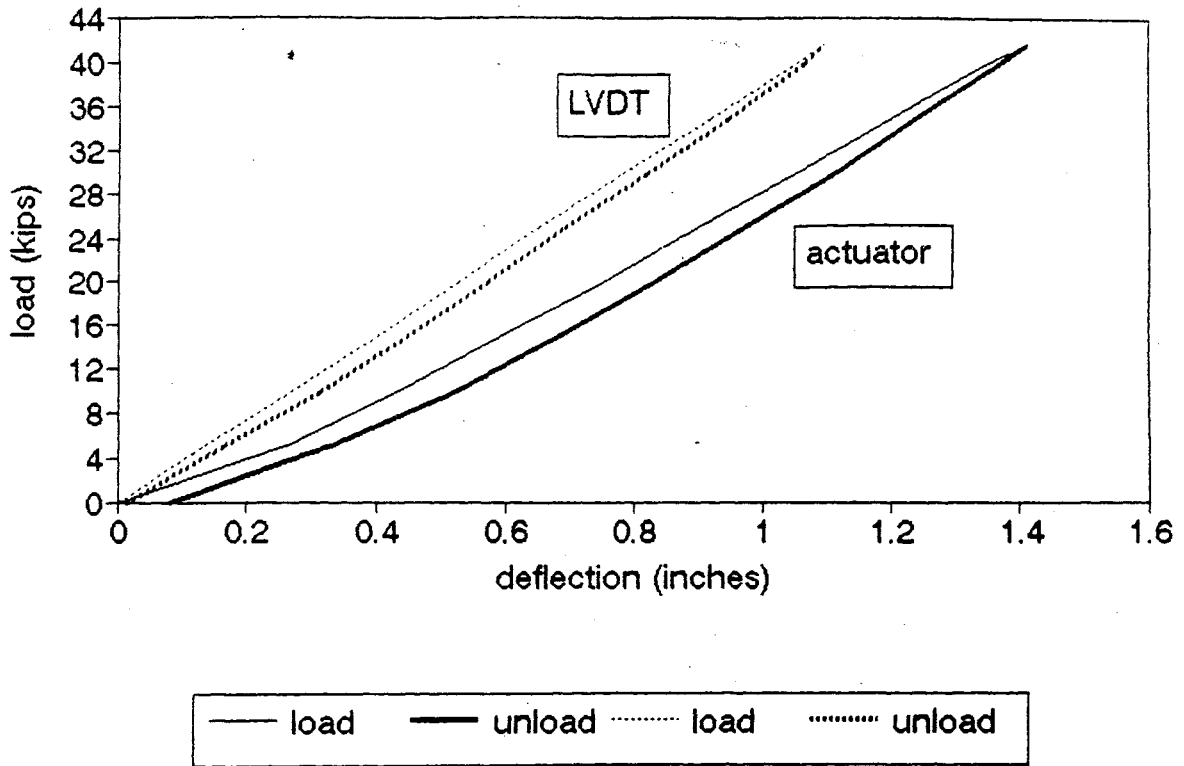
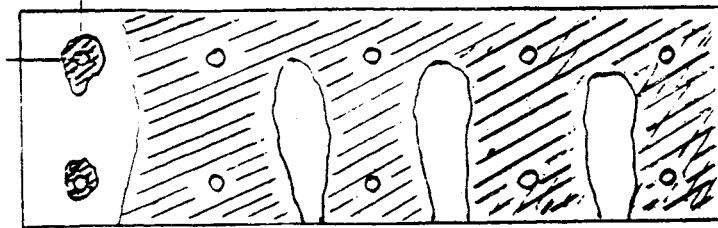




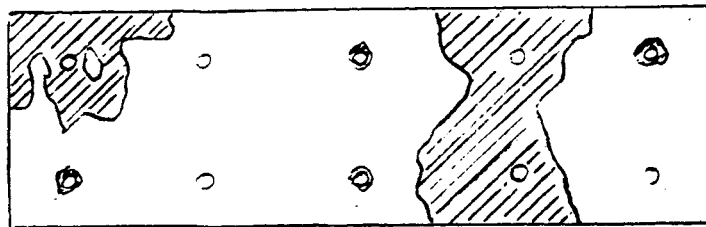
Figure 42 - Monotonic Test at 41.6 kips.



HORIZONTAL: 1"=5'
 VERTICAL: 1"=5'



 NO VOIDS
 VOIDS

(a) Portland mix



DRAWN TO SCALE

HORIZONTAL: 1"=5'
 VERTICAL: 1"=5'

 NO VOIDS
 VOIDS

(b) Conbrextra S

Figure 43 - Results of pumping.

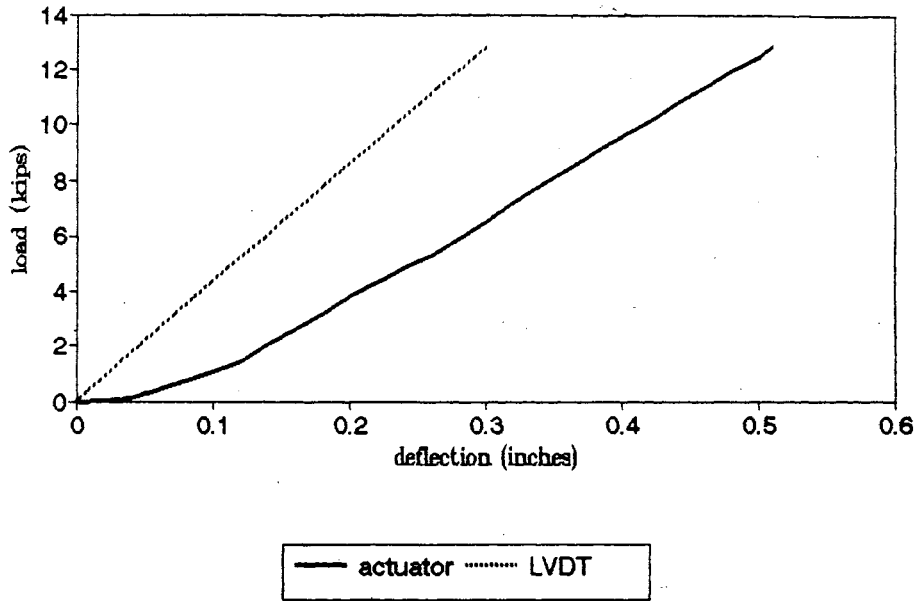


Figure 44 - Initial load-deflection curve for the Conbextra test.

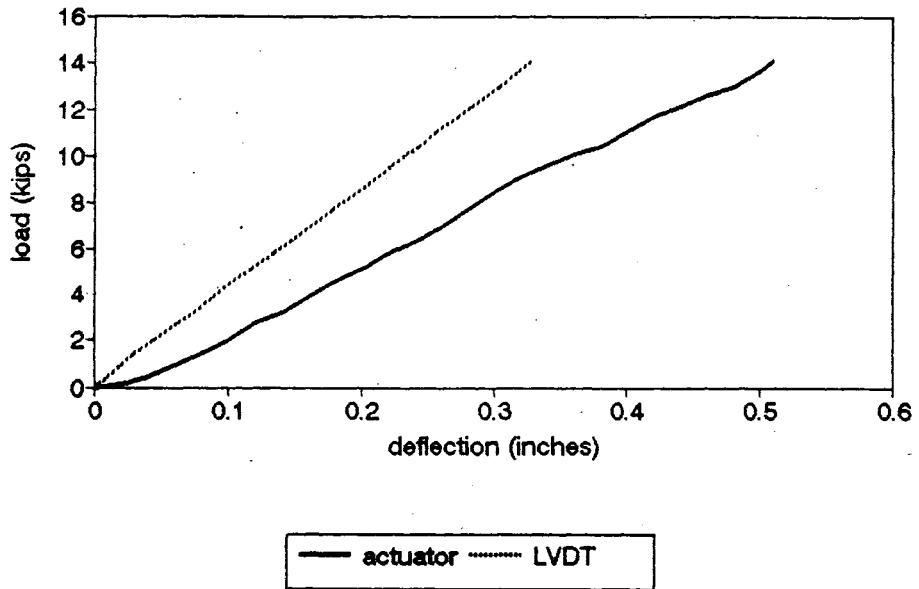


Figure 45 - Initial load-deflection curve for Portland cement test.

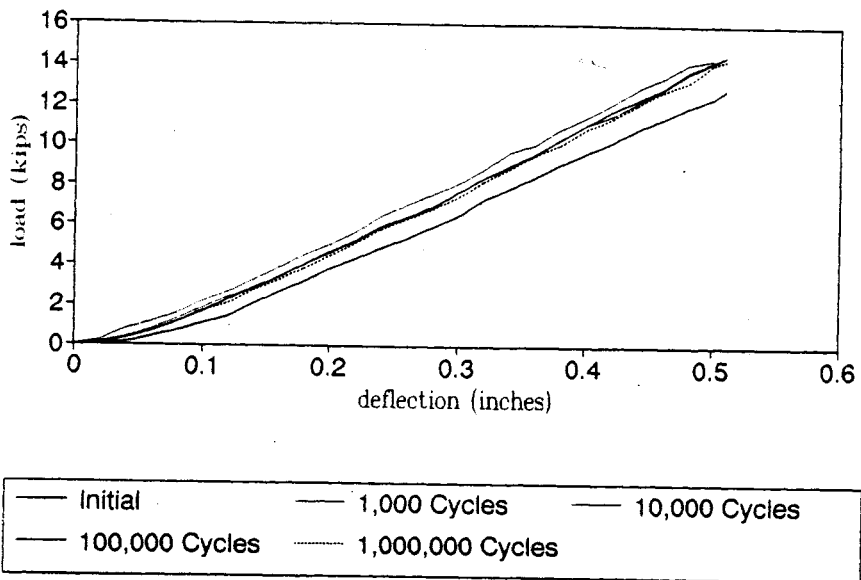


Figure 46 - Fatigue results for the Conbextra test (actuator).

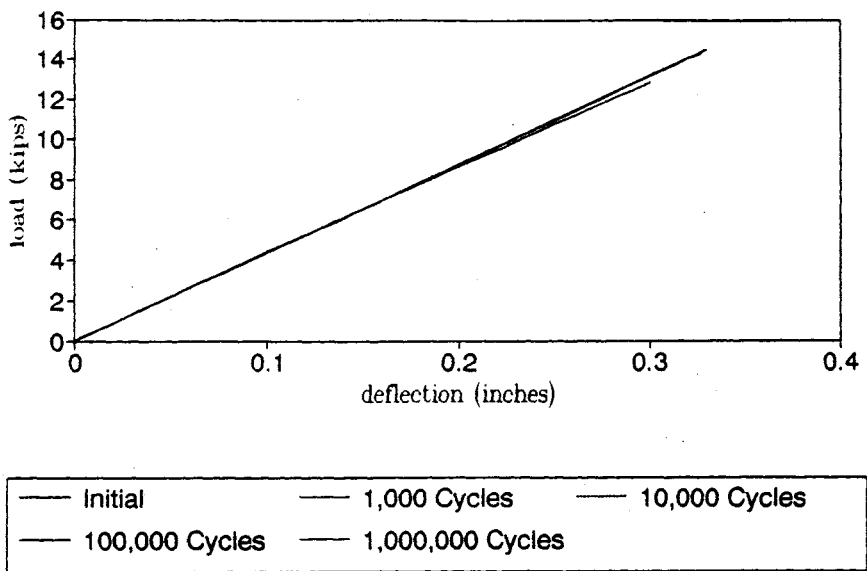


Figure 47 - Fatigue results for the Conbextra test (external LVDT).

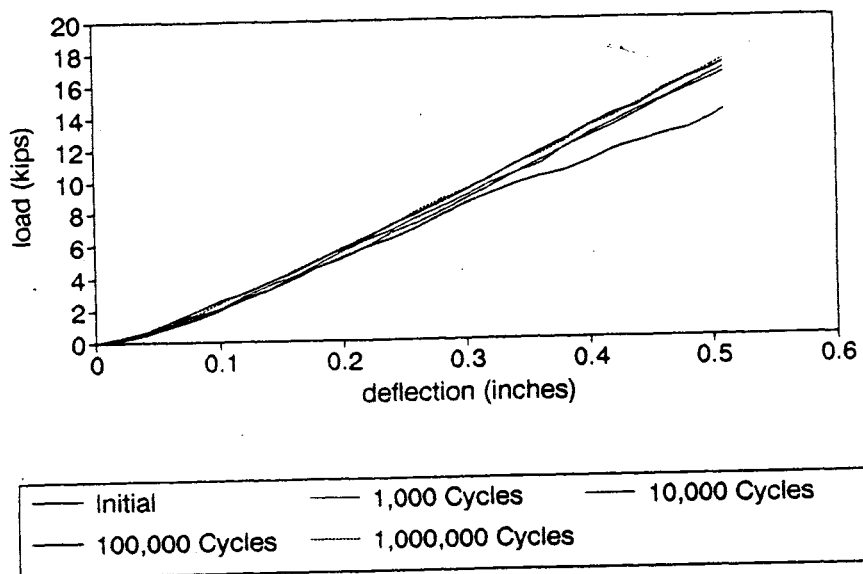


Figure 48 - Fatigue results for the Portland cement test (actuator).

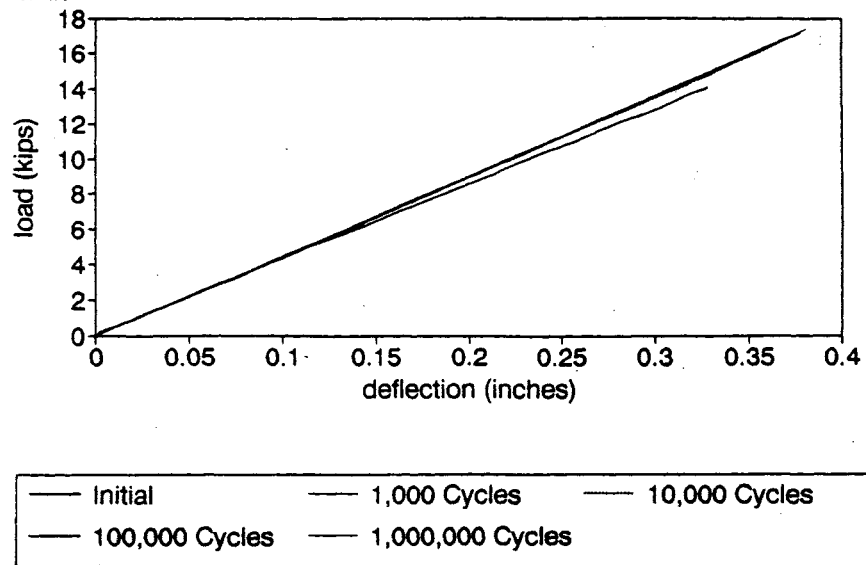


Figure 49 - Fatigue results for the Portland cement test (external LVDT).

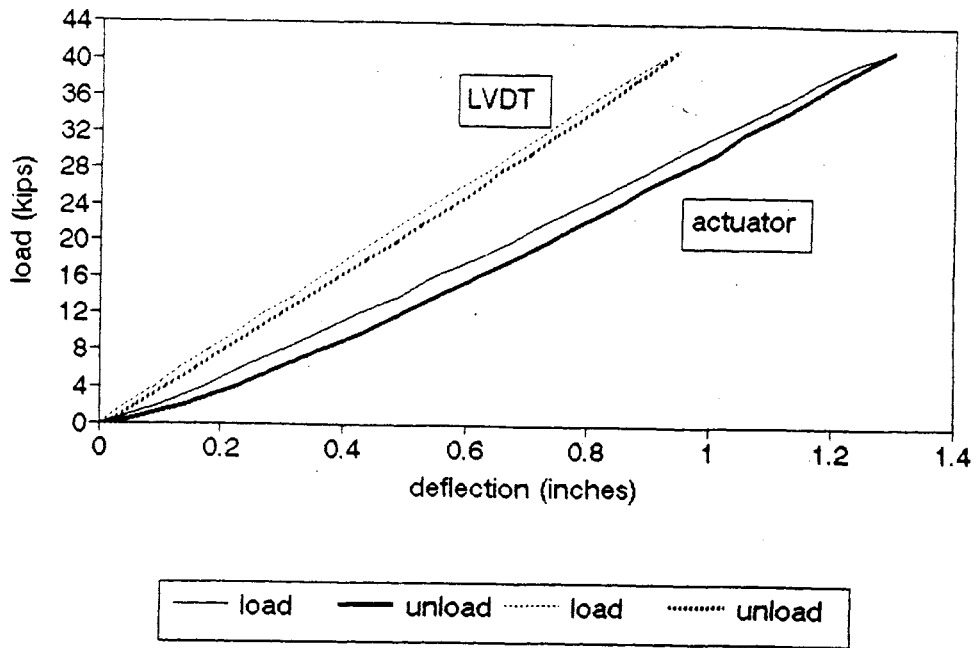


Figure 50 - Load-deflection curves for Conbrextra S at 41.5 kips.

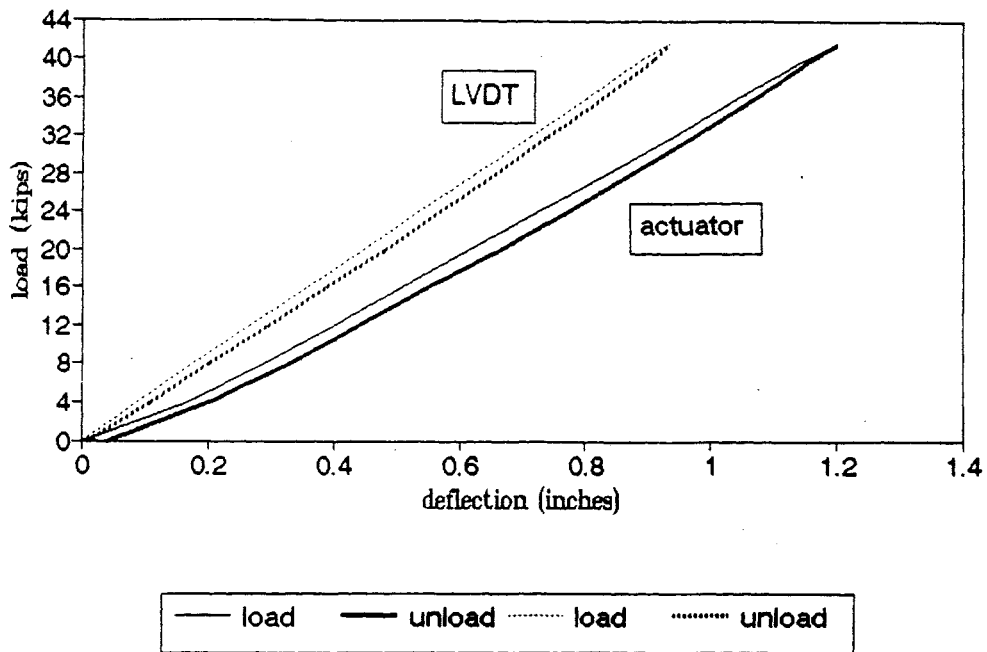
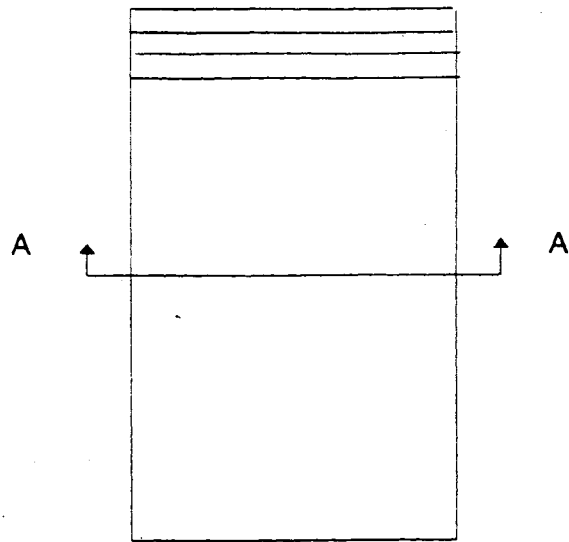
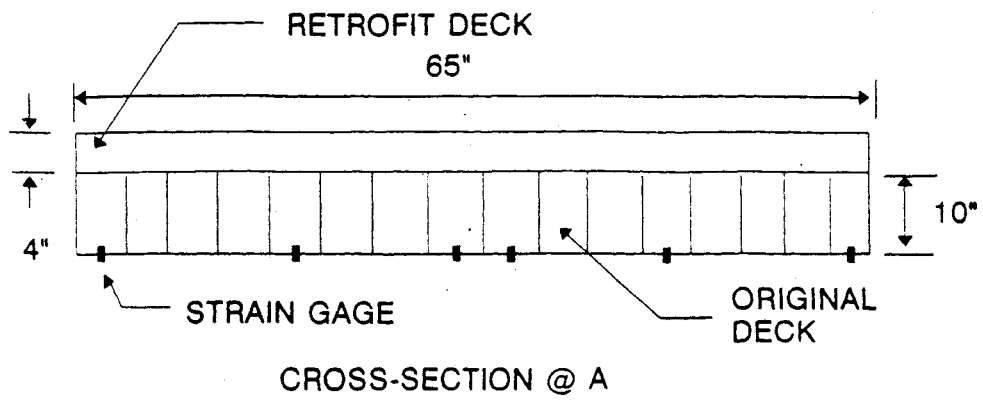


Figure 51 - Load-deflection curves for Portland cement at 41.5 kips.



PLAN VIEW

Figure 52 - Strain gage layout.

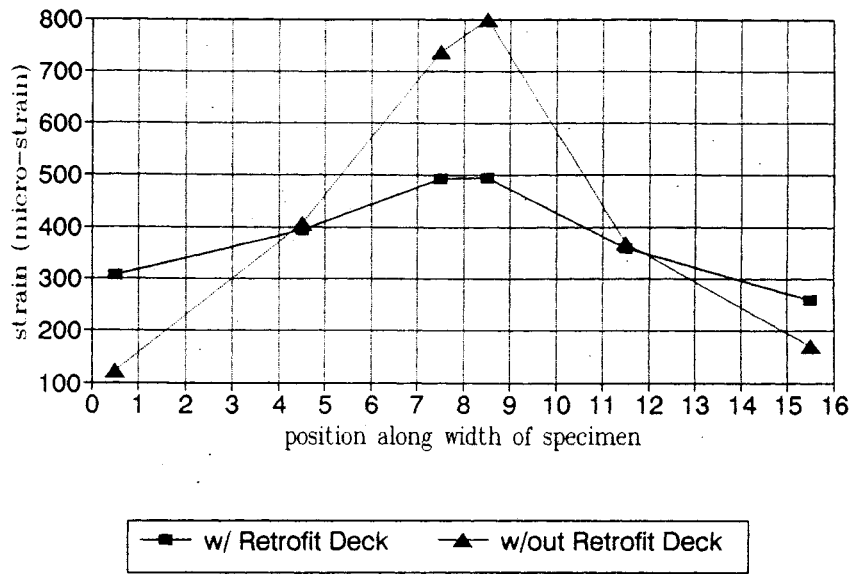


Figure 53 - Transverse load distribution (Conbrextra at 10 kips).

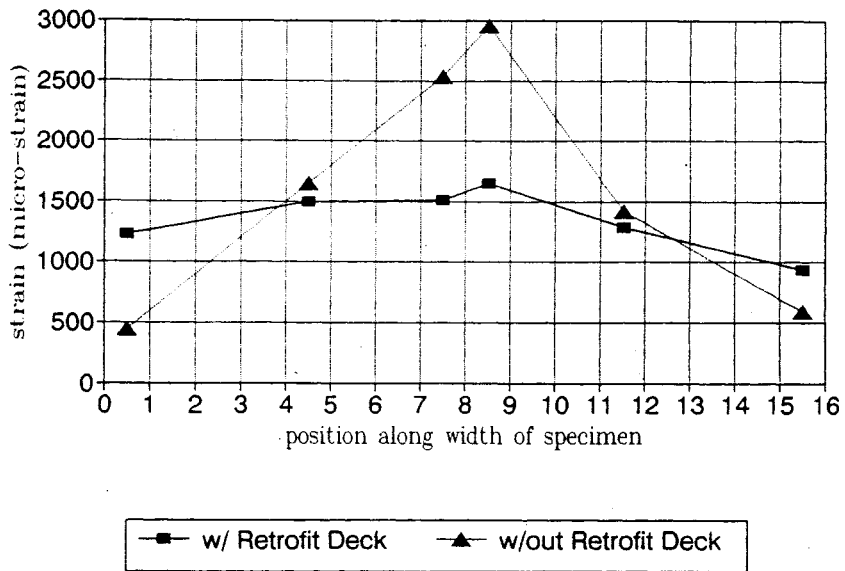


Figure 54 - Transverse load distribution (Conbrextra at 41.5 kips).

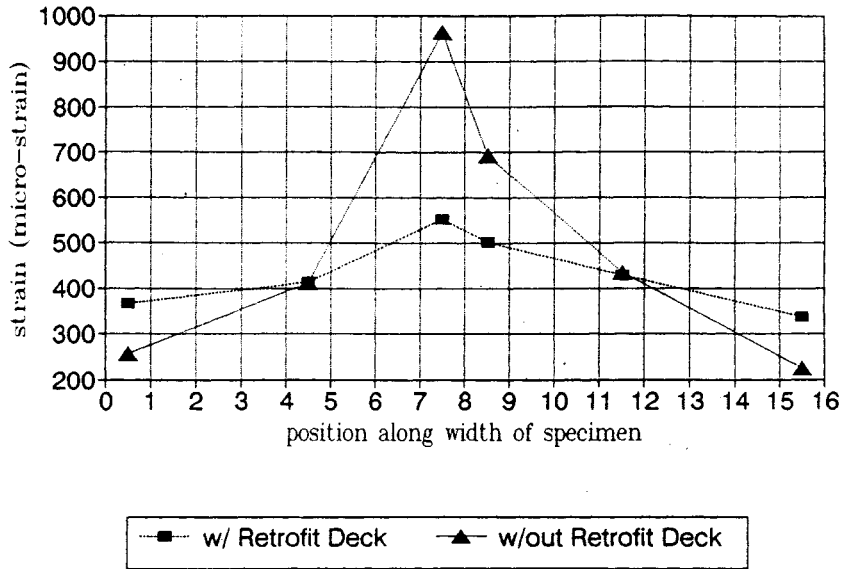


Figure 55 - Transverse load distribution (Portland cement at 10 kips).

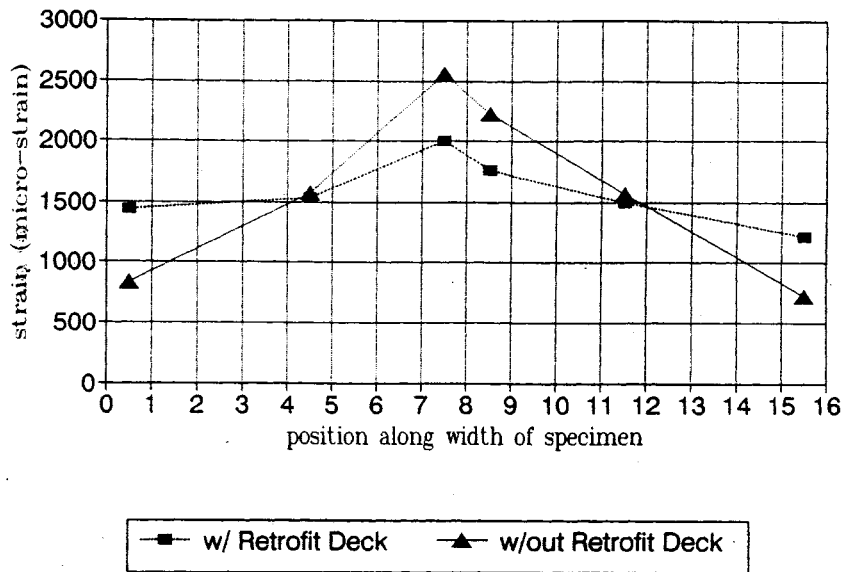


Figure 56 - Transverse load distribution (Portland cement at 41.5 kips).

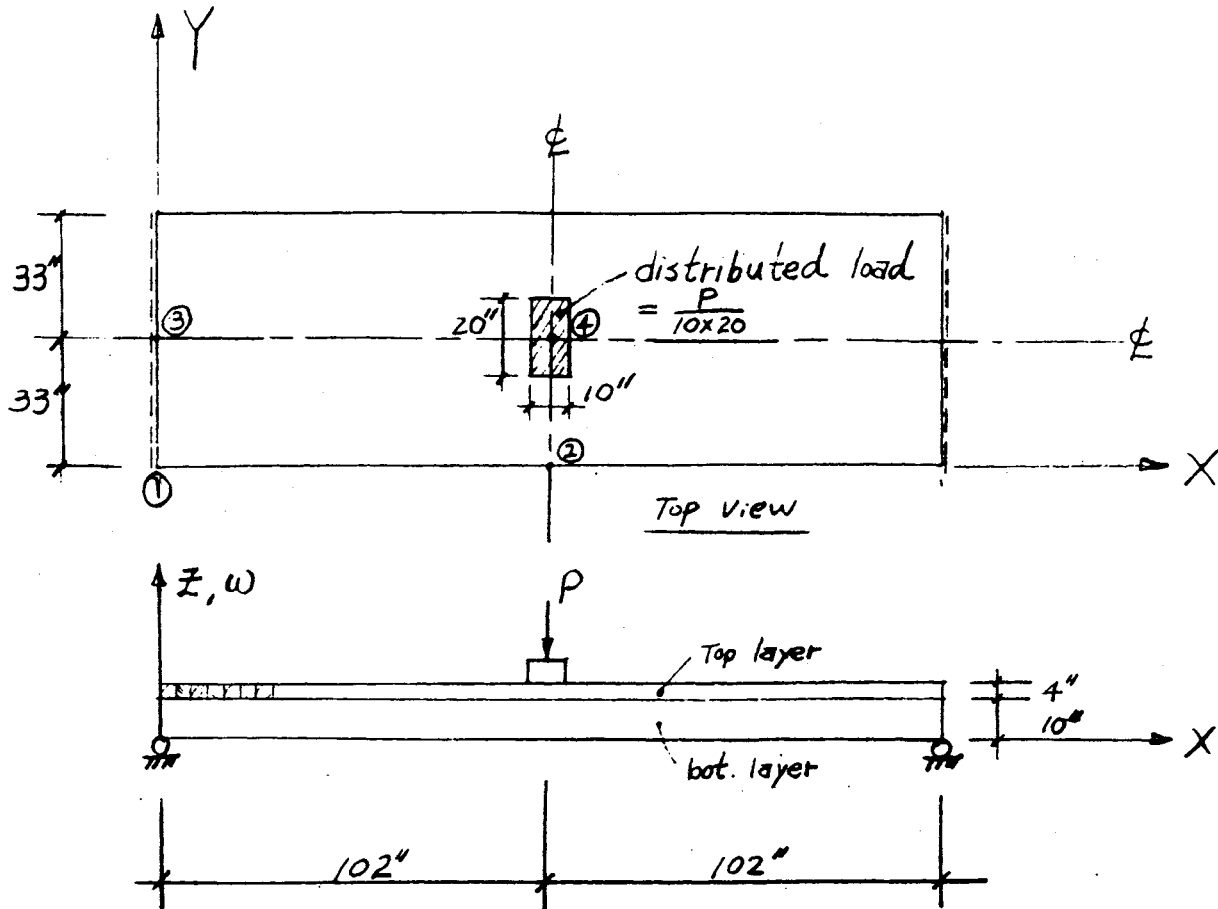


Figure 57 - Dimensions of laboratory model.

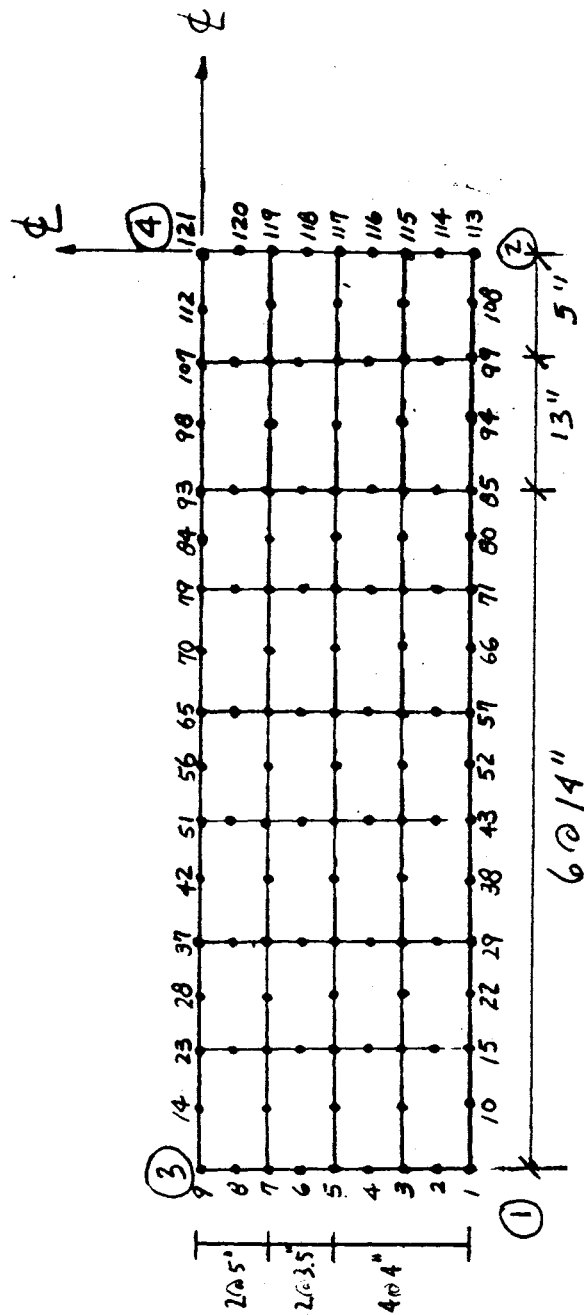


Figure 58 - Nodal layout for finite element analysis.

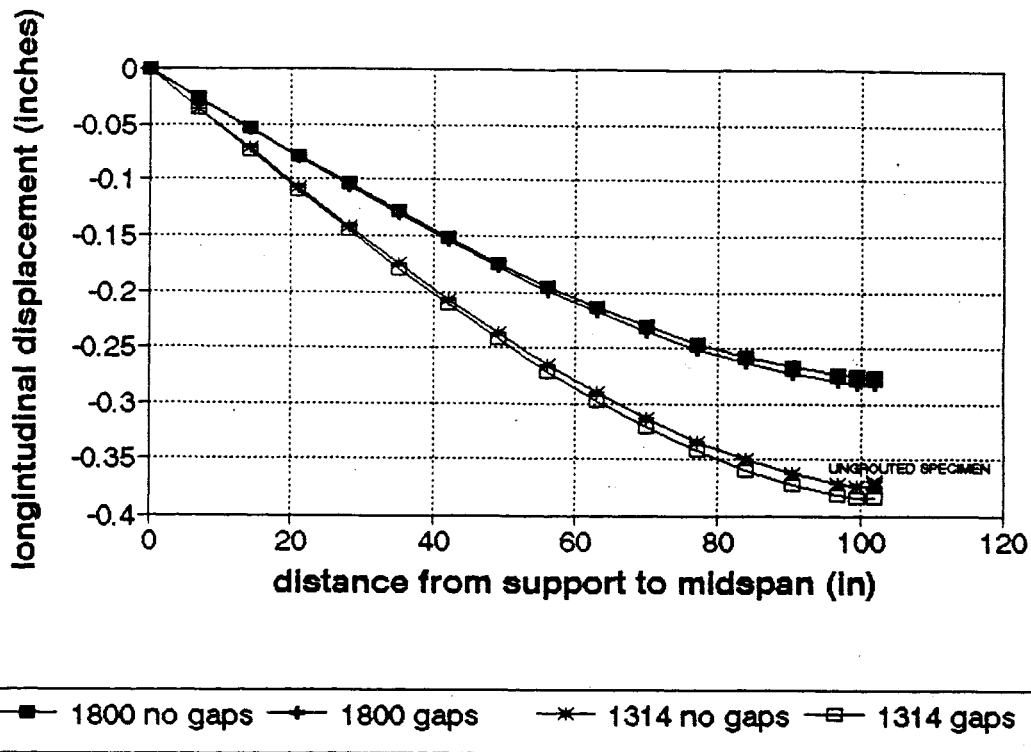


Figure 59 - Longitudinal deflections for analytical model (ungrouted).

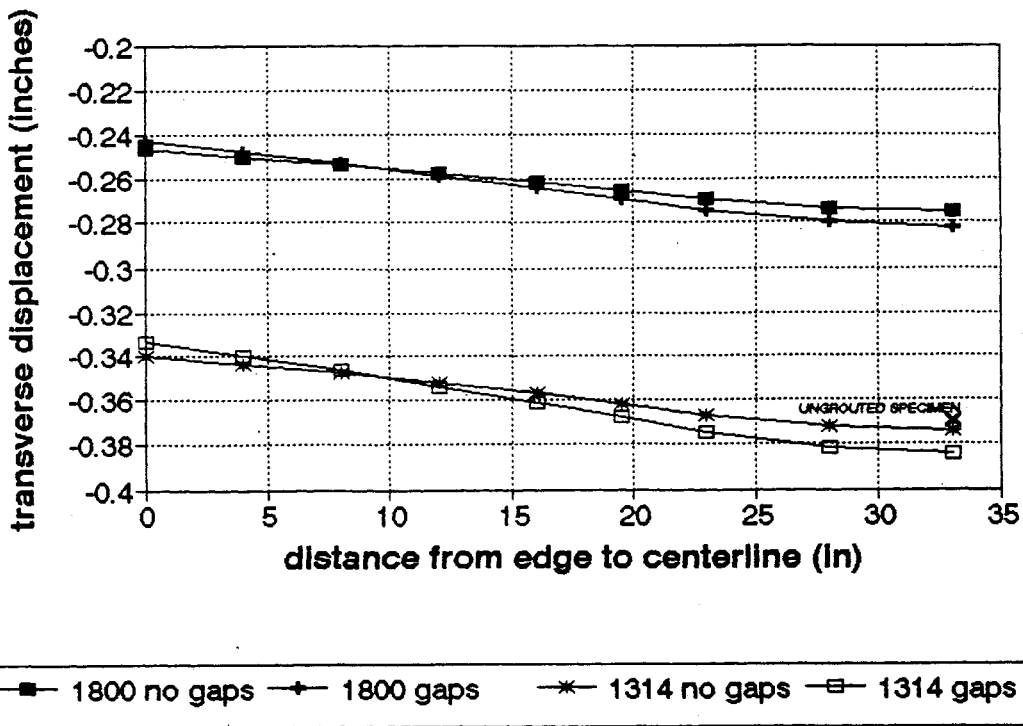


Figure 60 - Transverse deflections for analytical model (ungrouted).

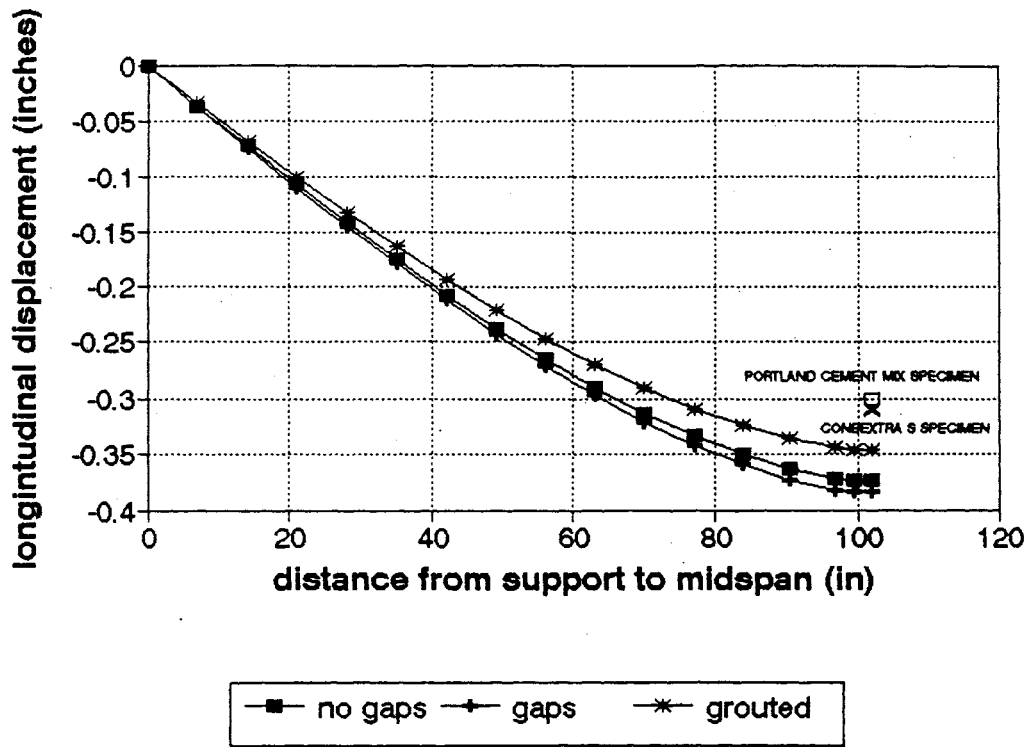


Figure 61 - Longitudinal deflections for analytical model (grouted).

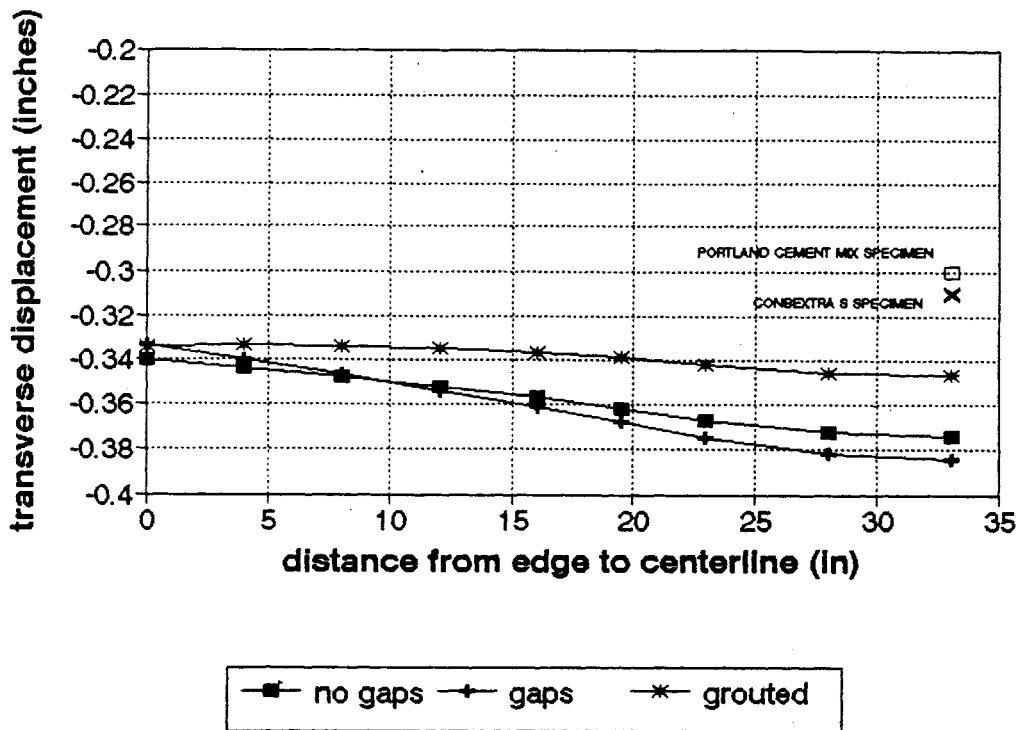


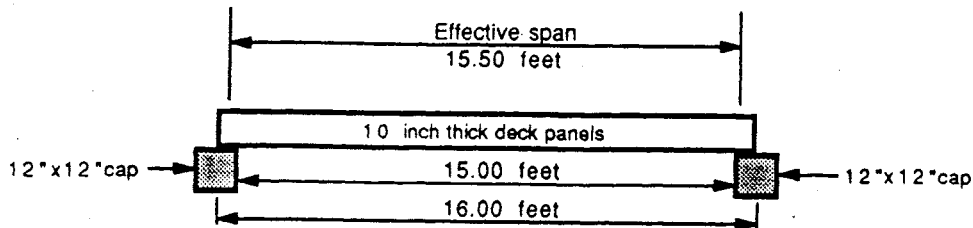
Figure 62 - Transverse deflections for analytical model (grouted).

APPENDIX A

LONGITUDINAL DECK DESIGN COMPUTATIONS 16' DECK PANELS

GIVEN INFORMATION:

DESIGN LOAD: AASHTO HS-20	INTERMEDIATE SPAN, SIMPLE SUPPORTS
SPAN LENGTH: 16.00 FEET	EFFECTIVE SPAN LENGTH: 15.50 FEET
DECK THICKNESS: 10 INCHES	SURFACE THICKNESS: 3 INCHES
DECK MATERIAL: Douglas Fir, No. 1 And Better	
WHEEL LOAD DISTRIBUTION: In direction of span = point load. (Ref. AASHTO 3.25.2)	
In direction normal to span = width of the wheel plus twice thickness of deck.	
20.00 + 2(10) = 40.00 inches = 3.33 feet	



DEAD LOAD:

Surfacing:	0.25 x 3.33 x 1' x 150 lbs/cu ft =	125.0 lbs/L.F.
Decking:	0.83 x 3.33 x 1' x 50 lbs/cu ft =	138.9 lbs/L.F.
	Dead load unit weight = w =	263.9 lbs/L.F.

MOMENT COMPUTATIONS:

Dead load moment = $\frac{wL^2}{8} = \frac{263.9 \times 15.50^2}{8} \times 12 = 95,099 \text{ in-lb}$

Live load moment = $[(. \text{AASHTO HS-20})/2] \times 12,000$

$[(124.0)/2] \times 12,000 = \frac{744,000 \text{ in-lb}}{839,099 \text{ in-lb}}$

Total Moment = M =

SECTION MODULUS OF DECK SECTION:

$$S = \frac{bd^2}{6} = \frac{40.00 \times 10^2}{6} = 667 \text{ in}^3$$

ACTUAL EXTREME FIBER STRESS:

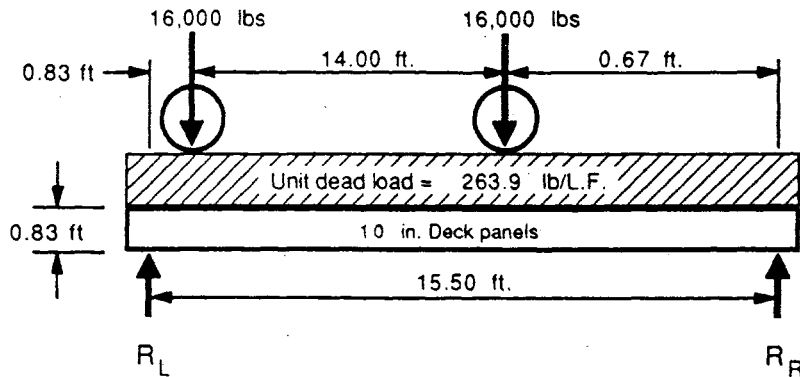
$$f_b = \frac{M}{S} = \frac{839,099}{667} = 1,259 \text{ psi} < 1521 \text{ psi O K!}$$

LONGITUDINAL DECK DESIGN
 HORIZONTAL SHEAR STRESS COMPUTATIONS
 16' DECK PANELS

HORIZONTAL SHEAR STRESS:

RATIONAL METHOD:

The calculations are in compliance with the National Design Specifications for Wood Construction (NDS Section 3.4.4).



$$R_L = 16,000 (14.67 / 15.50) + 16,000 (0.67 / 15.50) + ((264) (15.50 / 2))$$

$$R_L = 15,140 + 688 + 2,045$$

$$R_L = 17,873 \text{ lb}$$

$$V = R_L (0.83 \times 264) = 17,873 - 220 = 17,653 \text{ lb}$$

$$f_v = \frac{3V}{2bd} = \frac{3 \times 17,653}{2 \times 40 \times 10} = 66.2 \text{ psi} < 126 = 1.33 \times 95 \text{ OK!}$$

$$V_v = \frac{V}{bd} = \frac{17,653}{40 \times 10} = 44.1 \text{ psi very small OK!}$$

REQUIRED WIDTH OF BEARING AT END OF PANEL:

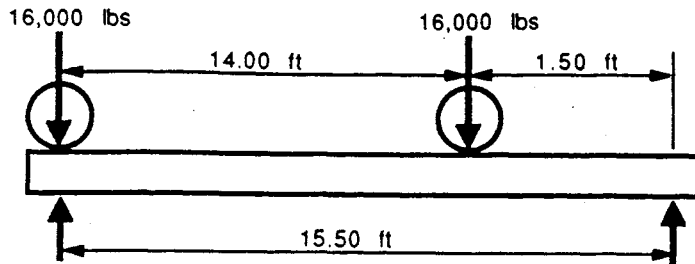
Allowable compression perpendicular to grain = 625 psi

This is the same for both the deck planks and the caps.

$$\text{Required width} = \frac{17,873}{40 \times 625} = 0.71 \text{ inches}$$

LONGITUDINAL DECK DESIGN
 COMPUTATIONS FOR
 16' DECK PANELS SPLICE

CHECK HORIZONTAL SHEAR, WITH WHEEL AT SUPPORT:



$$R_L = 17,548 \text{ lbs}$$

$$R_R = 14,452 \text{ lbs}$$

$$R_L = 16,000 + 16,000 (1.50 / 15.50) = 17,548 \text{ lbs}$$

$$\text{Distribution width} = 10.00 + 10.00 + 20.00 = 40.00 \text{ inches}$$

$$\text{Distributed load} = \frac{17,548 \text{ lbs}}{40.00 \text{ in}} = 439 \text{ lb/in}$$

$$\text{For 4 in plank} = 439 \times 4 = 1,755 \text{ lbs} = V$$

$$f_v = \frac{3V}{2bd} = \frac{3 \times 1,755}{2 \times 4 \times 10} = 65.8 \text{ psi} = \text{unit shear on plane of contact in splice}$$

SHEAR AT PLANE OF CONTACT:

The plane of contact for the shiplap joint between panels is also the neutral axis of the deck; therefore, the maximum shear occurs on this surface.

The joint is 4 inches wide.

$$\text{Shear per lineal foot of joint} = 65.8 \times 12 \times 4 = 3,159 \text{ lbs/L.F.}$$

$$\text{Area of } 5/8 \text{ inch Drive Spike} = 0.306 \text{ sq in}$$

$$\text{Strength in single shear} = 0.306 \text{ sq in} \times 20,000 \text{ psi} = 6,120 \text{ lbs}$$

$$\text{Strength of wood in bearing} = 0.625 \text{ in} \times 5 \text{ in} \times 2,020 \text{ psi} = 6,313 \text{ lbs}$$

The Drive Spikes in single shear is less than the wood in end grain bearing and governs.

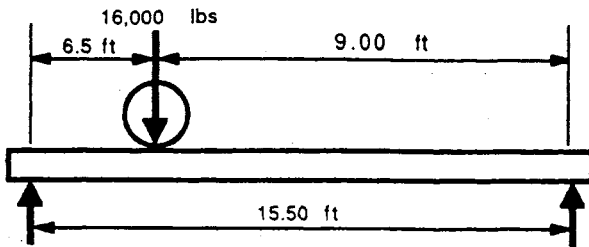
$$\text{Drive Spike spacing at support} = \frac{6,120 \text{ lbs}}{3,159 \text{ lbs/L.F.}} = 1.94 \text{ ft or } 23.3 \text{ in}$$

LONGITUDINAL DECK DESIGN
 COMPUTATIONS FOR
 16' DECK PANELS SPLICE

SPACING OF DRIVE SPIKES:

DESIGN CONDITIONS:

Drive spike spacing = 1.75 ft
 Wheel at 6.5 ft from centerline of support



$$R_L = \frac{9.00 \times 16,000}{15.50}$$

$$R_L = 9,290 \text{ lbs}$$

$$R_R = 6,710 \text{ lbs}$$

$$R_L = 9,290 \text{ lbs}$$

$$R_R = 6,710 \text{ lbs}$$

$$\text{Distributed load : } 9,290 / 40.00 = 232 \text{ lbs/in} \quad 232 \times 4 = 929 \text{ lbs} = V$$

$$\text{Shear at plane of contact : } F_v = \frac{3V}{2bd} = \frac{3 \times 929}{2 \times 4 \times 10} = 34.8 \text{ psi}$$

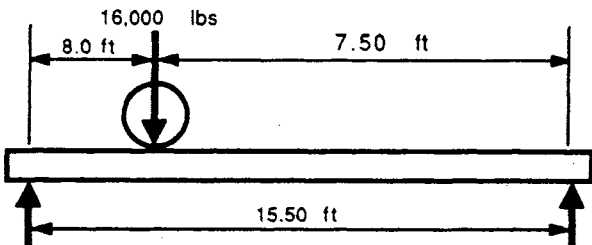
$$\text{Shear per L.F. of joint : } 34.8 \times 12 \times 4 = 1,672 \text{ lbs per L.F.}$$

$$\text{Max. spike sp. : } (6,120 \text{ lbs per spike}) / (1,672 \text{ lbs/L.F.}) = 3.7 \text{ ft} \\ = 44 \text{ in} > 21 \text{ OK}$$

SPACING OF DRIVE SPIKES:

DESIGN CONDITIONS:

Drive spike spacing = 2.00 ft
 Wheel at 8.0 ft from centerline of support



$$R_L = \frac{7.50 \times 16,000}{15.50}$$

$$R_L = 7,742 \text{ lbs}$$

$$R_R = 8,258 \text{ lbs}$$

$$R_L = 7,742 \text{ lbs}$$

$$R_R = 8,258 \text{ lbs}$$

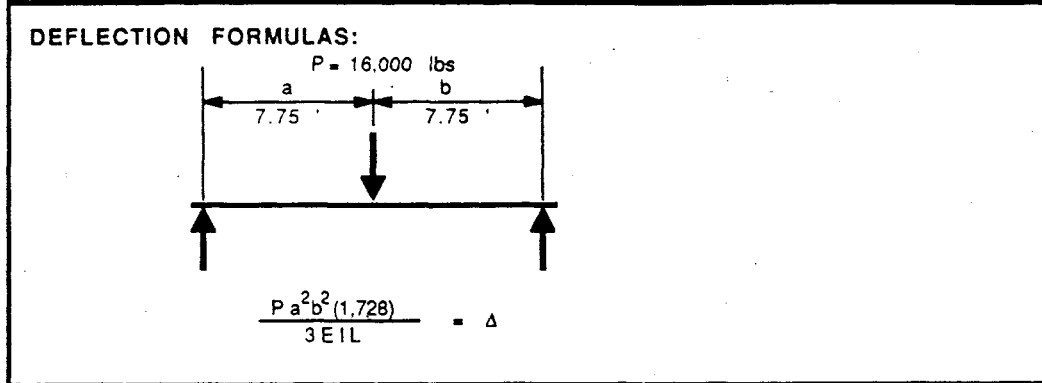
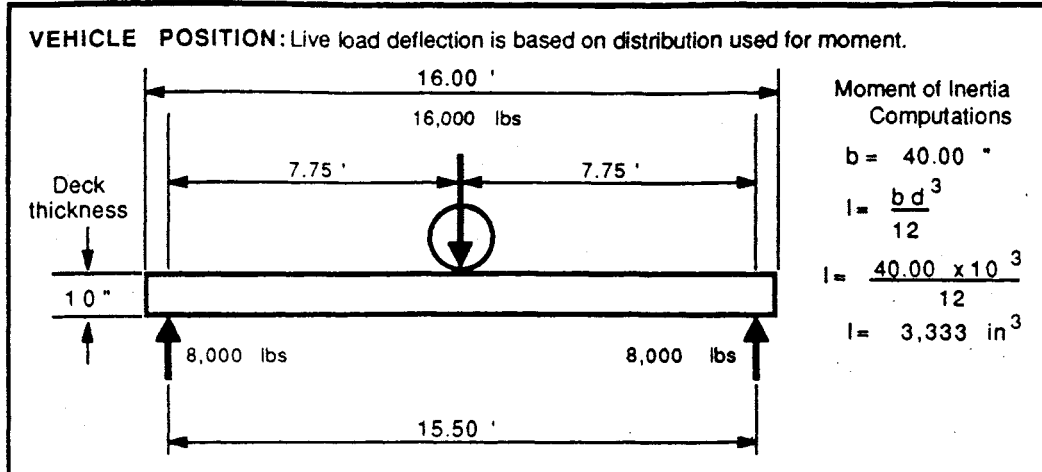
$$\text{Distributed load : } 7,742 / 40.00 = 194 \text{ lbs/in} \quad 194 \times 4 = 774 \text{ lbs} = V$$

$$\text{Shear at plane of contact : } F_v = \frac{3V}{2bd} = \frac{3 \times 774}{2 \times 4 \times 10} = 29.0 \text{ psi}$$

$$\text{Shear per L.F. of joint : } 29.0 \times 12 \times 4 = 1,394 \text{ lbs per L.F.}$$

$$\text{Max. spike sp. : } (6,120 \text{ lbs per spike}) / (1,394 \text{ lbs/L.F.}) = 4.4 \text{ ft} \\ = 53 \text{ in} > 24 \text{ OK}$$

LONGITUDINAL DECK DESIGN
 DEFLECTION CALCULATIONS
 16 ft. SPAN



CALCULATIONS:

$$\frac{16,000 \times 7.75^2 \times 7.75^2 \times 1,728}{3 \times 1,800,000 \times 3,333 \times 15.50} = 0.357 \text{ "}$$

TOTAL APPLIED LOAD DEFLECTION = 0.357"

$$L/\Delta = \frac{15.50 \times 12}{0.357} = 520$$

LONGITUDINAL DECK DESIGN
RATING CALCULATIONS
16 ft. SPAN DECK

DATA:

Dead load moment = $M_{DL} = 95,099$ in-lb
Live load moment = $M_{LL} = 744,000$ in-lb
Maximum dead load shear = $V_{DL} = 1,825$ lb
Maximum live load shear = $V_{LL} = 17,548$ lb
Section modulus of deck section = $S = 667$ in³
Cross sectional area of deck section = $A = 400$ sq in

Calculated ratings based on flexure:

$$f_{bDL} = \frac{M_{DL}}{S} = \frac{95,099}{667} = 142.6 \text{ psi}$$

$$f_{bLL} = \frac{M_{LL}}{S} = \frac{744,000}{667} = 1,116.0 \text{ psi}$$

$$\text{Inventory Rating} = \frac{(F_{\text{Allowable}}) - f_{bDL}}{f_{bLL}} \times 20$$

$$\text{Inv. (Flexure)} = \frac{1,521 \text{ psi} - 142.6 \text{ psi}}{1,116.0 \text{ psi}} \times 20 = \text{HS } 24.7$$

$$\text{Operating Rating} = \frac{(F_{\text{Allowable}})(1.33) - f_{bDL}}{f_{bLL}} \times 20$$

$$\text{Opr. (Flexure)} = \frac{(1,521 \text{ psi} \times 1.33) - 142.6 \text{ psi}}{1,116.0 \text{ psi}} \times 20 = \text{HS } 33.7$$

Calculated ratings based on shear at (d) from support:

$$f_{vDL} = \frac{3V_{DL}}{2A} = \frac{3 \times 1,825}{2 \times 400} = 6.8 \text{ psi}$$

$$f_{vLL} = \frac{3V_{LL}}{2A} = \frac{3 \times 17,548}{2 \times 400} = 65.8 \text{ psi}$$

$$\text{Inv. (Shear)} = \frac{95 \text{ psi} - 6.8 \text{ psi}}{65.8 \text{ psi}} \times 20 = \text{HS } 26.8$$

$$\text{Opr. (Shear)} = \frac{(95 \text{ psi} \times 1.33) - 6.8 \text{ psi}}{65.8 \text{ psi}} \times 20 = \text{HS } 36.3$$

Controlling Ratings:

Inventory Rating = **HS 24.7**

Operating Rating = **HS 33.7**

